May 2018

# Preliminary Investigation of Tensile Strength and Impact Characterization Of Cementitious Composite Incorporating Carbon Nanotubes

Robabeh Jazaei
robabeh.jazaei@gmail.com

# PRELIMINARY INVESTIGATION OF TENSILE STRENGTH AND IMPACT CHARACTERIZATION OF CEMENTITIOUS COMPOSITE INCORPORATING CARBON NANOTUBES

By

Robabeh Jazaei

Bachelor of Science in Civil Engineering
Shahrood University of Technology, Iran
2002

Master of Science in Civil Engineering
Azad University, Central Tehran Branch, Iran
2009

A dissertation submitted in partial fulfillment
of the requirements for the

Doctor of Philosophy – Civil and Environmental Engineering

Department of Civil and Environmental Engineering and Construction
Howard R. Hughes College of Engineering

The Graduate College
University of Nevada, Las Vegas
May 2018

UNLV | GRADUATE COLLEGE

## Dissertation Approval

The Graduate College
The University of Nevada, Las Vegas

April 10, 2018

This dissertation prepared by

Robabeh Jazaei

entitled

Preliminary Investigation of Tensile Strength and Impact Characterization of Cementitious Composite Incorporating Carbon Nanotubes

is approved in partial fulfillment of the requirements for the degree of

Doctor of Philosophy in Engineering - Civil and Environmental Engineering
Department of Civil and Environmental Engineering and Construction

Moses Karakouzian, Ph.D.
*Examination Committee Co-Chair*

Kathryn Hausbeck Korgan, Ph.D.
*Graduate College Interim Dean*

Brendan O'Toole, Ph.D.
*Examination Committee Co-Chair*

Ying Tian, Ph.D.
*Examination Committee Member*

Pramen Shrestha, Ph.D.
*Graduate College Faculty Representative*

# Abstract

Cement has been largely used in the construction industry, specifically as a matrix for concrete. Recently, a new generation of cement-based composite that greatly increases mechanical properties is replacing conventional concrete. With periodic advances in the field, researchers considered particles with high-aspect ratios such as Carbon Nanotubes (CNTs) to reinforce cement matrices. Although there is not much literature to draw upon in research, some research on improving tensile strength of cementitious composite incorporating with CNTs does exist. However, there had been no evidence of investigation into impact strength until this study.

Most papers presented examined the effect of multi-walled carbon nanotubes, but very few investigated single-walled carbon nanotubes (SWCNTs), and none of the research compared SWCNTs with multi-walled carbon nanotubes (MWCNTs), and hybrid CNTs (50% of MWCNTs and 50% SWCNTs) in cementitious composites.

The aim of this research is to assess and compare the effect on tensile and impact strength of cementitious composite of reinforcing cement with functionalized (-COOH) SWCNTs, MWCNTs, and hybrid CNTs. Additionally, the lack of standard mixing and test procedures for nanomaterials with cement is considered.

The first objective of this research was to enhance effectiveness of CNTs' dispersion in water with a sonicator, and to develop the procedure that can be replicated and perhaps standardized for cementitious nanocomposite. The most important objective of this research was to assess and compare the effect of reinforcing cementitious composite with single-walled, multi-walled, and hybrid carbon nanotubes. This process reveals the best low dosage (less than 1.0%) of MWCNTs and SWCNTs on energy absorption under drop-weight impact test. Among several methods of impact testing, two velocity-based impact tests are classified as low-velocity (quasi-static) and high-velocity (dynamic) tests. The drop-weight test is one

of many low-velocity impact tests in which the velocity of the striking body is lower than 10 m/s. The ACI 544.2R-89 report is followed and modified for this specific nanocomposite.

The third objective of this investigation was to measure tensile splitting strength of the nanocomposites. The splitting tensile test is incompliance with ASTM 496/ 496M-04 standard However, the specimens are scaled down and the test procedure is modified for this specific class of nanocomposite.

The energy absorption of cementitious composite reinforced with SWCNTs, MWCNTs and hybrid CNTs were measured and compared. Investigation of cementitious composite incorporating CNTs indicated reduced brittleness throughout, changing diagonal to radial failure mechanism.

Hybrid CNTs' reinforcement performed outstandingly at decreasing crack propagation and debris spatter of specimens subjected to impact load. Additionally, the impact strength of cementitious nanocomposite incorporating 0.4% hybrid carbon nanotubes by weight of cement increased. However, more experiments should be conducted. Lastly, tensile strength and ductility of hybrid reinforced cementitious nanocomposite improved, and failure mechanism was investigated.

# Acknowledgements

It is with enormous gratitude that I acknowledge my advisor, Professor Moses Karakouzian; my co-advisor and Chair of Mechanical Engineering Department, Professor Brendan O'Toole; and my doctoral committee members. Without my committee chair's and co-chair's insightful comments, encouragement, and precious support, completing an interdisciplinary dissertation would have been impossible. I am grateful that Dr. Karakouzian and Dr. O'Toole provided me enough guidance, several meetings, and challenging questions from conception to completion of my research. Without their support, creativity, and novel ideas my interdisciplinary research would not have developed as it has.

I would also like to extend my thanks to Dr. Jaeyun Moon from the Mechanical Engineering Department for her guidance, training, and support for my research, as well as for 24-hour access to her laboratory and research facilities. I am thankful to Dr. Minghua Ren from Geoscience department for assisting me in utilizing not only Field Emission Scanning Electron Microscope, but also for proper analysis and interpretation of the FESEM images.

I gratefully acknowledge Dr. Samad Gharehdaghi, who always brought novel ideas to the table as we discussed my research challenges. His contribution to my Ph.D. degree includes, but is not limited to, encouraging, mentoring, advising, and collaborating throughout all steps of my doctoral research.

Last but not least, I would like to express my deepest and sincerest gratitude to my family and my husband for supporting me spiritually throughout my education and career as well as my life. Special thanks to my mother Keshvar Khanoom Mazinani, and my sisters Fatemeh and Seddighe Jazaei, who not only enlighten my perspective, but also give me courage to challenge my potential. I am forever indebted to my family for providing the opportunity to fulfill my dreams. Without their selflessness and the support that they provided me beyond and above what I expected, I could not have accomplished much.

This milestone is dedicated to my amazing family for the love, care, and support that they provided me as I conducted this research.

# Table of Contents

# List of Tables

# List of Figures

# List of Abbreviations

ACI……..……..…

…. American Concrete Institute

CNT……

……..……. Carbon Nanotubes

FESEM……Field Emission

Scanning Electron Microscopy

HPC……..…

…. High-Performance Concrete

HSC

……..

…. High-Strength Concrete

MWCNTs……

Multi-Walled Carbon Nanotubes

NEC……..

.... Nano-Engineered Concrete

SWCNTs……..….... Single-

Walled Carbon Nanotubes

UHPC……. Ultra-

High-Performance Concrete

# CHAPTER 1 INTRODUCTION

## 1.1 General

Over the last century, researchers have continuously enhanced concrete's mechanical properties, including its toughness. Those efforts have resulted in the creation of three main classes of concrete: high-strength, high-performance, and ultra-high-performance. Despite substantial improvements in engineering properties, brittleness and insufficient toughness still are two weaknesses of cement-based composites. Reinforcing cementitious composite with carbon nanotubes (CNTs) is a promising and effective method to address both problems.

## 1.2 Scope of Research

This research focused on two main mechanical properties of concrete that are drawbacks for concrete structures: tensile and impact strength. Additionally, unpredictable concrete failure is problematic for residents' safety. The scope of this research involves investigating three main effects of reinforcing cement mortar:

1. Developing mixing and dispersion process for three types of carbon nanotubes: multi-walled carbon nanotubes (MWCNTs), single-walled carbon nanotubes (SWCNTs), and hybrid with ratio of 50% of multi-walled and single-walled carbon nanotubes (HCNTs).
2. The effect of reinforcing the cement matrix with multi-walled carbon nanotubes, single-walled carbon nanotubes and hybrid carbon nanotubes on splitting tensile strength.
3. Investigating the failure mechanism of cementitious nanocomposite incorporating multi-walled carbon nanotubes, single-walled carbon nanotubes and hybrid carbon nanotubes under splitting tensile and low-velocity impact test under splitting tensile and low-velocity impact test.

## 1.3 Research Objectives

The aim of this research is to investigate the mechanical properties of concrete with incorporated CNTs to focus on tensile strength and impact strength of cementitious nanocomposites. In particular, multi-walled, single-walled, and hybrid carbon-nanotube concrete specimens were investigated to determine the optimum CNTs mix proportion and the proper mixing technique. These research objectives encompass the following steps:

1. Different mixtures are prepared and tested. The mixtures include three concrete specimens with 0.2, 0.4, and 0.6 percent CNTs by weight of cement and one control mix. Each test is repeated three times. The water-to-cement ratio of 0.4 for impact test specimens and 0.5 for tensile test specimens is used. Cylindrical specimens with 50 mm diameter and 20 mm height are used for impact strength, and cylindrical specimens with 25 mm diameter and 50 mm height are used for tensile strength.
2. A dispersion method and a mixing method are developed with step-by-step procedures.
3. A sonicator is used to disperse multi-walled carbon nanotubes, single-walled carbon nanotubes, and hybrid carbon nanotubes into water solution.
4. The fracture sample is observed using a field emission electron microscope to ensure quality of dispersion.
5. Low-velocity drop-weight impact test and splitting test are conducted to assess and compare tensile and impact strengths.
6. The optimum percentage of multi-walled carbon nanotubes, single-walled carbon nanotubes and hybrid carbon nanotubes that archives the highest strength is identified.

Research plan flowchart shows the important steps of the experimental program in the figure 1

## 1.4 Research Plan

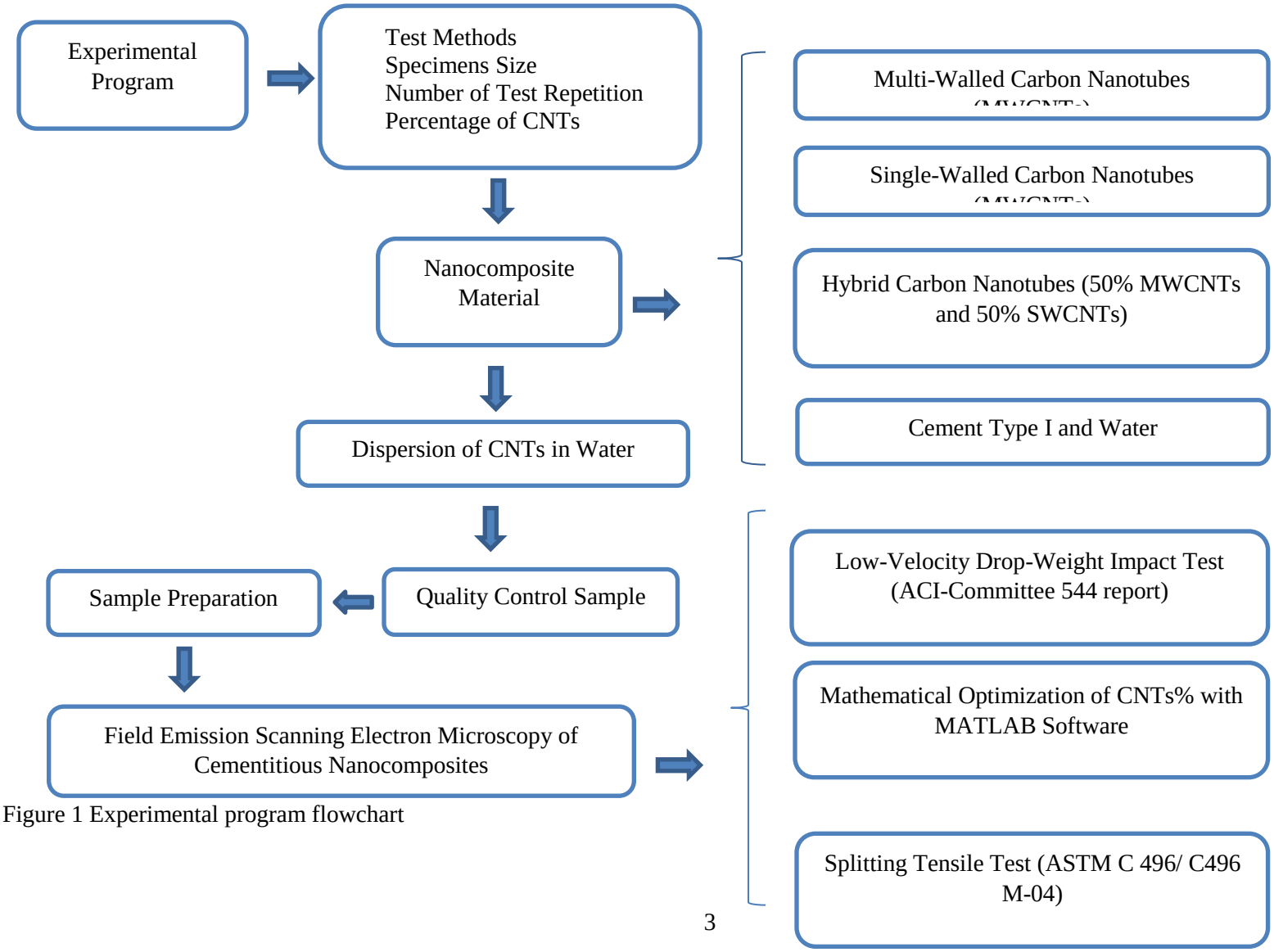


Figure 1 Experimental program flowchart

## 1.5 Organization of the Study

This dissertation consists of six chapters.

**Chapter 1** provides introductory information about motivation, scope, and objective(s) of research. This chapter describes the problem statement and the framework to achieve the experiment's objectives in a general step-by-step procedure.

**Chapter 2** defines carbon nanotubes, provides background, discusses the potential of carbon nanotubes for reinforcing concrete, and includes the literature review. An extensive survey of the relevant existing literature of previous research and technology identifies the knowledge gap that inspired this research.

**Chapter 3** provides the materials and describes the mixing procedure to produce cementitious nanocomposite. It describes the dispersion procedure and specimen preparation for field emission electron microscope observation. This chapter also explains the morphology of carbon nanotubes in cement mortar, then discusses and compares previous research on the effect of dispersion. The quality control of carbon nanotubes' dispersion is a prerequisite for synthesizing carbon nanotubes in cement matrices.

**Chapter 4** focuses on the splitting tensile test procedure and results. This chapter is an assessment and comparison of different cementitious nanocomposite incorporating multi-walled carbon nanotubes, single-walled carbon nanotubes, and hybrid carbon nanotubes. Additionally, the failure mechanism is described and compared to conventional concrete failure mechanism.

**Chapter 5** presents low-velocity impact test procedure according to drop-weight test of ACI report. This chapter also provides the results of an impact test by calculating static energy observation of cementitious nanocomposites. The failure pattern of the impact test is discussed. Additionally, mathematical analysis by MATLAB is provided to optimize the percentage of hybrid carbon nanotubes under impact test.

**Chapter 6** reveals the results, discusses the research findings, and provides suggestions for future research. The potential impact of this research for concrete structures is explained in this chapter as well.

# CHAPTER 2 LITERATURE REVIEW

## 2.1 Introduction

Cement has been largely used in the construction industry, specifically as a matrix for concrete. Conventional concrete turns into High-Strength or High-Performance Concrete (HSC, HPC) by utilizing smaller particle sizes. Even Ultra-High-Performance Concrete (UHPC) has been introduced. However, conventional materials are not able to compete with Nano-Engineered Concrete (NEC) due to the evolution of nanotechnology. Recently, a new generation of cement-based composite that greatly increases mechanical properties has begun replacing conventional concrete.

For over five decades, fibers of all types have been employed to augment the mechanical properties of cement-based composites. Traditional fibers include, but are not limited to, steel, glass, carbon, aramid, basalt, and other natural and synthetic materials. These mechanical properties of conventional cementitious materials are still relatively low due to cement's brittleness and poor bond in cement matrices; however, researchers are trying to enhance tensile strength and impact strength of cementitious composites using a variety of methods.

Periodic advances in the field have led to the development of decreasingly smaller fibers. Very recently, researchers considered particles with high-aspect ratios (length over diameter) and their implications for field. Particles or fibers of miniscule (nanometer) size effectively increased cementitious composite performance. Carbon nanotubes (CNTs) became known 25 years ago. The world of concrete will be revolutionized by this promising material that offers superior mechanical properties. CNTs' high strength, flexibility, and low weight contribute to the excellent quality of cementitious nanocomposites.

Carbon nanotubes (CNTs) became known 25 years ago. The world of concrete will be revolutionized by this promising material that offers superior mechanical properties. CNTs' high strength, flexibility, and low weight contribute to the excellent quality of cementitious nanocomposites.

The application of CNTs in cementitious materials is a newly emerging field. Therefore, the literature in the construction industry is still under development. It is justified then to further investigate CNTs in cementitious nanocomposites. The literature currently available focuses primarily on compression and flexural strength. Although there is not much literature to draw upon in research, some research exists on improving tensile strength of cementitious composite incorporating with CNTs, but there is no evidence of investigation into impact strength.

CNTs' hollow structure and high-aspect ratio causes CNTs to buckle when placed under compressive, torsional, or bending stress. However, standard single-walled carbon nanotubes (SWCNTs) can withstand pressure up to 25 GPa (3626 Ksi) without plastic or permanent deformation. Therefore, investigation of CNT composites is crucial in assessment of CNTs mechanical properties. Of the papers available, the vast majority were presented about the effect of multi-walled carbon nanotubes, but very few investigated single-walled carbon nanotubes, and none of the research compared SWCNTs with both MWCNTs and hybrid CNTs (50% of MWCNTs and 50% SWCNTs) in cementitious composites.

## 2.2 Carbon Nanotubes Definition

A CNT is a miniature cylindrical carbon structure with hexagonal graphite molecules attached at the edges. CNTs are very thin and long. The diameter is one nanometer (one billionth of a meter) and the length is up to several nanometers. Nanotubes look like powder or black soot, but they are actually rolled-up sheets of graphene that form hollow strands with walls that are only one atom thick.

## **2**.3 Single-Walled and Multi- Walled Carbon Nanotubes

The two main types of CNTs are Multi-Walled Carbon Nanotubes (MWCNTs) and Single-Walled Carbon Nanotubes (SWCNTs), both introduced about twenty-five years ago. SWCNTs came into production less than two years after the discovery of MWCNTs [1].

According to the US National Library of Medicine (NLM) and the National Institutes of Health (NIH), the tensile strength of SWCNT is a hundred times greater than steel. SWCNTs perform very well, even under enormous pressure. When an SWCNT is under a high compressive load, it bends, twists, kinks and buckles, but returns to the original structure because of its high elasticity [2]. Three distinct ways in which graphene can be rolled into tube are known as *Armchair*, *Zig-Zag* and *Chiral* [3].

Multi-Walled Carbon Nanotubes can be structurally rolled in two ways: the *Russian Doll* model and the *Parchment* model (See Figure 2) [2]. In the Russian Doll model, the carbon nanotube has additional interior carbon nanotube, and thus the outer tube's diameter is thickened (Figure 2). The Parchment model is similar to rolling up paper and is shown below.

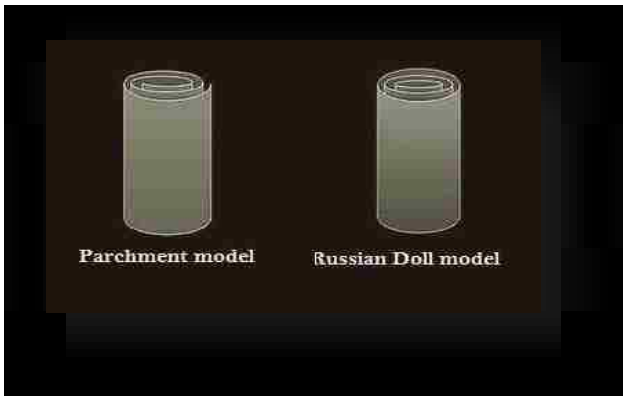


*Figure 2 Structural Rolling Graphene sheet methods [2]*

In civil engineering, newly emerging nanotechnologies have had a significant impact on cementitious concrete properties [4]. CNTs have become popular over the last decade due to their ultra-high enhancement

of tensile strength. CNTs also considerably increase mechanical, thermal, and electrical properties. CNTs have a high-strength stiffness that is three to five times higher than steel.

## 2.4 Potential of Carbon Nanotubes in Construction Industry

Current applications of carbon nanotubes vary across fields, including uses in water purification systems, air filters, solar-cells, fire-protection technologies, polyethylene, sports equipment, synthetic muscles, gene therapy, tissue regeneration, cancer treatment, textiles, and space elevators. Due to the high strength-to-weight ratio of CNTs, they are also extensively used in the aerospace, military, medical, and automotive industries.

CNT use has extended to provide an alternative for rehabilitating existing construction, bridges, and cellular phone antennas, as well as preventing damage, fatigue, or loss of cross section due to corrosion for both concrete and steel structures. Thus, CNTs have proven cost-effective solutions in these fields. However, due to a lack of research, they are not currently applied to cement composites. Thus, the benefits of CNTs have remained out of reach for those working with cement composites. Yet, in this area, potential applications of CNTs could be innumerable, especially if combined with typical cementitious products.

## 2.5 Prior Research Works on Application of CNTs in Construction Industry

In 2012, Sadiq Muhammad investigated the reinforcement of Cement-Based Matrices with graphite nano materials, which included carbon nanotube, nano fiber and graphite nanoplatelet (Figure 3). The aim of Muhammad's study was to evaluate mechanical properties, control micro-cracks, and investigate energy absorption, frictional pull out, and durability of cement nanocomposite. The materials applied were Portland cement type I, silica fume, crushed silica sand, sand, superplasticizer, and nano-material (CNTs, nano fiber, and graphite nanoplatelet) [5].

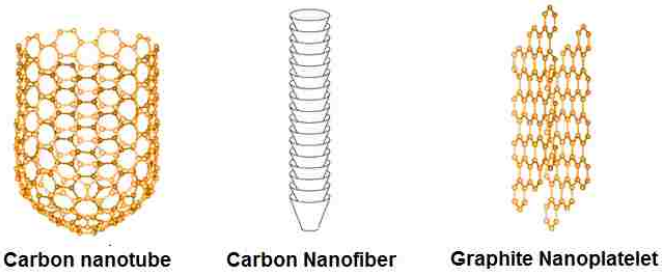


*Figure 3 Carbon nanotubes, carbon nanofiber, and graphene nanoplatelet [5]*

Results showed that MWCNTs had the highest elastic modulus, tensile strength, and thermal conductivity. However, MWCNTs cost more than other nano particles as can be seen in Table 1, below [5].

*Table 1. Typical properties of graphite nanomaterials and carbon fiber [5]*

| Graphite Nanomat. | Length, μm | Dia., nm | Aspect Ratio | Surface Area, $m^2/g$ | Elastic Modulus, GPa * | Tensile Strength, GPa * | Thermal Conductivity, W/m.K * | Cost, $/kg |
|---|---|---|---|---|---|---|---|---|
| MWNT | 20 | 20 | 1,000 | 500 | 1,200 *** | 350 *** | 2,800 *** | 45 ** |
| Nanofiber | 50 | 100 | 500 | 500 | 240 | 3 | 1,950 | 10 **** |
| Nanoplatelet | 3 | 10 | 300 | 100 | 1,000 | ~(10-20) | 250 | 10 ***** |
| CarbonFiber | 1,000 | 7,000 | 140 | 16 | 350 | 3 | 600 | 12 |

** Property measured in basal plane or along length*

*** Mid-term price target*

**** Measurements are 'true' values based on wall cross-sectional area*

***** Mid-term price target- Pyrograf Product Inc; a subsidiary of ASZ*

****** Mid-term price target- XG Sciences*

In 2015, Muhammad Maqbool Sadiq's comprehensive research on cementitious nanocomposite was patented as "Ultra High-Performance Concrete Reinforced with low cost graphite nanomaterials and microfibers, and method of production" (patent US 8951343 B2) [6].

Zhito Chen et al (2016), used 0.67% plasma synthesized carbon nanotubes (p-CNTs) to improve dispersion and flexural strength of Ultra High-Performance Concrete (UHPC) from 12.5 to 21.2 Mpa. The length of

MWCNTs was 10-30 μm with an outer diameter of 10-30 μm and 90-95% purity (Surface area>140-180 m2/g). Greater surface areas create more bonding with cement matrixes. In order to disperse MWCNTs, water was used as a solvent in a 30-minute ultrasonic bath. The results indicated that CNTs stay dispersed up to 3 days [7].

Mohamed O. Mohsen et al (2016), investigated the effect of mixing duration on flexural strength of non-treated MWCNTs (0.03, 0.08, 0.15, or 0.25%) cementitious composites. The length of the MWCNTs were 10-30 μm, the outside diameter, 10-20 μm, and the surface area, greater than 200 m2/g, with 95% above purity. Mixing time durations of 1.5, 15, 30, and 60 minutes were implemented. The results also indicated that the specimen with 0.25% MWCNTs to cement weight fraction with 60 minutes mixing duration provided the greatest increase in flexural strength. SEM pictures provided more detail regarding decreased void in cementitious composite [8].

B.S. Sindu et al (2014), conducted research on the effects of adding MWCNTs [0.093, 0.22, 0.42, 0.72, and 1.2% by weight of cement (%)] with a diameter of 0.1296 μm (E=9.382 TPa and Poisson ratio of 0.3) into cementitious composite (Figure 4). The mixture included Portland cement, water, and MWCNTs. The aim of this numerical (Finite Element Method) research was to analyze cementitious composite for a simply supported beam of 165x26mm, where mechanical properties enhancement was measured [9].

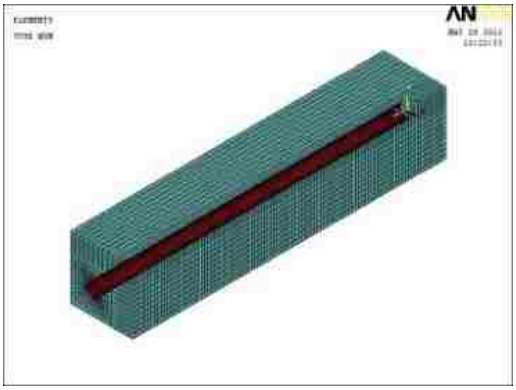

*Figure 4 Quarter model of RVE of cement reinforced with four CNTs [9]*

Mehdi Eftekhari et al (2015), studied the dynamic fracture behavior of CNT Reinforced Concrete under an impact load. This numerical study proved an increase of energy absorption under dynamic load as well as increases in compressive strength (26%), and tensile strength (32%). The depth of projectile penetration was noticeably reduced when CNTs were added to reinforced concrete [10].

In 2012 S.K. Annamalai, researched the effects of using CNTs to seal cracks (Figure 5) and holes in buildings. In a cube sample of concrete, cracks were sealed with two, four, and eight grams of CNT additive, shown in Figure 6. The optimum amount of CNTs was 20% of total sealant. The compressive strength of cube was enhanced up to 37.5% [11].

*Figure 5 Experimental set up for testing of cubes for compressive strength [11]*

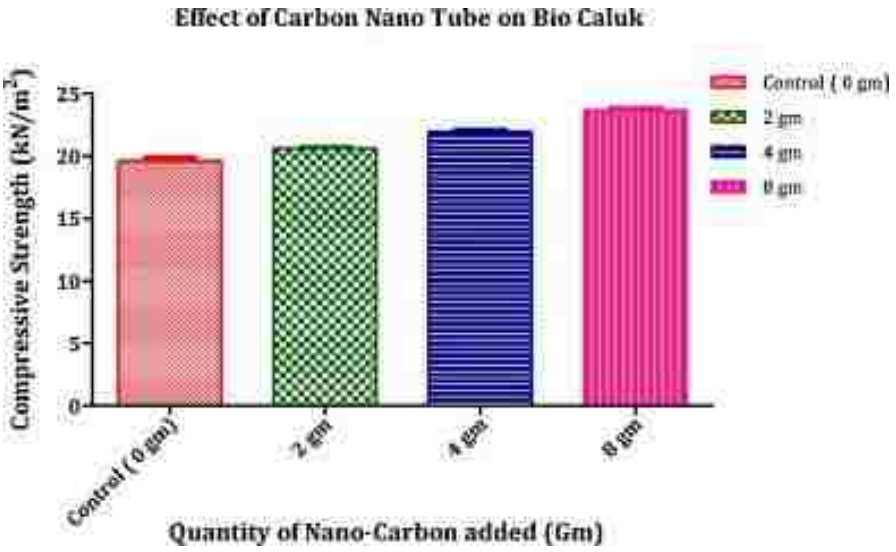


*Figure 6. Comparison of compressive strength of different sealants [11]*

H. Shen et al investigated the impact of functionally graded CNTs composite on Carbon Nanotube Reinforced Concrete (CNTRC) in 2015. Both nonlinear bending behavior and the buckling and vibration response were computationally studied. The results showed that adding 20% CNTs to total mixture improves CNTRC responses to nonlinear bending, buckling, and vibration [12].

H. K. Kim et al (2014), reported that adding 0.1, 0.3, and? or? 0.5% CNTs to cement mortar while decreasing water/cement ratio improves the stability of piezo-resistance (conductivity resistance) under a cyclic load (Figure 7). The mixture included cement, silica fume, crushed sand, water, super-plasticizer, and CNTs [13].

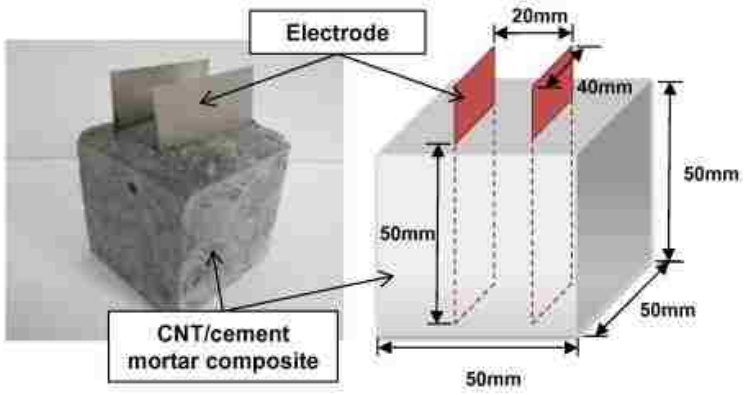


*Figure 7. Conductivity test [13]*

In 2016, G.M. Kim et al investigated the effect on the heating element when CNTs were added to cementitious composite. In this study, 0.1, 0.3, 0.6, 1, and 2% CNT, silica fume, and poly-carboxylic acid base super-plasticizer were mixed. The results showed that using up to 0.6% of CNTs improves heating conductivity. Additionally, the electrical resistivity of CNT embedded cementitious composite related to heat generation capacity. Beyond 0.6% of CNTs, additive electrical resistivity rapidly decreased [14].

*Table 2. Summary of test results in previous studies on electrically conductive concretes [14]*

| Conductive filler | Steel fibers and steel shavings | Steel fibers | Carbon products | Stainless steel fibers and graphite | CNT 0.6% | CNT 2% |
|---|---|---|---|---|---|---|
| Electrical resistivity (Ω cm) | 7500 | 748.33 | 5100 | 400 | 145.2 | 68.1 |
| TI (°C)* | 38.7 | 41.3 | 47 | 25 | 34.6 | 67.8 |
| Heating rate (°C/min) | 0.83 | 1.8 | 1.2 | 0.41 | 2.41 | 7.98 |

*TI (°C): temperature increase from ambient temperature to terminal temperature within 1 hou*

Heyong-Ki Kim (2015) indicated the use of CNTs in cement composite and RC decreases chloride penetration in Figures 8 and 9. The mixture included cement, water, silica fume, super-plasticizer and 0, 0.3, and 0.6% CNT, tested in saturated and dry conditions. The results showed 0.6% CNTs mixture in dry conditions (Figure 10) has minimal conductivity [15].

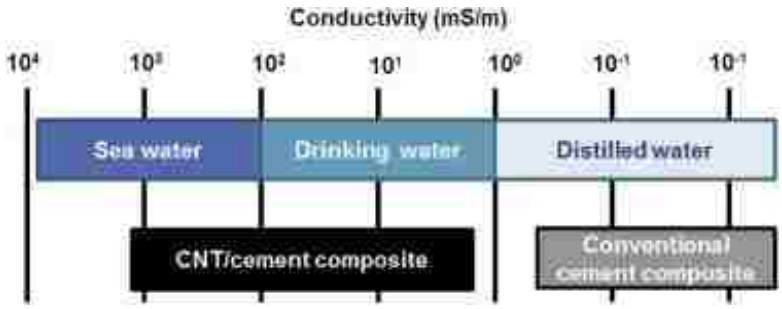


*Figure 8. Conductivity ranges of various types of water and cement composites [15]*

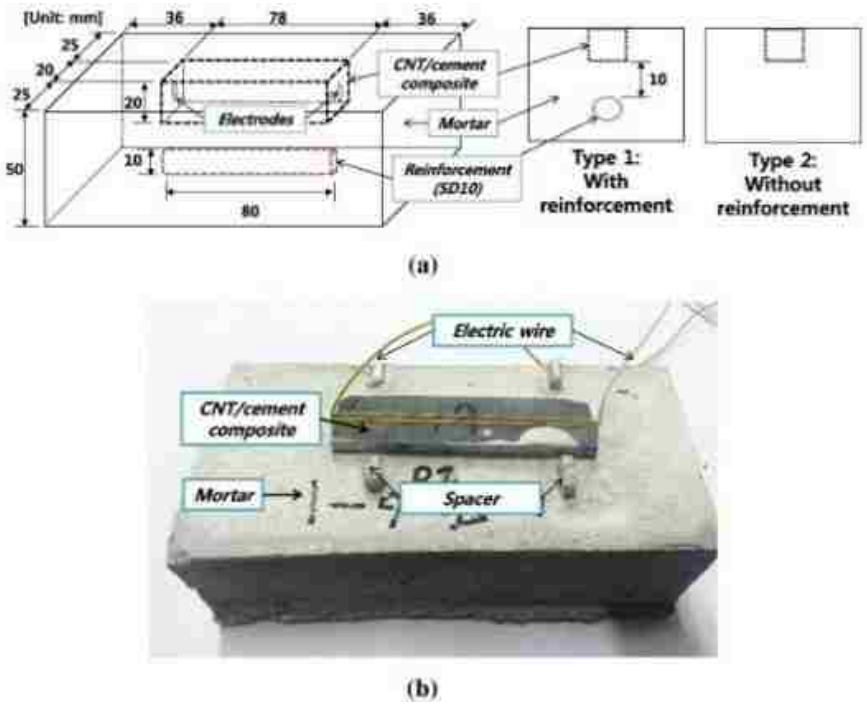


*Figure 9. Specimens for evaluating the effect of reinforcement on conductivity of CNT/cement composites in concrete structure: (a) schematics and (b) actual shapes [15]*

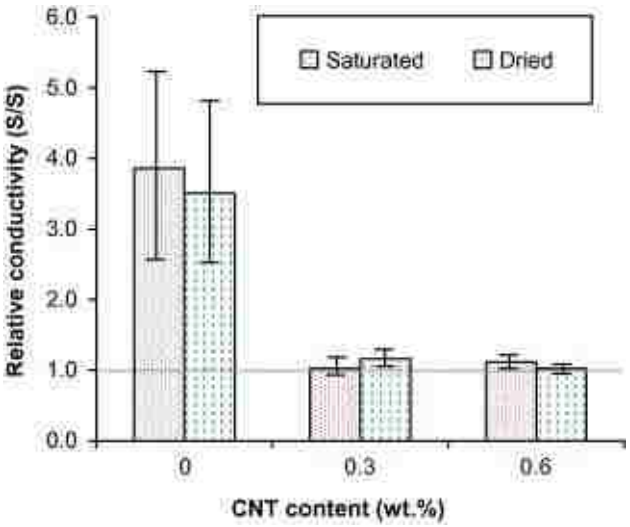


*Figure 10. Relative conductivities of CNT/cement composites embedded in cement mortar with reinforcement [15]*

H.K. Kim, 2014, conducted research on the effect of improving dispersion of CNTs by adding silica fume. The findings indicated an enhancement in mechanical and electrical properties in cement composite. The mixture contained CNTs that were 0, 0.15, 0.3% by weight of cement and 0, 10, 20, and 30% silica fume by weight of cement [16].

Rafat Saddique et al, 2014, reported a review paper on CNTs properties compared to plain cement paste. The summary of collected papers discussed the improvements of CNT composite (either cement mortar or concrete) compared to other classes of concrete. The CNT composite demonstrated denser micro-structure to control shrinkage and provided higher Young's modulus, higher flexural strength, higher compressive strength under high strain loading, and a good interaction between CNTs and fly ash in cement matrix as a filler [1].

Peter Synoski et al, 2015, investigated the improvement of mechanical fracture of cement mortar containing Portland cement, silica fume, and plain MWCNTs, MWCNTs treated (Length of 0.5-40 μm and diameter of 20-40 μm), and silica carbon nanotubes groups. The silica functional groups increased cement hydration

in the first 24 hours. Moreover, fracture toughness and frictional bond between matrix and reinforcement was enhanced [17].

I.W. Nam et al, 2012, investigated the influence of Silica Fume (SF), nylon fiber, and super-plasticizer incorporated with MWCNT cement composites on Electromagnetic Interference Shielding (EMISE). Electromagnetic Interference (EMI) is concerned with the amount of electromagnetic waves that are either absorbed or reflected. It causes the growth of tumors in the human body, so the composite material in the study provides protection from harmful electromagnetic waves. The frequency range of 45 MHz-18 GHz was used in the study. MWCNTs with 0, 0.3, 0.6, and 1% weight of cement and purity of 96.2% and SF of 0, 10, 20, and 30% by weight of cement SF were tested. The results in Figure 11 showed that adding 0.6 wt% of MWCNT and 20 wt% of SF to cement matrix improves EMISE [18].

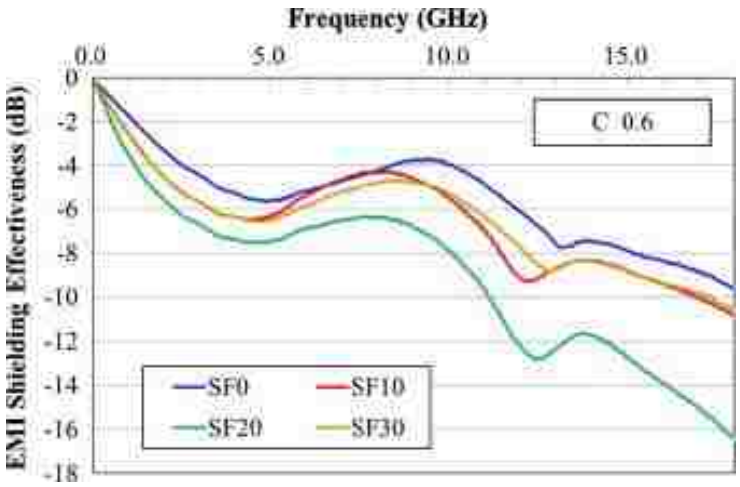


*Figure 11. EMI shielding effectiveness of specimens where 0–30% SF has been added to cement matrices to which 0.6 wt. % MWCNT has been added [18]*

Kean-Khoon Chew et al, 2011, conducted research on the reinforcement of Calcium Phosphate Cement (CPC) composite with MWCNTs and Bovine Serum Albumin (BSA) for injectable bone. The MWCNTs were functionalized CNTs (MWCNTs–OH and MWCNTs–COOH, diameter of 30–50 nm and length of ≈30 μm). CPC incorporated with 0.5wt% MWCNTs and BSA showed the highest compressive strength. In this paperthe authors investigated compressive strength, among other mechanical properties, but structural

characterization tests included scanning electron microscopy (SEM), X-ray diffraction (XRD) analysis, and Fourier transform infrared (FTIR) spectroscopy was used to determine crystalline structure of composite, specific surface functional groups in Figure 12.

In order to measure how injectable the composite matrix was, a 10-mm syringe was filled with CPC paste. *Injectability* was qualitatively assessed and evaluated by extruding the paste through a disposable syringe, and then calculated from the equation below:

Percentage of CPC extruded paste= Mass of extruded CPC paste/ Original mass of CPC paste inside the syringe *100[%].

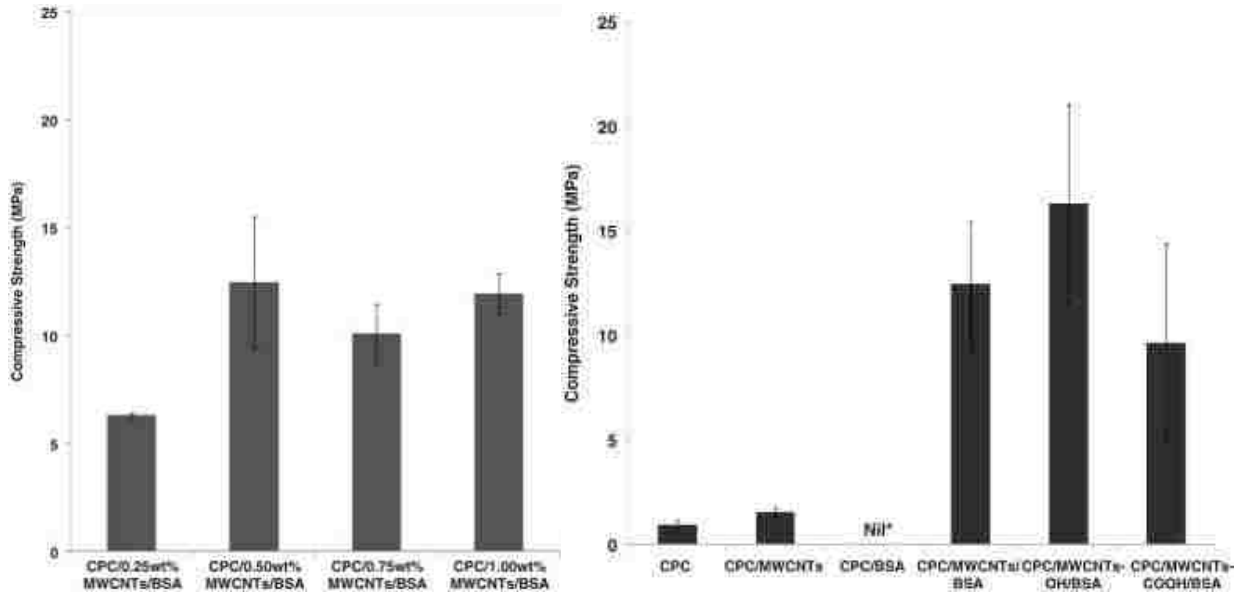


*Figure 12. The comparison of compressive strength value of CPC/MWCNTs/BSA composites containing different percentages by weight of pristine MWCNTs. All composites have a BSA content of 15 wt%. Data are presented as mean ± 1 standard deviation [19]*

After injection of the composite paste, bone defects and miniscule pores and cracks were filled. The results demonstrated that the mechanical properties of the composite were significantly improved. Not only did matrix injectability improve, but compressive strength of the composite increased to 16.3 Mpa. Pristine

MWCNTs, hydroxylated MWCNTs (MWCNTs–OH), and carboxylate MWCNTs (MWCNTs–COOH) with a diameter of 30–50 μm and length of ≈30 μm were used in the test [19].

Mehdi Eftekhari et al, 2016, conducted numerical research on the nonlinear behavior of CNT-reinforced Calcium Silicate Hydrate (C-S-H) composite with a focus on its structure. The CNT models used were *Armchair* and *Zigzag*, where the study showed that the tensile, compressive, and shear strengths of the Armchair CNTs are higher compared to Zigzag CNTs. However, the Armchair has less interfacial resistance than Zigzag CNTs (Figure 13). Higher interfacial resistance between CNTs and composite allows efficient bridging behavior between cement and CNT reinforcements and prevents crack propagation.

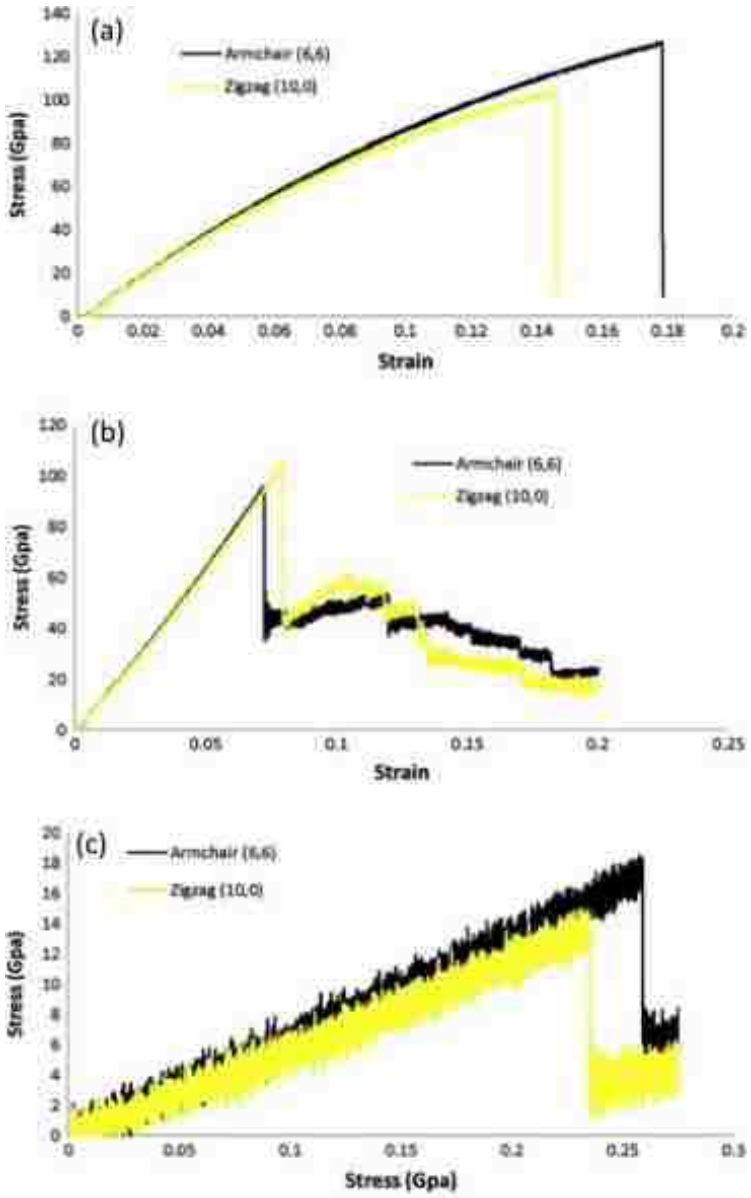


*Figure 13. Stress–strain curves of CNT, (a) tensile, (b) compressive, (c) shear. (For interpretation of the references to colour in this figure legend, please refer to the web version of this article.) [20]*

*Table 3. Mechanical strengths for the CNT [20]*

| Models | Tensile strength (Gpa) | Compressive strength (Gpa) | Shear strength (Gpa) |
|---|---|---|---|
| Armchair (6,6) | 126.71 | 95.96 | 18.51 |
| Zigzag (10,0) | 104.74 | 105.14 | 14.94 |

The numerical analysis determined tensile strength of composite in the Z direction to be up to 6 GPa, which allows CNTs' bridging to function efficiently (Figure 14 and 15). CNTs composite bridge cracks can be seen in the Figure 14. Additionally, shear strength in a silicate layer plan is twice as strong as any other plan. However, in higher ranges of compressive stress (compressive strain about 0.025), local buckling occurs to CNT particles. This is caused by a compressive strength reduction [20].

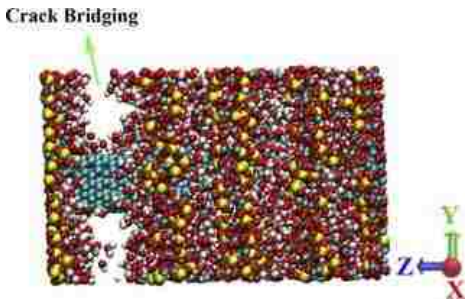


*Figure 14. CNT crack bridging behavior in CNT-reinforced C–S–H. (For interpretation of the references to color in this figure legend, refer to the web version of this article.)[20]*

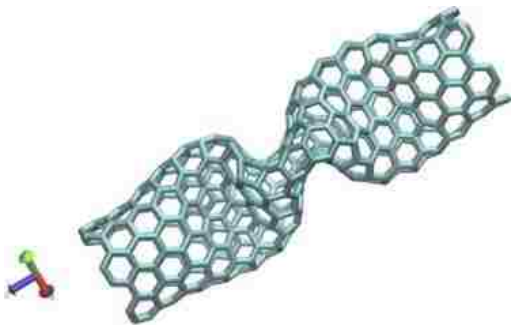

*Figure 15. Local shell buckling of CNT in the C–S–H medium (the C–S–H atoms are removed for clarity). (For interpretation of the references to color in this figure legend, refer to the web version of this article.)[20]*

Mehdi Eftekhari et al, 2014, investigated the hydration model of CNT-reinforced concrete through numerical research. The findings (Figure 17-19) indicated that fracture energy of concrete with longer CNTs increased. Moreover, the propagation of cracks was lower (Figure 16), while the Modulus of elasticity and Poisson's ratio did not improve [21].

*Table 4. Geometrical properties of CNTs [21]*

| Type | Diameter (Å) | Length/diameter |
|---|---|---|
| Armchair (10, 10) | 6.78 | 14.75 |
| Zigzag (17, 0) | 6.65 | 15.04 |
| Armchair (10, 10)/(15, 15) | 10.17 | 9.83 |
| Zigzag (17, 0)/(26, 0) | 10.18 | 9.82 |

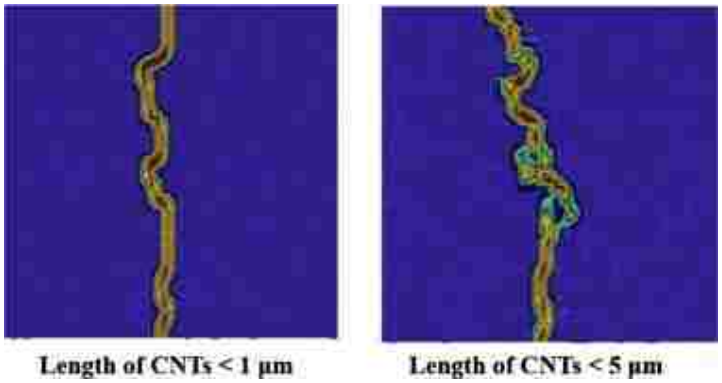


*Figure 16. Crack pattern in samples with different CNT length [21]*

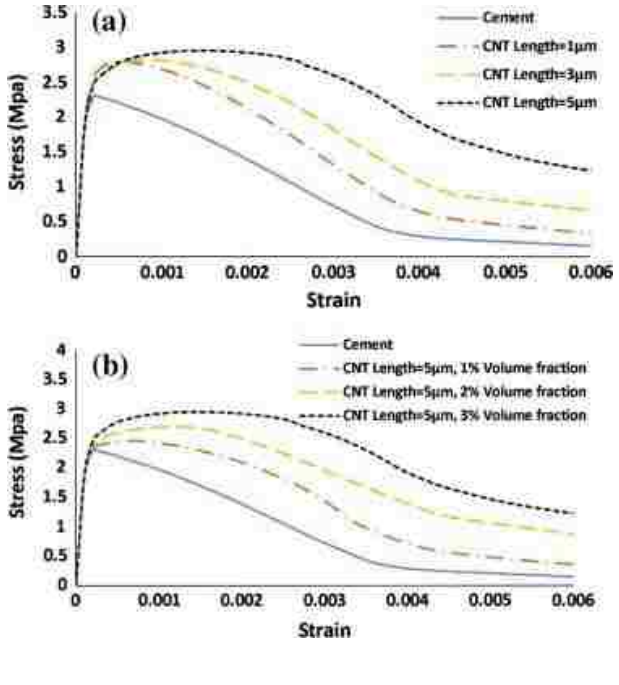


*Figure 17. Stress–strain curve for the cement and CNT-reinforce cement; (a) 3% CNT volume fraction and (b) CNT with the length of 5 µm [21]*

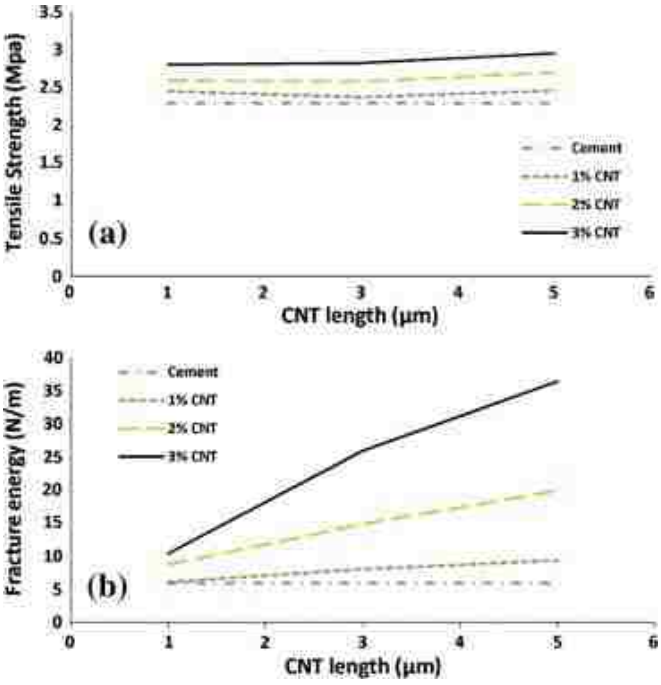


*Figure 17. Tensile strength and (b) fracture energy of the CNT-reinforced cement [21]*

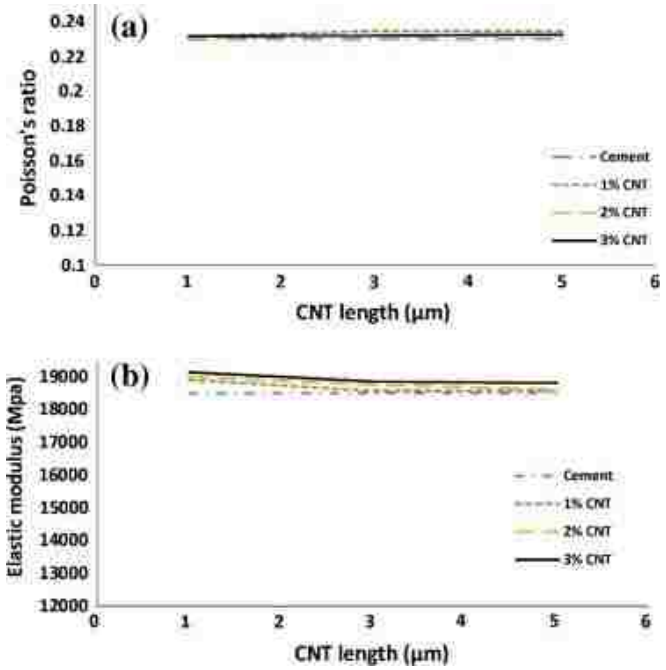


*Figure 18. (a) Poisson's ratio and (b) elastic modulus of the CNT-reinforced cement [21]*

## 2.6 Previous Research on Scanning Electron Microscope

Improving properties of cementitious nanocomposite for mechanical engineering purposes is influenced by the quality of carbon nanotube dispersion. The more uniformly the carbon nanotubes are dispersed, the stronger the engineering properties of the composite. However, it is challenging to assess uniformity of carbon nanotube dispersion. Therefore, the dispersion of CNT in cementitious nanocomposite should be evaluated before producing a specimen. In this research, to ensure minimum CNT agglomeration and maximum dispersion, two prototype samples were made for assessment by a non-destructive test.

Two classes of electron microscopes include Scanning Electron Microscope (SEM) and Field Emission Electron Microscope (FESEM). However, FESEM provides images with higher resolution and magnification especially for cementitious nanocomposite as CNTs are dominated by cement crystals, and so that class of microscope was used.

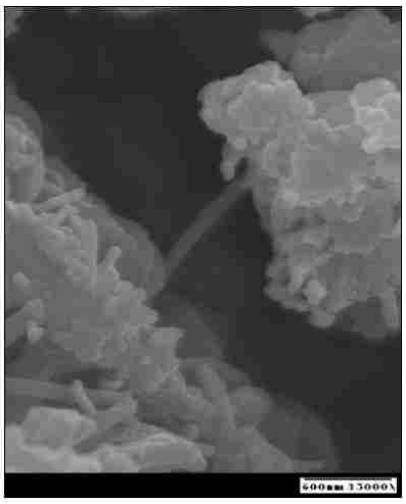

*Figure 19 SEM image showing CNT holding cement compounds [22]*

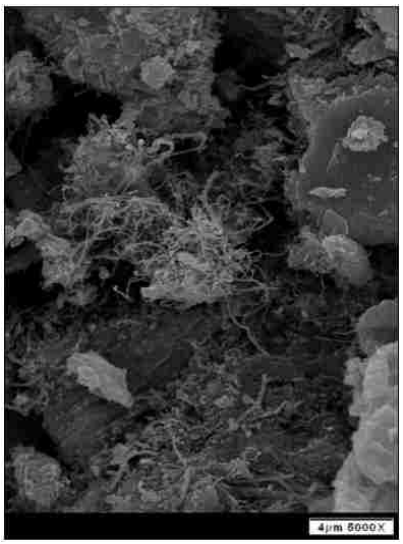

*Figure 20. SEM micrographs of fracture surface of (a) cement/CNT composite containing 0.05 wt% original CNTs; (b) cement/PVA/a-CNT composite containing 0.05 wt% a-CNTs and 0.5 wt% PVA; (c) Zoomed SEM image of the box region in (b) (W/C = 0.3 and maintain [22]*

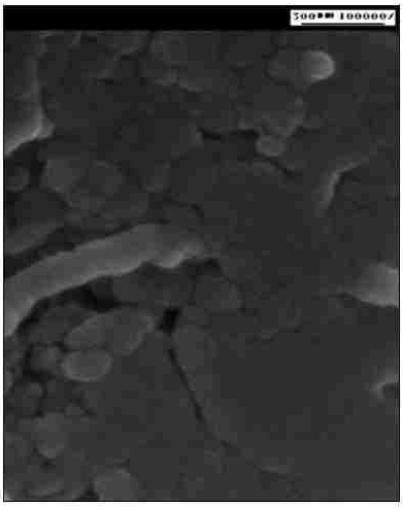

*Figure 21. SEM images of different samples. a: CPC power of sample 2; b: fracture surface of CPC sample 9 after setting; c, d: morphology of RGO on the fracture surface of sample 2 after setting; e: morphology of RGO on the fracture surface of sample 6 a[22]*

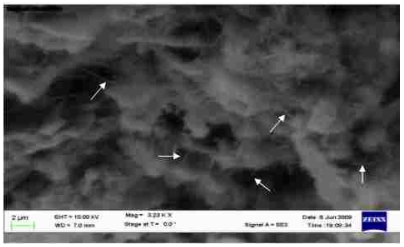

*Figure 22. The agglomeration of CNTs [7]*

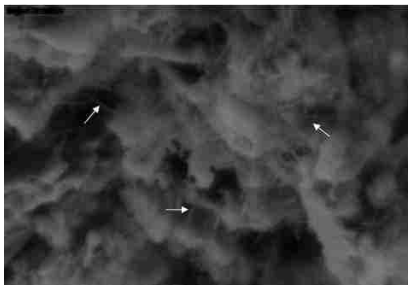

*Figure 23. SEM image of 0.03% CNT/cement specimen [8]*

*Figure 24.SEM image of dispersed MWCNTs in water [26]*

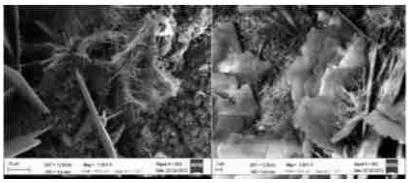

*Figure 25. MWCNT agglomeration in cement hydrates [26]*

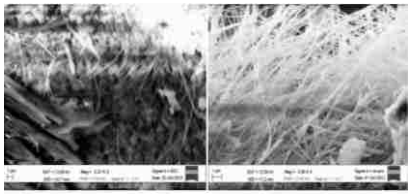

*Figure 26.(a) SEM and (b) TEM images of MWCNTs [25]*

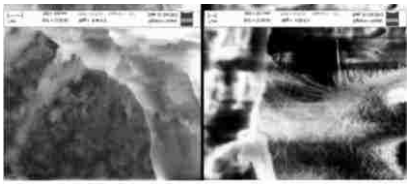

*Figure 27.Close spacing of nanomaterials within the matrix [5]*


*Figure 28. Dense matrix [5]*

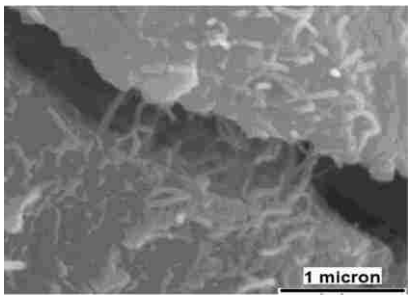


*Figure 29.Uniform dispersion of nanotubes within the matrix [5]*

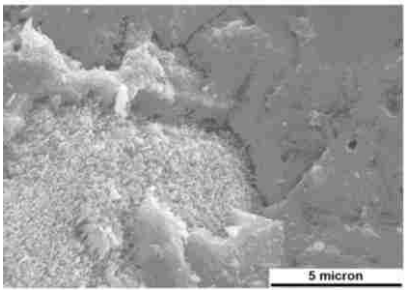


*Figure 30. Arrest and deflection of a micro-crack by a bundle of cnfs within the cementitious [5]*

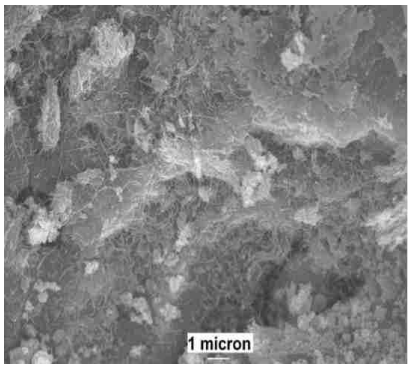


*Figure 31. Bridging of micro-cracks by acid-functionalized graphite nanomaterials introduced into cementitious matrices at 0.08% volume fraction [5]*

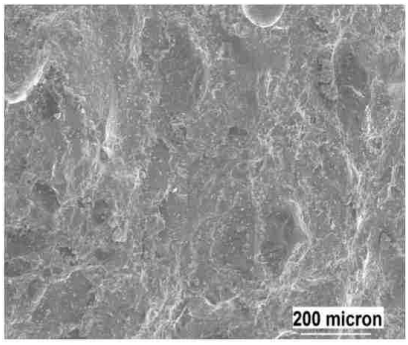


*Figure 32. Functionalized MWCNT B, and SEM images of the fractured surface of a cementitious matrix with 0.04 vol.% of functionalized MWCNT [5]*

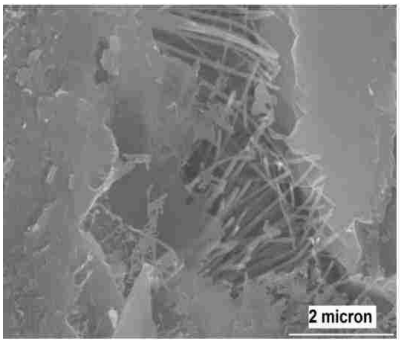


*Figure 33.(a) 0.1% CNF Cement composite with 0.5 w/c and (b) 0.2% CNF cement composite with 0. 5w/c [24]*

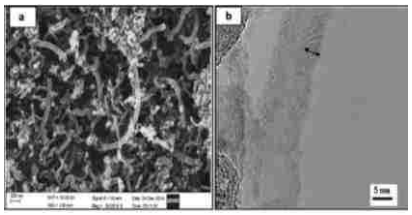


*Figure 34 (a) 0.1% CNF Cement composite with 0.45 w/c and (b) 0.2% CNF cement composite with 0.45w/c. Mohanam, [24]*

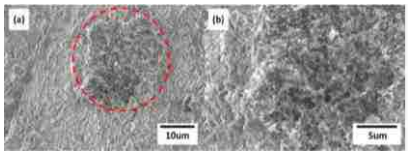


*Figure 35. (a) 0.1% CNF Cement composite with 0.40 w/c and (b) (b) 0.2% CNF cement composite with 0.40w/c. Mohanam, [24]*

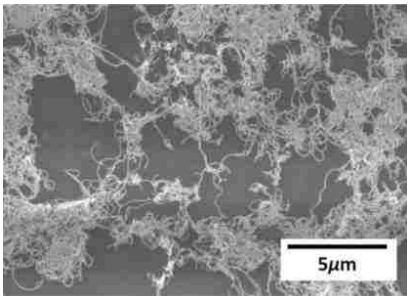


*Figure 36 SEM images of 28-day crushed [23]*

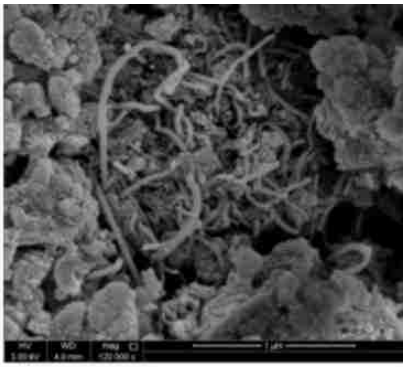

*Figure 37 CNTs dispersion within cement matrix [23]*

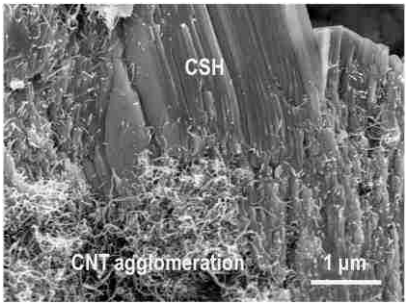


*Figure 38 CNTs dispersion within cement matrix [23]*

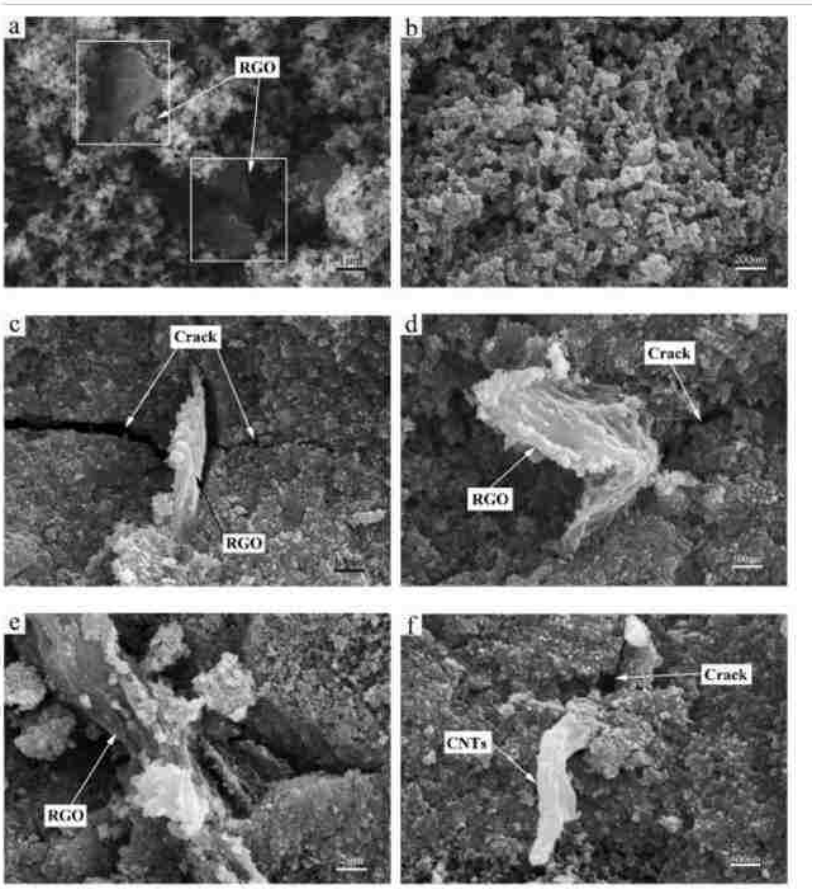


Figure 39 CNT embedded in cement matrix. [22]

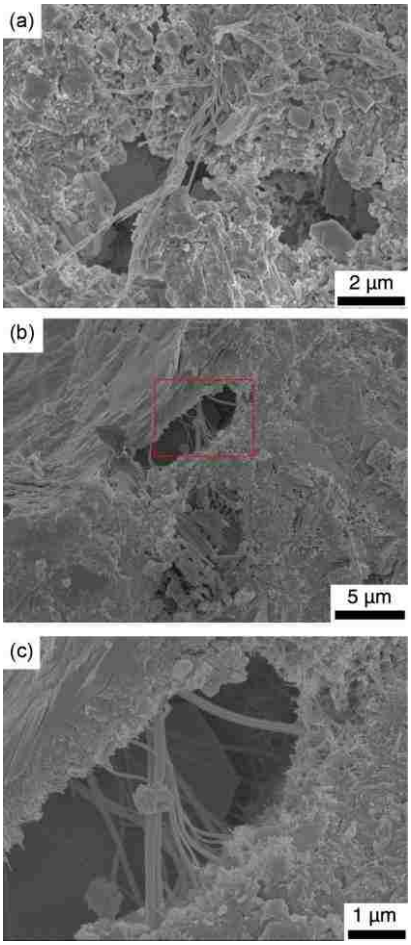


Figure 40 Dispersion of a 1% CNTs in cement matrix [22]

## 2.7 Literature Review Summary and Gaps

The above literature review indicates:

1. Preliminary studies show the potential of CNTs in increasing mechanical properties of cement-based composites. However, not all aspects of nanocomposites have been investigated. Some research consists of basic studies with an emphasis on improving cementitious composite.
2. Almost all studies focused on MWCNT, not SWCNT.
3. Much numerical research used Final Element Method (FEM), but was not validated through experimentation. Instead, the models were simulated using a simple cubic model or beams with rebar.
4. None of the research has examined a hybridization of MWCNT and SWCNT.
5. Dispersion is a serious issue in mixing CNTs, but it was neglected in the literature.
6. Particle size, distribution, and the amount of super plasticizer is not emphasized in any of the studies.
7. There is little research on the effect of CNTs on mechanical properties of cement-based composites, while there are a large number of studies on the thermal and electrical conductivity of CNTs [58].
8. Some of literature compares different nano-fibers and MWCNT.
9. Comparisons were made between different treated MWCNTs.
10. The only hybrid system studied used MWCNTs and microfibers.
11. The optimum percentage of CNTs varied from 0.01% to 2.00% in previous studies

# CHAPTER 3 PROCEDURE

## Phase I Study: Dispersion Procedure of Carbon Nanotubes, Cementitious Nanocomposite Mixing Method, Prototype Sample Assessment with FESEM

## 3.1 Introduction

Despite the exceptionally high strength and outstanding mechanical properties that CNT additives provide for cement-based composite, there are still two obstacles that must be overcome to reach maximum potential strength of carbon nanotubes reinforcement.

The first issue is that CNTs tend to bundle and adhere together because of Van der Waals forces. The second issue is that CNTs are considered hydrophobic material and do not disperse in water because they are not able to interfacial bond with cement matrix. Therefore, the most challenging part of producing cementitious nanocomposite is dispersion of carbon nanotubes in water and bonding water and carbon atoms to achieve a homogeneous liquid for the cement matrix.

Contemporary methods for simultaneously achieving high dispersion and de-agglomeration includes using ultrasonic technique and using functionalized CNTs. Many researchers used Carboxylate acid functionalized carbon nanotubes, various solvents; centrifuge stirring CNTs, and heating after sonication of CNT to increase dispersion effectiveness and enhancement. In fact, the covalent bond between CNTs' sidewall and chemical functionalization increases bonding between CNTs and the composite matrix. In this research both methods were utilized to discern the best outcome.

## 3.2 Materials Used

### *Single-Walled and Multi-Walled Carbon Nanotubes:*

In this study, Single-Walled (SWCNTs) and Multi-Walled Carbon Nanotubes (MWCNTs) for Research and Development (R&D) were used because compared to R&D CNTs, the higher tendency of entanglement for commercialized CNTs causes the CNT dispersion process to be more challenging. The SWCNTs' and MWCNTs' properties are shown in Table 5.

*Table 5. Physical attributes of all SWCNT and MWCNT*

| Type of Carbon Nanotubes | SWCNTs | MWCNTs | Dimension |
|---|---|---|---|
| OD (outside diameter) | 1-4 | 30-50 | nm |
| Length | 5-30 | 10-20 | nm |
| Purity | >90wt% | >95wt% | - |
| Ash | <1.5wt% | <1.5wt% | - |
| SSA (specific surface area) | >407 | >60 | m^2/g |
| EC (electrical conductivity) | $10^2$ | $10^2$ | s/cm |

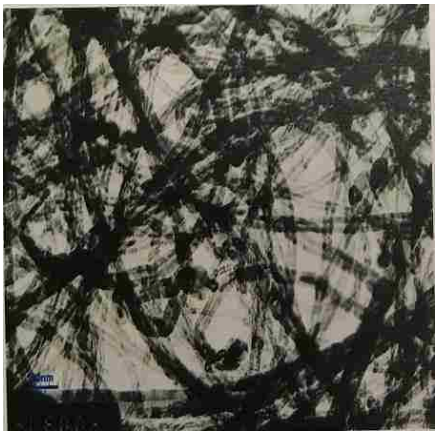

*Figure 41. Transmission Electron Microscopy (TEM) image of MWCNTs with purity of greater than 95wt % with 30-50 nm OD (Source: Cheap Tubes)*

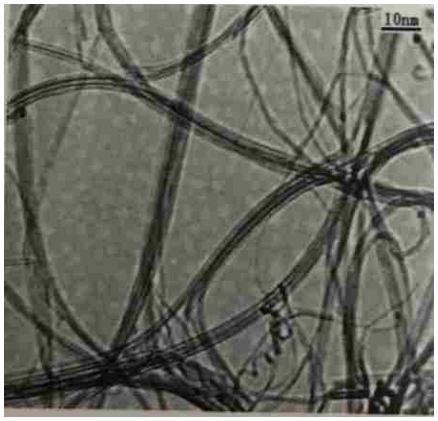


*Figure 42. Transmission Electron Microscopy (TEM) image of SWCNTs with purity of greater than 90wt % with 1-4 nm OD (Source: Cheap Tubes)*

To assess the effect(s) of MWCNTs and SWCNTs and to eliminate other contributors' additives in nano-cementitious composite's mechanical properties, neither additives nor superplasticizer was added to the matrix.

Nanotubes with aspect ratio >>1 are considered one of the best reinforcements to compensate for strength reduction. By using graphene to enhance mechanical properties makes carbon nanotubes the best candidate for cementitious-composite reinforcement [28]. Carbon nanofibers also offer a bridge effect, incorporating carbon nanotubes to facilitate conductivity within the composites [29-31].

## *Mixing Cement:*

Ordinary Type I Portland (ASTM C150) cement was used in this experiment. The cement was stored in the lab in an air-tight plastic container to avoid hydration of cement in the lab. Type I cement contains 50% C3S, 24% C2S, 11% C3A, and 8% C4AF.

## *Mixing water*

For this experiment, filtered water from the Science and Engineering Building at the University of Nevada, Las Vegas was used as water mixture.

## 3.2 Mixing Technique

To achieve high dispersion and stabilization, modification of the dispersion process occurs throughout the making of quality control samples. The following steps demonstrate the dispersion procedure:

### *Scale materials*

The small amount of CNTs should measure accurately due to light weight of CNTs and usage percentage. The scale used to measure CNTs was METER AE 200, which was calibrated with analytical balances division of 0.0001gram. The calibration process and tools are shown in Figure 43.a and 43.b.

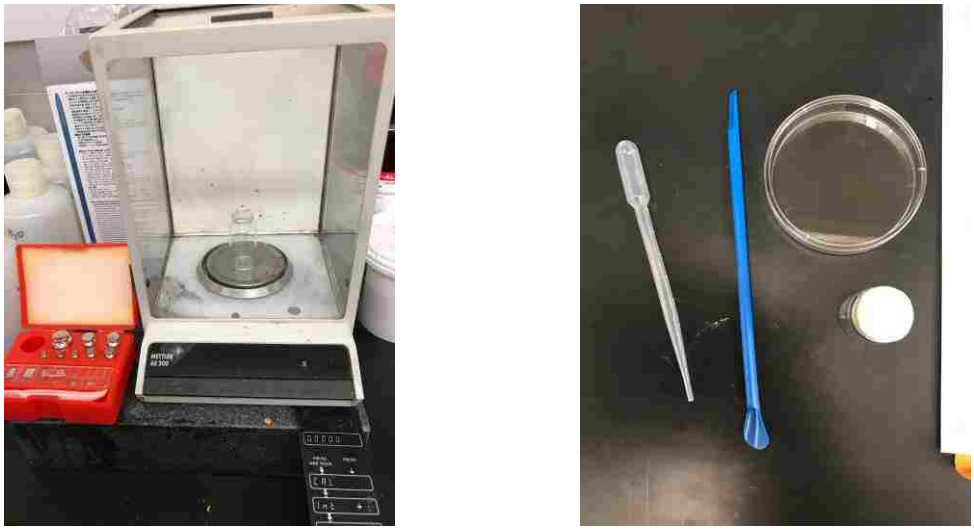

(a) (b)

*Figure 43. a) Scale CNTs with METER AE 200 b) Tools to measure the small amount of water and CNTs*

### *Mixing carbon nanotubes with water*

Water was scaled separately (Figure 44a), and then required CNTs were added gradually (Figure 44b). A water-to-cement ratio of 0.4 was used for impact test specimens, and one of 0.5 was used for tensile test specimens.

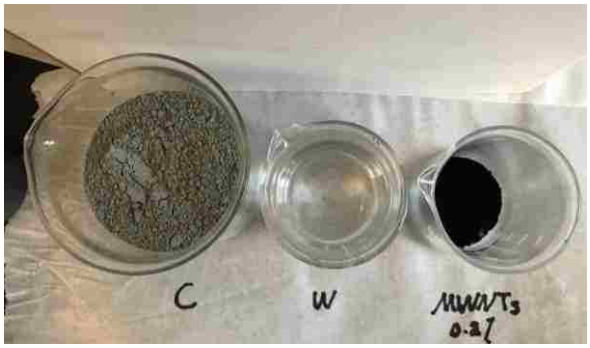


(a)


(b)

*Figure 44. (a) Cement, water, and multi-walled carbon nanotubes were scaled (b) MWCNTs were gradually added to water*

## *Stirring and Functionalized CNTs*

Manual stirring of SWCNTs and MWCNTs with water creates an unstable mixture as shown in Figure 46a; after a few minutes, the carbon nanotubes are deposited Figure 46b. The CNTs used in this research are COOH (carboxylate group) functionalized CNTs provide a hydrophilic surface for CNTs, which makes for better dispersion in water [31]. Additionally, after dispersion of COOH-group CNTs, the matrix is stable for a longer time.


(a)


(b)

*Figure 45. Manual stirring CNTs within water (a) After mixing (b) After 5 minutes*

## *3.4 Dispersion Method*

The most challenging part of producing cementitious nanocomposite is dispersion of carbon nanotubes, especially SWCNTs compared to MWCNTs, because of Van der Waals forces among them. In theory, uniform dispersion of MWCNTs and SWCNTs is required to achieve high potential of carbon nanotubes. However, there is no standard procedure to disperse carbon nanotubes. The most commonly used method is to produce well-dispersed carbon nanotubes using ultrasonic vibration energy [32] to split up bundles of carbon nanotubes. Therefore, mechanical agitation is needed for proper CNT dispersion. Ultrasonic high-frequency sound waves were used with programmable QSONICA Q500 [33-36] sonicator (Fig 46). Sonication of CNTs overcomes the bonding force and break down intermolecular bonds and allow water to react with CNTs. However, excessive use of ultrasonic energy may damage the carbon nanotubes structures and decrease CNTs' desirable properties.

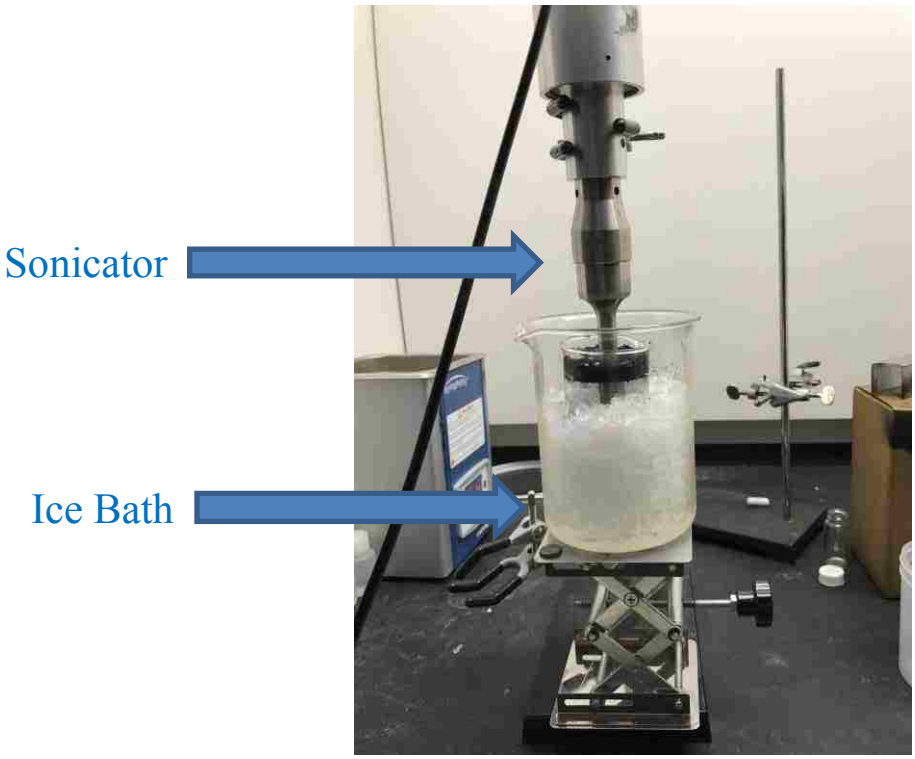


*Figure 46. Sonicators (QSONICA Q500)*

The chemical reaction of CNTs and water under ultrasonic mixture generate considerable heat energy. Therefore, an ice bath is required to prevent rapid evaporation of mixture during sonication process (Figure 47a).

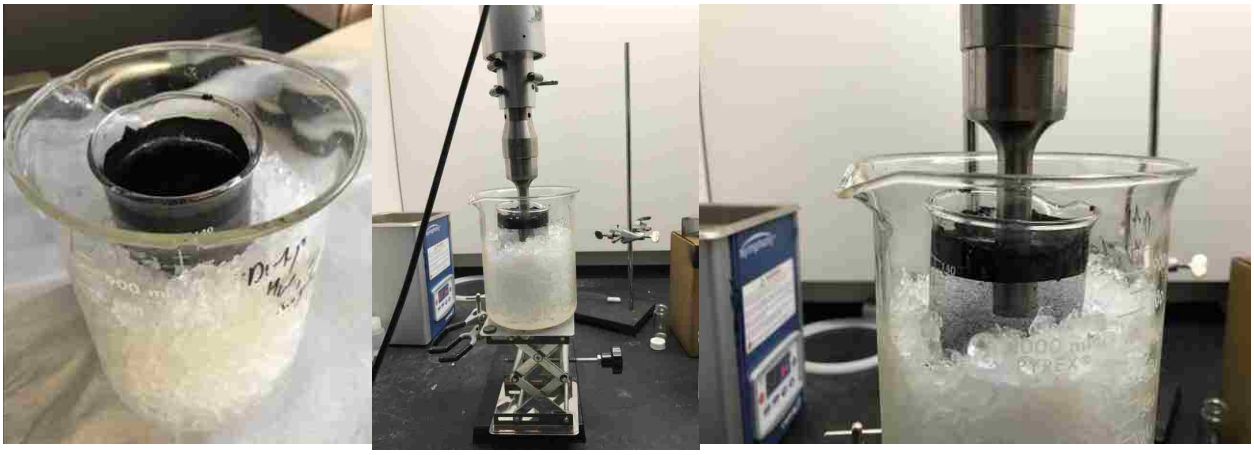

(a) (b) (c)

*Figure 47. (a) Ice bath (b) and (c) Adjusting sonicator probe*

### *3.4.1 Program Sonicator*

Time and amplitude were set to 20 minutes and 30% relatively. The total time of sonication was an hour (three 20-minute cycles). Due to high energy of the sonicator, the ice bath must be replaced regularly. An adjustable pulse time was programmed to be on for three seconds and off for two seconds to prevent excessive heat buildup. An elapsed time indicator recorded the amount of time the dispersion process took to complete (Figure 48).


*Figure 48. Misonix Q500 sonicator adjust energy, pulse, amplitude and time*

Before all the ice in the ice bath has melted, a new ice bath is applied during sonication of carbon nanotubes. The sonicator probe must be under water to disperse the carbon nanotubes (Figure 48b and c). As ice begins melting during the sonication process, the probe may be placed outside the matrix, especially when a larger amount of carbon nanotubes disperses (Figure 49). Additionally, SWCNTs release more heat energy during the sonication process, and an ice bath may need to be applied several times. The final dispersion product is a homogeneous black liquid that is stable for approximately three days (Figure 50).

*Figure 49. Melted ice bath and application of new ice bath*


*Figure 50. Dispersed multi-walled carbon nanotubes after an hour sonication at amplitude of 30%*

## *3.4.2 Mixing Cement with Dispersed Carbon Nanotubes*

Adding carbon nanotubes decreased the setting time for cementitious composite due to accelerating cement hydration. The specimens of this experiment scaled down so mechanical mixtures could not be utilized. Additionally, a standard mix procedure from ASTM and/or ACI has not provided a procedure for nanocomposite. Manual mixing of dispersed carbon nanotubes and cement had to be completed in 1to 2 minutes due to the quick hardening of cementitious nanocomposite matrix. Additionally, a control mix was produced without any CNTS for comparison purposes.

*Figure 51. Mixing disperse carbon nanotubes with cement*

### *3.4.2.1 Molding procedure:*

In accordance with ASTM C 109, after casting the cement mortar, the side of the cement mortar was tapped lightly to allow air bubbles to raise to the surface of cement mortar and break to avoid any void in the hardened cement mortar. The impact mold was cylindrical, with a 50-mm diameter and 20 mm height. The tensile mold was also cylindrical, with a 25-mm diameter and 55 mm height. The cementitious nanocomposite matrix was placed into a mold in two equal levels for impact specimens and three equal levels for tensile specimens. Air bubbles in carbon nanotube mixtures cause void and diminish strength in cementitious nanocomposites, so to remove air bubbles through the cement matrix, a small steel rod was jabbed into each layer, and the molds were tapped 3to 4 times after each layer was jabbed. The top of cementitious nanocomposite cylinder was struck off with the rod.

### *3.4.2.2 Orbital shaker:*

To shake, stir, and make the cementitious nanocomposite mix homogeneous, an orbital shaker VWR OS-500 (Figure 52a) was used for 10 minutes at a speed of 4. This shaker facilitated air bubble travel to the composite surface (Figure 52b and c).


(a)

(b)

(c)

*Figure 52 (a) Shaker VWR OS-500 (b) air bubble came to the mixture surface (c) shaking nano-cementitious specimens orbitally*

***3.4.2.3 Curing Procedure:***

All molds were capped, marked, and placed in ambient temperature until the cementitious nanocomposite mix was set up. After 24 hours, the specimens were unmolded in compliance with ASTM C 192 [34-35].

*Figure 53. Impact and tensile cementitious nanocomposite specimen curing*

## 3.5 Sample Preparation for Field Emission Scanning Electron Microscopic

## Step 1-Desiccating Process

Sample preparation is one the most important aspects of microscopy investigation. Peroration of fractured quality control samples of cementitious nanocomposite with desiccator were completed before FESEM. This process helps to remove all air molecules out of the electron's path during FE scanning with an electron microscope. When the specimen contains moisture in some spots, the FESEM image is darker, as shown in Fig. 54a, but Fig. 54b captured a clear image from a dried sample**.**

*Figure 54. a) Fractured specimen b) drying in desiccator*

Additionally, to check the dispersion in hardened prototype specimen for the FESEM test, the specimen should be fractured in small pieces because a broken surface provides a better absorption opportunity for CNTs. Cement crystals often grow on the surface of specimen (Figure 56).

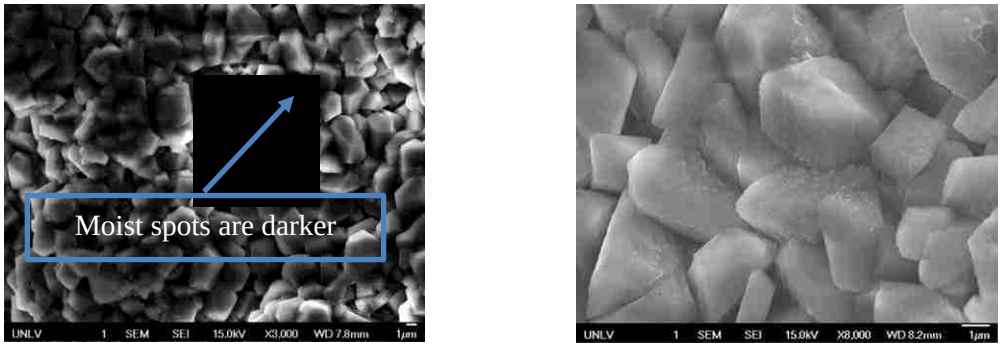


(a) (b)

*Figure 55. FESEM of cementitious composite surface crystals (a) contained some moisture (b) dried nano sample*

## Step 2-Gold Coating of Specimen

The electron microscope is based on electron discharge; therefore, the specimen must be dried to produce a clear image. Non-conducting materials such as cement generate a charge on the surface and disturbs image clarity, and when electrons hit cement, they cannot penetrate it. However, a CNT is a conductive material that allows electrons move inside it. To avoid surface charging, coating the sample with conductive material

is the best solution to provide a path for electron flow. Silver, copper, and gold are the best conductive metals. Gold coating the prototype sample should be done prior to FESEM.

The Super Cressington 108 auto sputter coater utilizes ionization of argon to deposit gold atoms as an extremely thin layer onto the fractured specimen (Figure 56). The coating process consists of charge deduction and allows the FESEM scanning electron microscope to generate a clear image because gold coating creates a path for electrons within the specimen. Note that a thick layer of coating also leads to an obscured image and will prevent the capture of the finest details. In this research deposition, gold-coating time was 20 seconds, and the measurement range was from 0-35mA/mbar.


*Figure 56. Coating the sample with gold for better electron discharge (Cressington 108 auto sputter coater)*

## Step 3-Place Specimen in FESEM

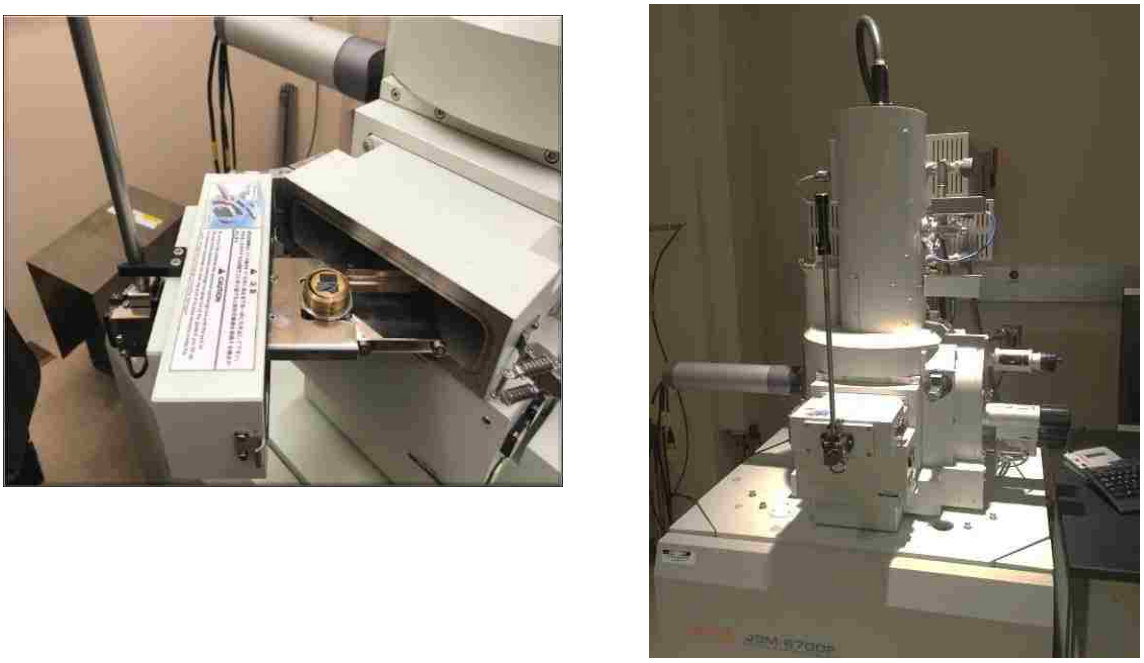

*Figure 57. FESEM scanning electron microscope (JEOL) JSM-6700F*

*Figure 58. Placing sample for scanning electron microscope*

## 3.6 Quality Control Sample Preparation

Improving the mechanical engineering properties of cementitious nanocomposite is influenced by the quality of carbon nanotubes' dispersion. The better the carbon nanotubes are dispersed, the stronger the engineering properties of composite. However, it is challenging to assess the uniformity of carbon nanotube dispersion. Therefore, the dispersion of CNT in cementitious nanocomposite should be evaluated before producing a specimen. In this research, to ensure minimum CNT agglomeration and maximum dispersion, two prototype samples were assessed by a non-destructive test.

The prototype sample was made with cement, 0.2% multi-walled carbon nanotubes by weight of cement, mixed with water to a cement ratio of 0.4 (Table 6). Complying with ASTM C 109, after casting the cement mortar, the sides of the mold were tapped lightly to allow air bubbles to enter the cement mortar surface and avoid voiding in the hardened cement mortar. The specimen was kept in an oiled mold for 24 hours in moist conditions.

Next, the specimens were demolded and immersed in water until the day before the sample was dried and coated with a thin layer of gold. The Field Emission Scanning Electron Microscope (FESEM) image test was implemented for 7 days.

*Table 6. Mix Design for Quality Control Sample*

| Materials | Weight | Unit |
|---|---|---|
| Cement | 112.38 | gr |
| Water | 44.95 | gr |
| MWCNTs (0.2%) | 0.22 | gr |
| Cement Mortar | 157.55 | gr |

Sonication process time was two 30-minute sessions (total of 60 minutes), with amplitude of 20%, and a one-minute break interval between the two sonications. In this mix, due to low w/c ratio, more water was

added to the mixture to improve workability. MWCNTs cannot disperse in water without sonication. Therefore, the MWCNTs cannot be recognized in the FESEM images and cementitious crystals dominate the mixtures. Additionally, there is not sufficient bond with MWCNTs and cement crystals. In addition, the thin gold-coating layer was not applied for this sample.


*Figure 59. Quality control sample for FESEM*

## 3.7 Filed Emission Scanning Electron Microscope for Quality Control Sample

The FESEM chamber requires a small sample. Therefore, the first specimen was fractured and tested in the FESEM instrument. To dry the specimen, a desiccator was used. The sample stayed in the desiccator for 24 hours to ensure it was dry enough to allow FESEM electrons to go through the specimen. This sample was not coated. The results indicated CNT agglomeration due to uniform dispersion and poor connection between cement crystal and multi-walled carbon nanotubes.

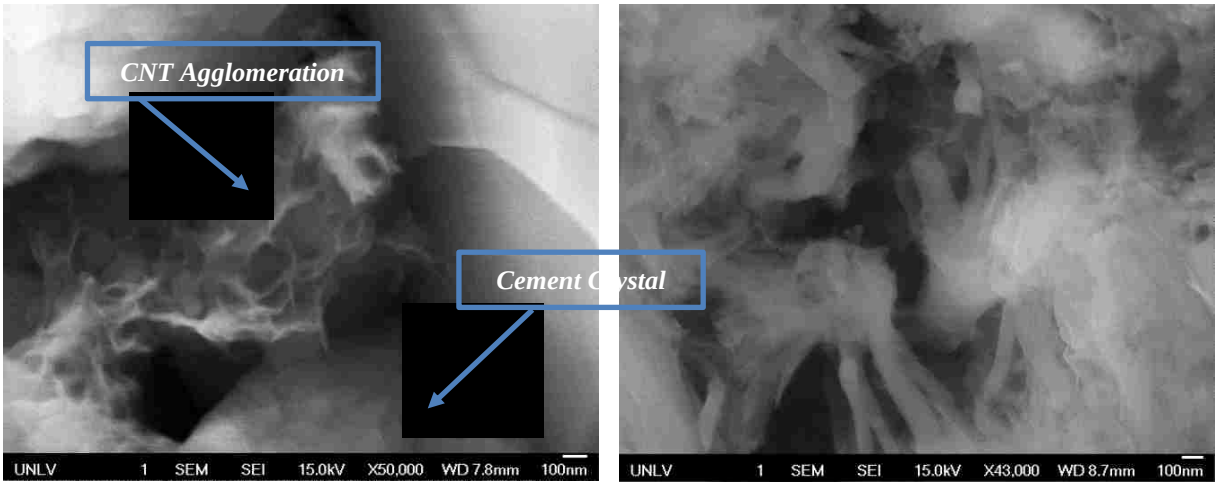


*Figure 60. The CNT was not dispersed uniformly. Growing cement crystal and agglomerated MWCNTs*

Two classes of electron microscopes include Scanning Electron Microscope (SEM) and Field Emission Electron Microscope (FESEM). However, FESEM provides images with higher resolution and magnification especially for cementitious nanocomposite, as CNTs are dominated by cement crystals (Fig. 60).

The FESEM is composed of high-vacuum equipment that allows electrons to move through the specimen and provide high resolution pictures. FESEM indicates the morphology and crystallography of cement-based nanocomposite. In this research, the FESEM instrument was used instead of SEM due to high-magnification images that FESEM provides. Additionally, SWCNTs are finer than MWCNTs, and FESEM provides high-quality images.

## 3.8 FESEM Results

The FESEM is a powerful device in nanoscience and nanotechnology that enables researchers to observe and analyze nanomaterials [36-41]. Recent progress in nanomaterials has utilized FESEM as a controlling instrument to check the fine structure of multi-walled and single-walled carbon nanotubes.

After 28 days of curing the specimens, a crushed specimen was prepared for FESEM imaging to assess the uniformity of CNT distribution within the cement matrix. This is necessary to evaluate the sonication process before producing more cementitious nanocomposites. Once the sonication process indicated fair CNT dispersion, that procedure was applied to all specimen preparation. CNT agglomeration leads to lower strength in cementitious nanocomposite. However, FESEM images were used as quality control assessment in this research to ensure effectiveness of CNT integration in the cement matrix.

Morphological analysis throughout FESEM indicated uniform dispersion of MWCNTS in the matrix and bounding between MWCNTs and cement crystals (Fig 61).

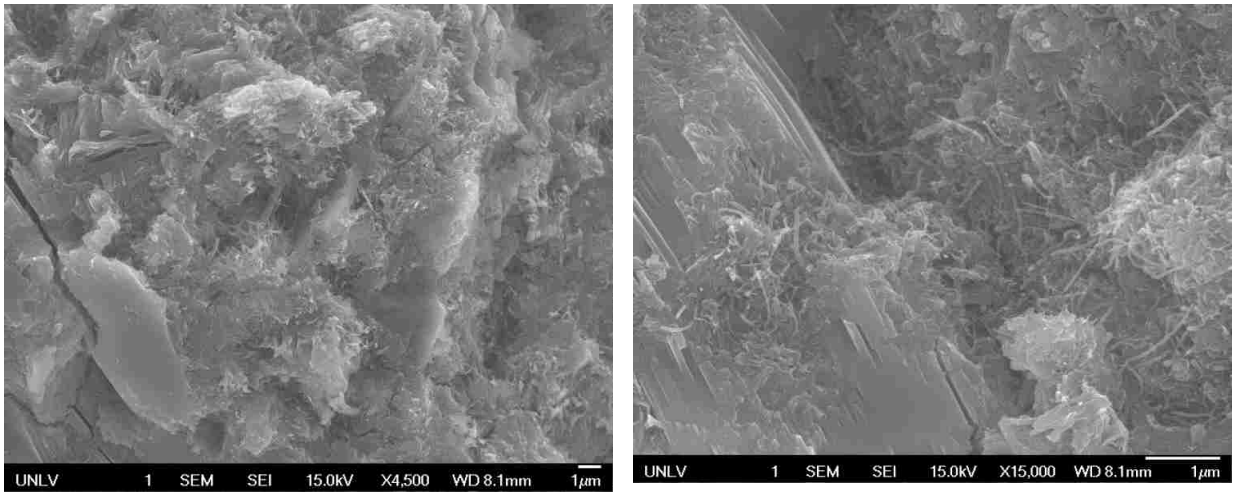


*Figure 61. Percolation of dispersed MWCNTs within matrix and micro-crack bridge by multi-walled carbon nanotubes/bundle of MWCNTs within the cementitious matrix*

At the fractured edge, MWCNTs were pulled out from specimen. The MWCNTs bridged with cement crystals (Fig. 63).


*Figure 62. Image is on the age of fractured surface of sample*

Air void residing in cementitious nanocomposite is one of the challenges as carbon nanotubes are added to the cement matrix. A small amount of entrapped air void in cementitious nanocomposite substantially reduces the composite mechanical properties of hardened cementitious nanocomposite. Carbon nanotubes in both multi-walled and single-walled classes significantly add air void due to microstructural change in the cement matrix. Additionally, all classes of carbon nanotubes accelerate setting time of fresh cement paste. Therefore, the entrapped air voids created in fresh cement paste reduce the engineering properties of hardened cementitious nanocomposite. The mixing techniques of this research significantly decreased entrapped air void. As can be seen in Figure 64, the air void is on the order of a nanometer (129.60nm). Integrity of cementitious matrix offered ultra-higher strength as will be discussed in the next chapter.

Another challenge is crack propagation across entrapped air voids as load is applied. With proper CNT dispersion, cracks and trapped air voids still interrupt load transfer when cementitious nanocomposite is tested mechanically. The failure mechanism of cementitious nanocomposite was influenced by micro and nano voids. Cracks quickly propagated through the composite where these air bubbles occurred [42].

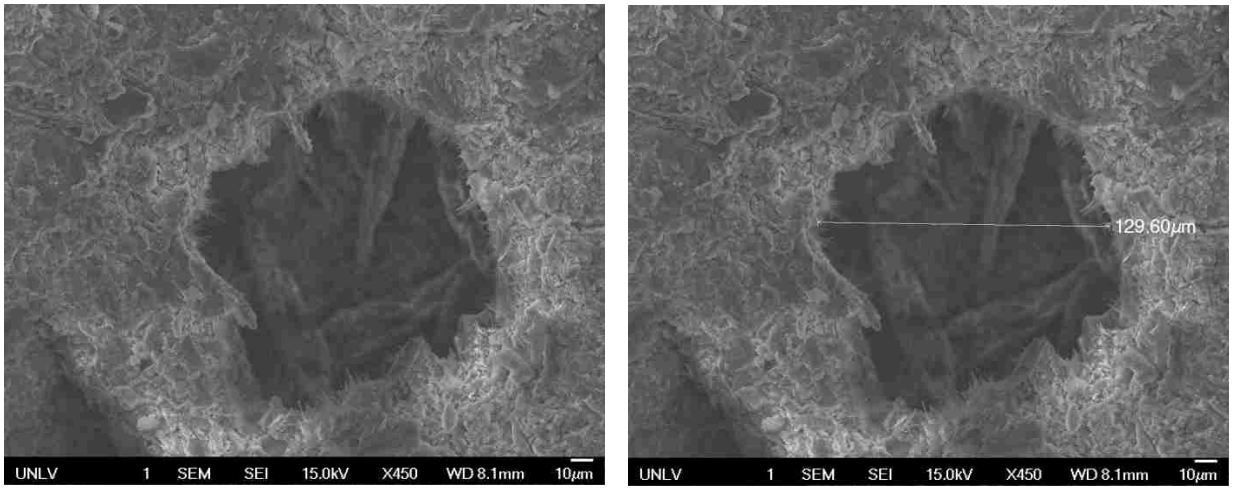


*Figure 63. The nano-scale void in cement-based nanocomposite*

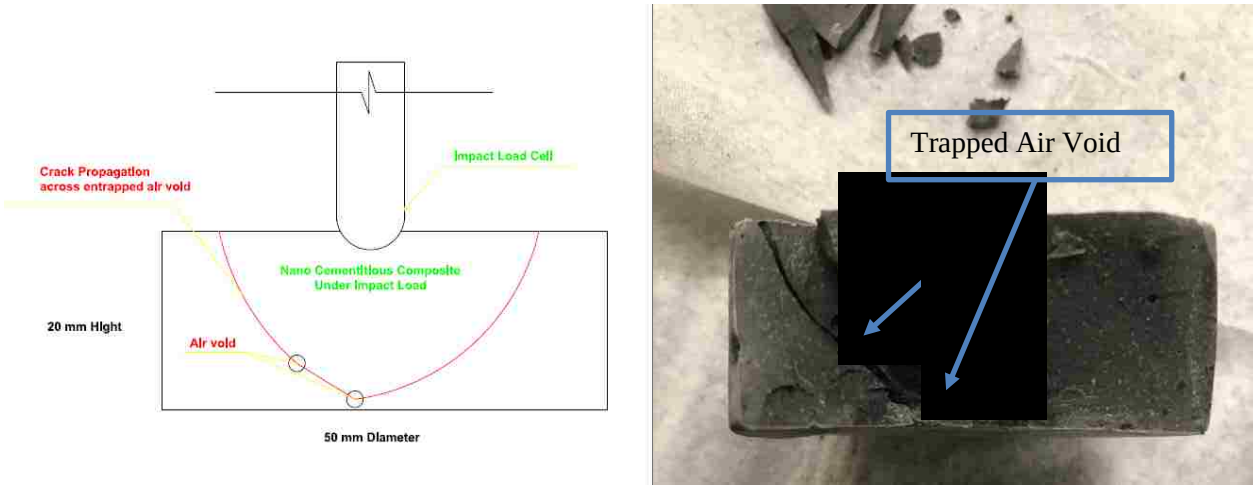


*Figure 64 Crack propagation across air void after impact load transferee within cementitious nanocomposite incorporating 0.2 wt% MWCNTs*

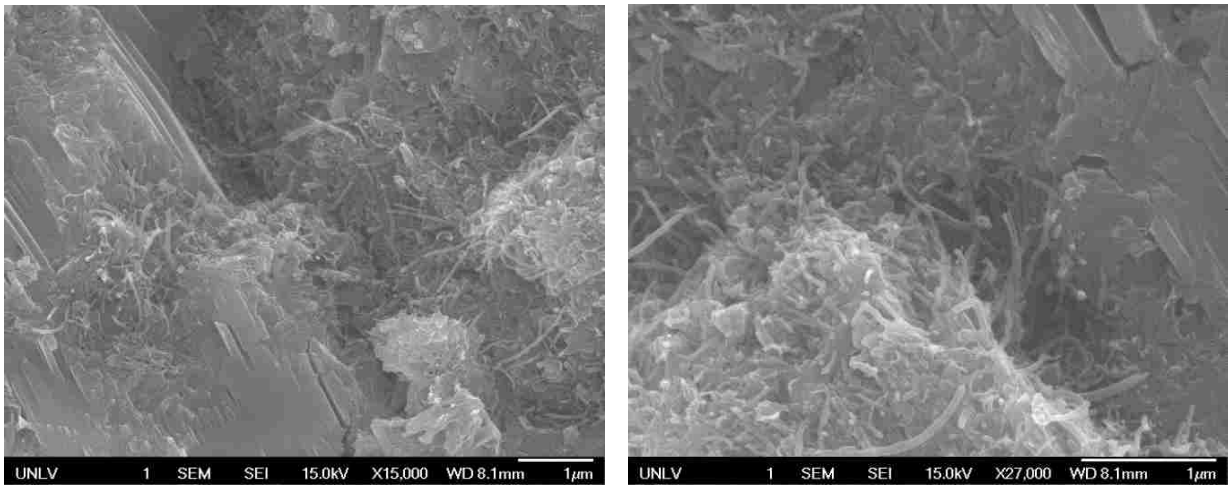


*Figure 65. Uniform dispersion of multi-walled Carbon nanotubes in the matrix and bounding MWCNTs and cement crystals*

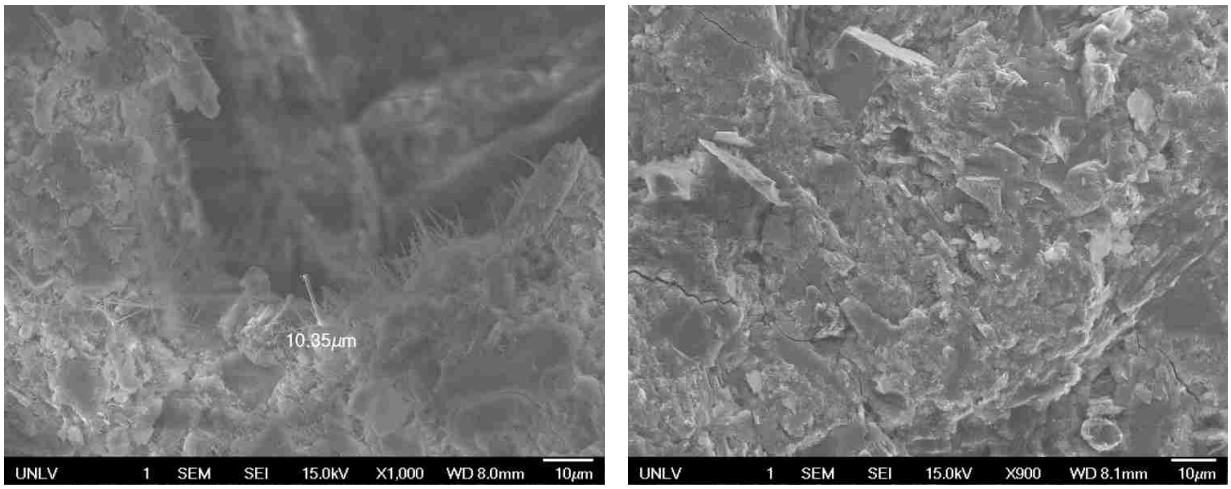


*Figure 66. Scanning electron microscope images of multi-walled carbon nanotubes cementitious composite paste (pulled-out MWCNTs on crack surface)*

# CHAPTER 4 TENSILE TEST RESULTS

## Phase II Study: Tensile Experimental Analysis to Investigate the Behavior of MWCNTS, SWCNTS, and Hybrid Reinforced in Cementitious Nanocomposites

## 4.1 Introduction

Concrete requires reinforcement with steel rebar and/or various classes of synthetic and natural fibers to compensate for its low tensile strength and ductility. However, steel rebar and steel fibers are vulnerable to corrosion and cause crack propagation along rebar. Additionally, these types of reinforcements are costly and add more weight to the concrete structure. Replacing such traditional reinforcements with Carbon Nanotube (CNT) reinforcement is a novel alternative for innovative and durable concrete structures. Nano-cement-based composites incorporating carbon nanotubes with advanced fabricating technology offer higher tensile splitting strength.

## 4.2 Effect of Scaling Down of Specimens

According to tensile ASTM C496/C496M-04 standards [50-63,63], the height–to-diameter ratio for splitting a tensile test specimen requires at least 2.0. In this experiment, the specimens for the tensile test were scaled down to cylinder with 25 mm diameter and 25 mm height.

*Table 7. Cylindrical tensile test sample geometry*

| Tensile Sample Geometry | | |
|---|---|---|
| d | 25 | mm |
| h | 50 | mm |

The effect of scaling down should be taken into consideration because as the specimen becomes smaller the accuracy of data will be affected. However, CNTs are currently an expensive material, and this class of nanocomposite experiment is under development. Additionally, test procedures and standards have not yet been developed. Therefore, the aim of this experiment was to assess the possibility of utilizing CNTs as the next generation of reinforcement.

## 4.3 Cementitious Composite with Different Mix Proportion

Splitting-tensile test matrices were reinforced by multi-walled carbon nanotubes (MWCNTs) and water cement ratio of 0.5. MWCNTs sonicated for an hour. Three samples incorporating 0.2wt%, 0.4wt%, and 0.6wt% of multi-walled carbon nanotubes were mixed as shown in the following table.

*Table 8. Mix design for cementitious nanocomposite incorporating multi-walled carbon nanotubes (all materials calculated based on weight of cement)*

| No. | MWCNTs | Materials | Sample (gr) | 3 Specimens |
|---|---|---|---|---|
| A-1 | 0.00wt% | Cement | 54.98 | 131.95 |
| B-1 | | MWCNTs | 0.00 | 0.00 |
| C-1 | | Water | 27.49 | 65.97 |
| A-2 | 0.20wt% | Cement | 54.98 | 131.95 |
| B-2 | | MWCNTs | 0.11 | 0.26 |
| C-2 | | Water | 27.49 | 65.97 |
| A-3 | 0.40wt% | Cement | 54.98 | 131.95 |
| B-3 | | MWCNTs | 0.22 | 0.53 |
| C-3 | | Water | 27.49 | 65.97 |
| A-4 | 0.60wt% | Cement | 54.98 | 131.95 |
| B-4 | | MWCNTs | 0.33 | 0.79 |
| C-4 | | Water | 27.49 | 65.97 |

Splitting-tensile test matrices were reinforced by single-walled carbon nanotubes and water cement ratio of 0.5. Single-walled carbon nanotubes sonicated for an hour. Three samples weighing 0.2wt%, 0.4wt%, and 0.6wt% of single-walled carbon nanotubes were mixed as on Table 9.

*Table 9. Mix design for cementitious nanocomposite incorporating single-walled carbon nanotubes (all materials calculated based on weight of cement)*

| No. | SWCNTs | Materials | Sample (gr) | 3 Specimens |
|---|---|---|---|---|
| A-1 | 0.00wt% | Cement | 54.98 | 131.95 |
| B-1 | | MWCNTs | 0.00 | 0.00 |
| C-1 | | Water | 27.49 | 65.97 |
| A-2 | 0.20wt% | Cement | 54.98 | 131.95 |
| B-2 | | MWCNTs | 0.11 | 0.26 |
| C-2 | | Water | 27.49 | 65.97 |
| A-3 | 0.40wt% | Cement | 54.98 | 131.95 |
| B-3 | | MWCNTs | 0.22 | 0.53 |
| C-3 | | Water | 27.49 | 65.97 |
| A-4 | 0.60wt% | Cement | 54.98 | 131.95 |
| B-4 | | MWCNTs | 0.33 | 0.79 |
| C-4 | | Water | 27.49 | 65.97 |

Splitting-tensile test matrix was reinforced by 50% multi-walled carbon nanotubes and 50% single-walled carbon nanotubes (hybrid) by weight of cement, and water cement ratio of 0.5. Hybrid CNTS sonicated for an hour. Three samples weighing 0.2wt%, 0.4wt%, and 0.6wt% of hybrid carbon nanotubes were mixed as shown in the following table.

*Table 10. Mix design for cementitious nanocomposite incorporating hybrid carbon nanotubes (all materials calculated based on weight of cement)*

| No. | MWCNTS | SWCNTs | Materials | Sample (gr) | 3 Specimens |
|---|---|---|---|---|---|
| A-1 | 0.00wt% | 0.00wt% | Cement | 54.98 | 131.95 |
| B-1 | | | MWCNTs | 0.00 | 0.00 |
| C-1 | | | Water | 27.49 | 65.97 |
| A-2 | 0.10wt% | 0.10wt% | Cement | 54.98 | 131.95 |
| B-2 | 0.1319gr | 0.1319gr | MWCNTs | 0.11 | 0.26 |
| C-2 | | | Water | 27.49 | 65.97 |
| A-3 | 0.20wt% | 0.20wt% | Cement | 54.98 | 131.95 |
| B-3 | 0.2638gr | 0.26389gr | MWCNTs | 0.11 | 0.26 |
| C-3 | | | Water | 27.49 | 65.97 |
| A-4 | 0.30wt% | 0.30wt% | Cement | 54.98 | 131.95 |
| B-4 | 0.3958gr | 0.3958gr | MWCNTs | 0.16 | 0.40 |
| C-4 | | | Water | 27.49 | 65.97 |

## 4.4 Splitting-Tensile Strength of Composite

Three distinct locations of cylindrical specimens were measured by an angle of 120˚. Additionally, diameter was measured at top, bottom, and middle of cylindrical specimens. The average value of length and diameter were recorded for splitting tensile strength calculation.

*Figure 67. Splitting-tensile nanocomposites specimens*

The splitting tensile test was performed by an electromechanical TNIUSTQDISER machine, with capacity of 5,000 for specimens (reinforced MWCNTs and SWCNTs) with lower tensile strength. However, specimens with hybrid reinforcement exceed the capacity of a compression machine, so the load cell was replaced with a higher capacity of 50,000lbf. Machine software operator recorded the results (Figure 70-71).

The cylindrical splitting specimens with a height of 50 mm and diameter of 25 mm were tested after 28 days of curing in water. The procedure of splitting tensile strength test was in compliance with ASTM C 496/C496M-04 "Standard Test Method for Splitting-Tensile Strength of Cylindrical Concrete Specimens," which is applicable for cylindrical concrete specimens. The tensile test for cementitious nanocomposite specimens was scaled down. The plywood bearing strip with a length of 70 mm, a width of 20 mm, and a thickness of 1.15 mm were placed on the top and bottom of cementitious nanocomposites (Figure 69). The loading rate (displacement velocity) was 0.35 inch per minute until the specimen reached maximum tensile strength, and continued loading until complete specimen failure. The specimen's crack propagation and failure mechanism were monitored. The CNT reinforcements mitigated more ductile behavior of nanocomposites.

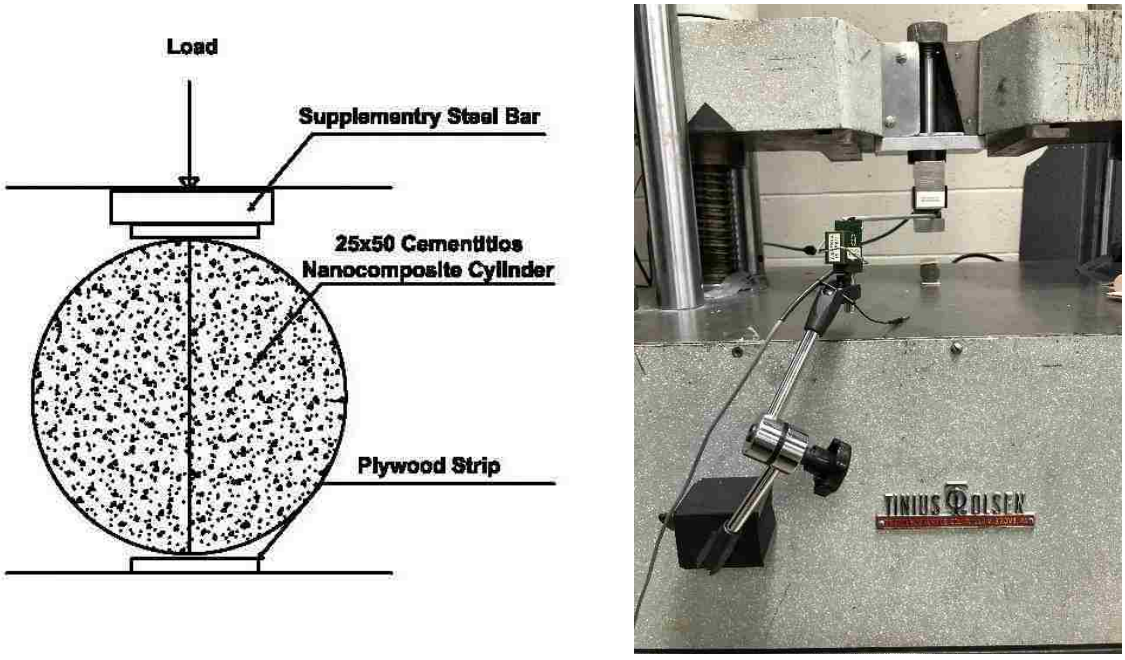


*Figure 68. Schematic test setup for splitting-tensile test and specimen test set up before applying load*

The maximum tensile strength was calculated as following equation.

$$f_t' = \frac{2P}{\pi LD}$$

Where

$f_t'$= Splitting-tensile strength of the cementitious nanocomposite, MPa (psi)

$P$= Ultimate load, KN(lbf)

$L$= Length of the cylindrical specimen, mm (in)

D= Diameter of the cylindrical specimen, mm (in)

*Figure 69. Load cell with 5,000lbf capacity for nanocomposites incorporating hybrid CNTs*

*Figure 70. Load cell with 5000lbf capacity for nanocomposites incorporating MWCNTs and SWCNTs*

## 4.5 Control Samples Failure Mechanism

Failure mechanism differences were detected between cement mortar specimens and specimens reinforced with MWCNTs, SWCNTs, and hybrid CNTs. The required load for ultimate failure of nanocomposite reinforced with hybrid CNTs exceeds the capacity of load-cell. Therefore, the load-cell was replaced with a new test set up, illustrated in Figure 71.

*Figure 71. Cement mortar sample failure mechanism in splitting tensile test (sudden cement mortar failure)*

## 4.6 Failure Mechanism of CNT-Reinforced Cementitious Nanocomposite

Comparing the failure mechanism of cement mortar (Figure73) under spiriting tensile test with CNT-reinforced cementitious nanocomposite presented considerable enhancement in ductility of the concrete [63-64]. Reinforcing cement mortar with hybrid CNT resulted in the most ductile failure pattern. As shown in the following pictures of failure mechanism of nanocomposite with hybrid CNT reinforcement (Figure 73), the crack developed under applied load in alignment with axial load.

This pattern of failure is similar to that of cement mortar, in which a crack initiates in the middle of the cross section, followed shortly afterward by specimen failure. In other words, in the sudden failure of concrete or cement mortar under flexural or tensile load, the load capacity of concrete is negligible after initiating the first crack [43-46]. Concrete is reinforced by rebar not only to transform sudden failure to predictable failure, but also to add tensile strength where concrete is in tension stress. Structural design for reinforced concrete is based on predictable failure where the concrete capacity in tension is negligible and rebar carries the entire tension forces.

However, cement mortar reinforced with carbon nanotubes offers tensile strength for concrete and transforms concrete's sudden failure to predictable failure. This is one of the vital components for structural health monitoring with enhancing durability of concrete structure.

As can be seen in Figure 73, after the first micro crack initiated and developed, nanocomposite incorporating 0.6wt% carbon nanotubes carried the load for a long time until it reached maximum strength. The uniqueness of this nanocomposite property generates a new class of advanced concrete reinforcement.

Another significant result of the figure 73 compared to conventional cement mortar is failure mechanism after maximum stress. The majority of concrete types are designed for compression because concrete materials are brittle. Fracturing occurs immediately after ultimate strength (maximum stress in the graph). However, in the nanocomposite, the failure mode was transformed to ductile materials. In other words, after

ultimate stress, the nanocomposite was still capable of carrying applied load. However, more experiments should be conducted with actual specimen's size and more test repetition to ensure the same pattern occurs.

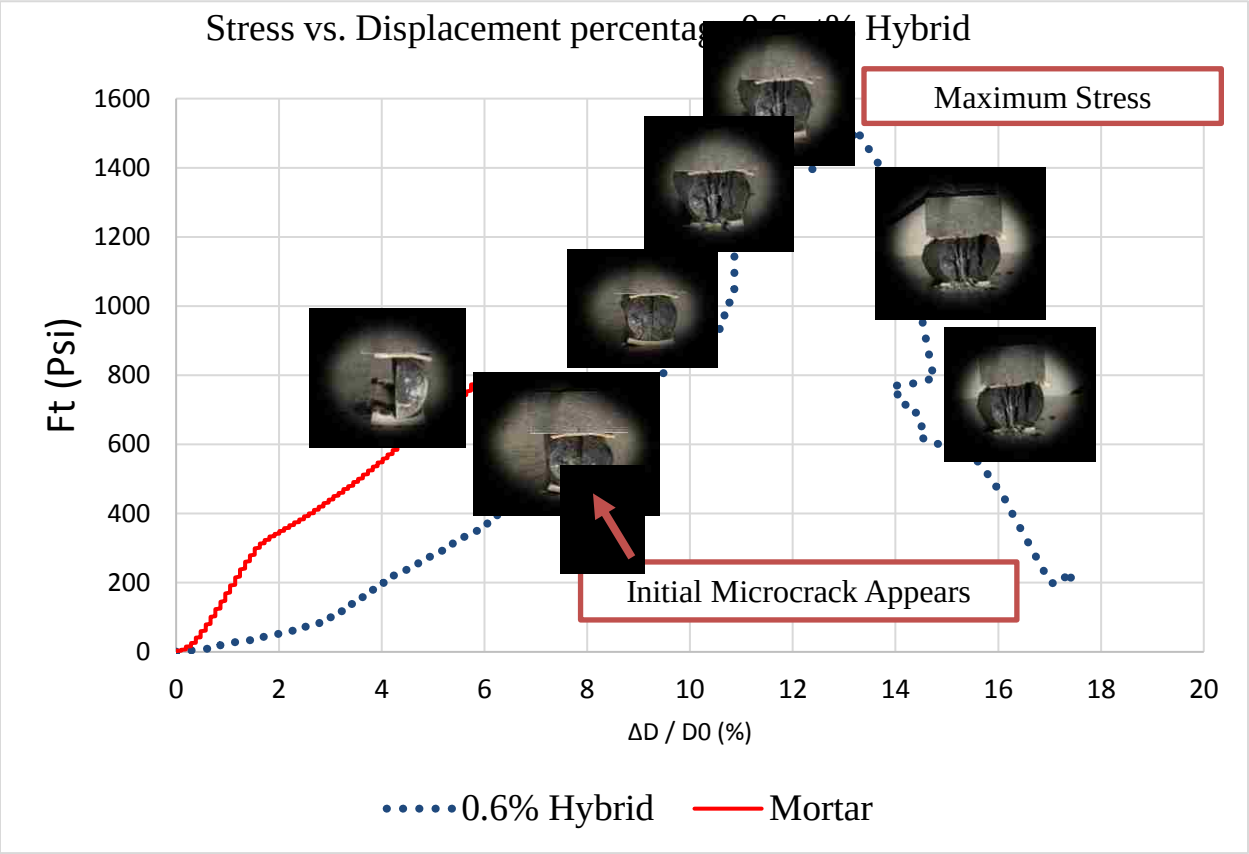


*Figure 72. Stress verses displacement percentage for nanocomposite reinforced by 0.6wt% hybrid carbon nanotubes*

In figure 72, D0 is the initial vertical distance between the underneath of load cell and the fixed table of Tinius Olsen Tensile Testing Machine which includes the diameter of the specimen (in vertical direction) and thickness of plywood strips, and D denotes the instantaneous value of this distance. Hence, ΔD/D0 does not measure the strain accurately; neither is it an accurate measurement of the vertical deformation of the specimen under the tensile load. However, it is helpful to compare the energy absorbed by different specimens qualitatively. Given that the same procedure is followed in conducting all tests and knowing that

the energy absorption is proportion to the area under the stress-strain curve, it can be concluded that the more the area under the Ft versus ΔD/D0 graph is the greater the energy absorption.

The failure pattern after developing the initial crack provides additional time before ultimate failure occurs in cement-based nanocomposites. The evolution of crack propagation on cementitious nanocomposite surface until ultimate specimen failure during splitting-tensile test was assessed in this experiment (Fig. 73).

The evolution of crack propagation on the nanocomposite surface until ultimate specimen failure during splitting-tensile test is presented in the Figure 74. The fracture mode did not occur after developing the first crack in the axial of cylindrical specimen. The vertical cracks repeated with applied load alignment.

The left part of the specimen had fallen apart exactly where an air void existed which indicated the importance of the mixing process of the composite to reach the maximum potential of carbon nanotubes reinforcement. The same pattern occurred through impact tests: Where air voids existed, cracks propagated (Figure 73).

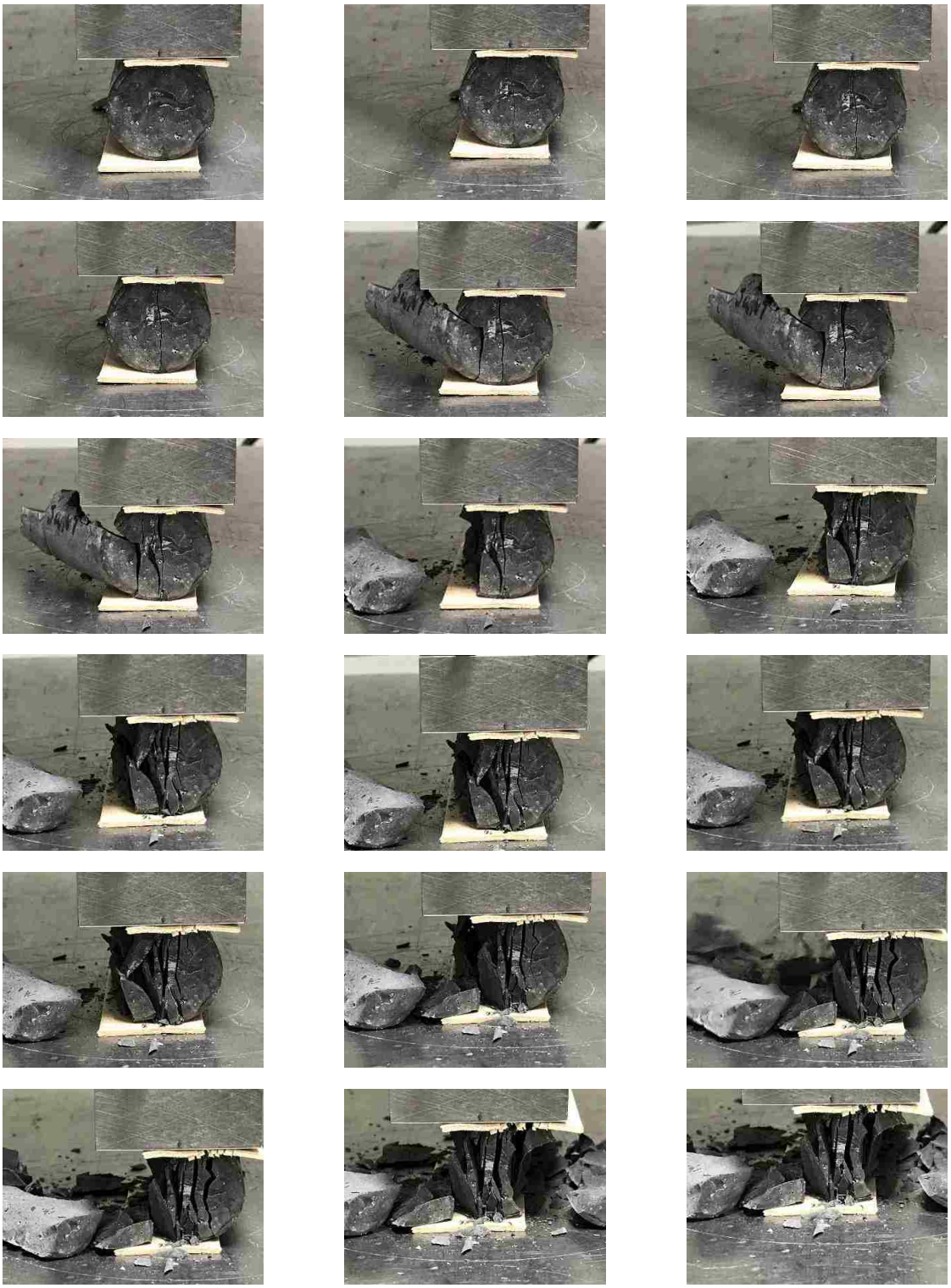

*Figure 73. Nanocomposite incorporating 0.4wt % hybrid carbonb nanotubes failure mechanism in splitting tensile test (ductile failure)*

## 4.7 Transformed Nanocomposite from Circular to Overall Shape

Another important finding of this experiment is that the nanocomposite failure mode was initiated from central axial aligned with applied load, but cementitious nanocomposite load capacity increased after the first crack initiated and propagated through vertical cross section axial. The deformation of cross section from circle to oval shape augmented tensile strength by 50% in cementitious nanocomposite incorporating hybrid carbon nanotubes when compared to conventional cement mortar.

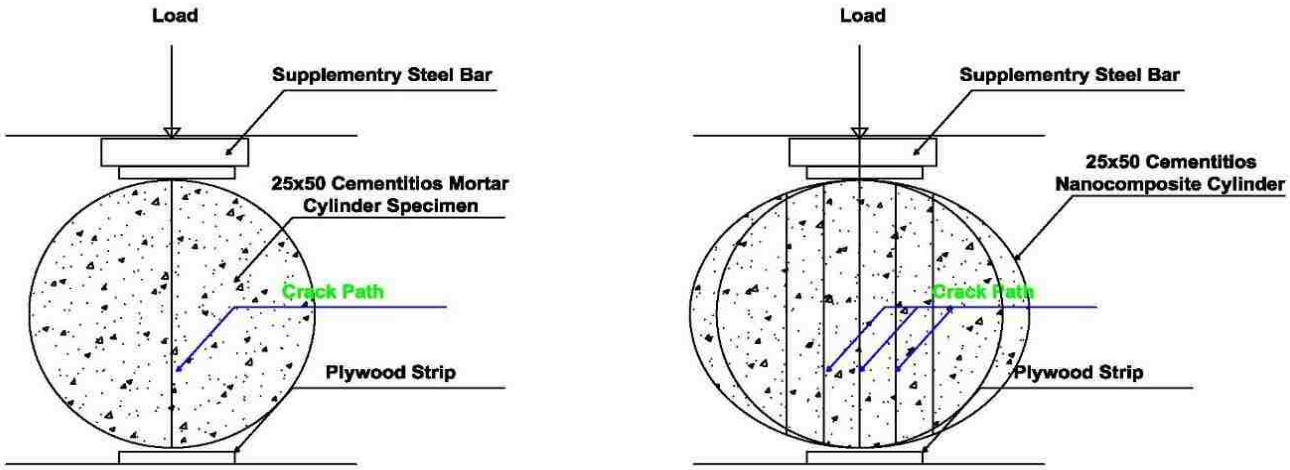


*Figure 74. Schematic fracture pattern of hybrid nanocomposite*

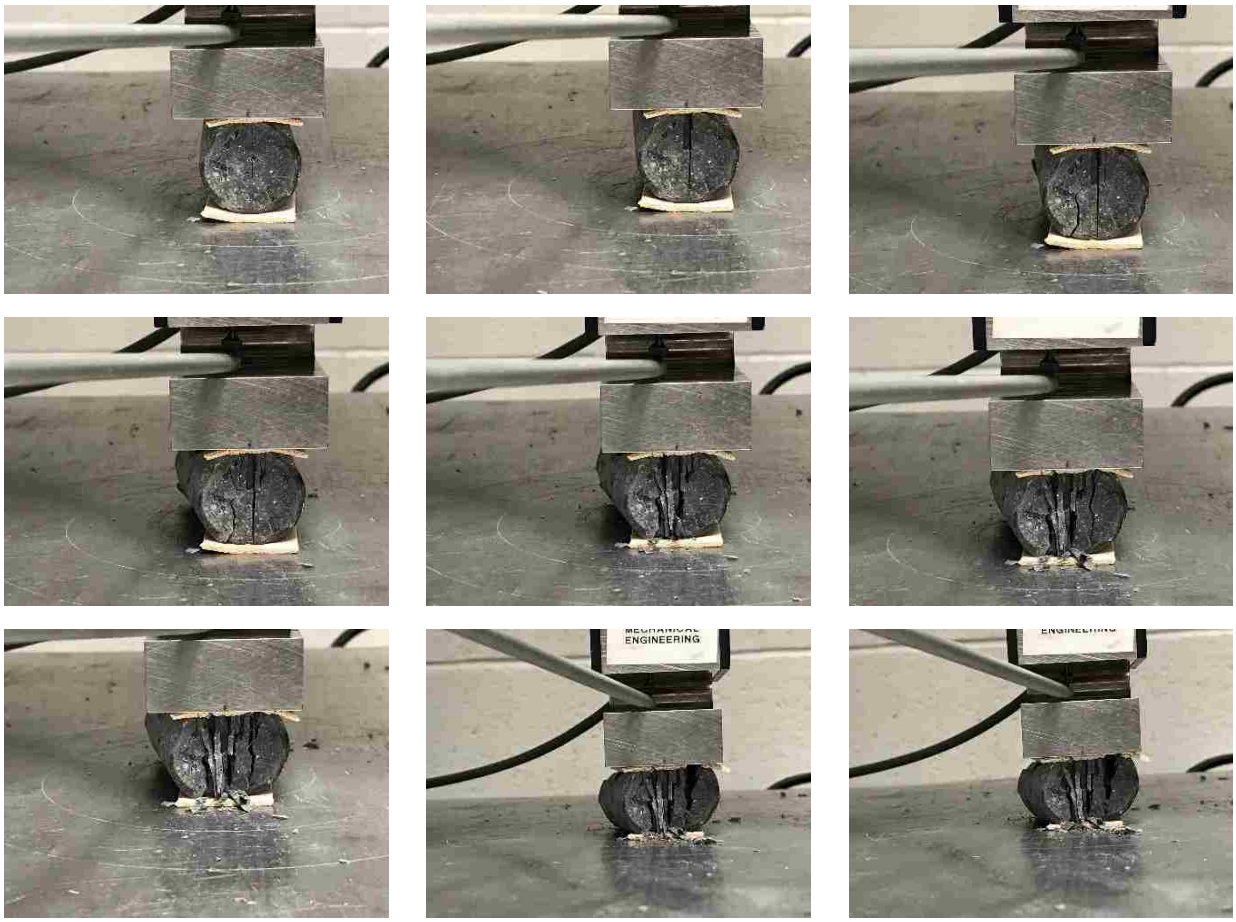


*Figure 75. Nanocomposite incorporating 0.4wt % hybrid carbon nanotubes failure mechanism in splitting tensile test (ductile failure and deformation of cross section from circular to oval shape)*

## 4.8 Comparison of Tensile Strength

This section compares the area under each graph to indicate how cementitious nanocomposite incorporating CNTs absorb more energy qualitatively. In other words, this section compares the toughness of each composte with a control sample to emphasize the improvement in failure mechanism.

The hybrid nanocomposites showed more ductile behavior compared to conventional concrete that is extremmly brittle. Concrete failure mechanism under static and dynamic load is identified as the first crack

occurs because shortly after that concrete collapses. However, in cementitious nanomaterilas, as shown in Figure 76, after the first crack happens approximately at 600 psi, the composite stress raises to 1500 psi.

Figure 76 shows that nanocomposite incorporating 0.6wt% hybrid carbopn nanotubes reached the maximum tensile strength compared to nanocomposites with 0.2wt% and 0.4wt%. This composite increased the tensile strength by approximetly 50% compared to cement mortar.

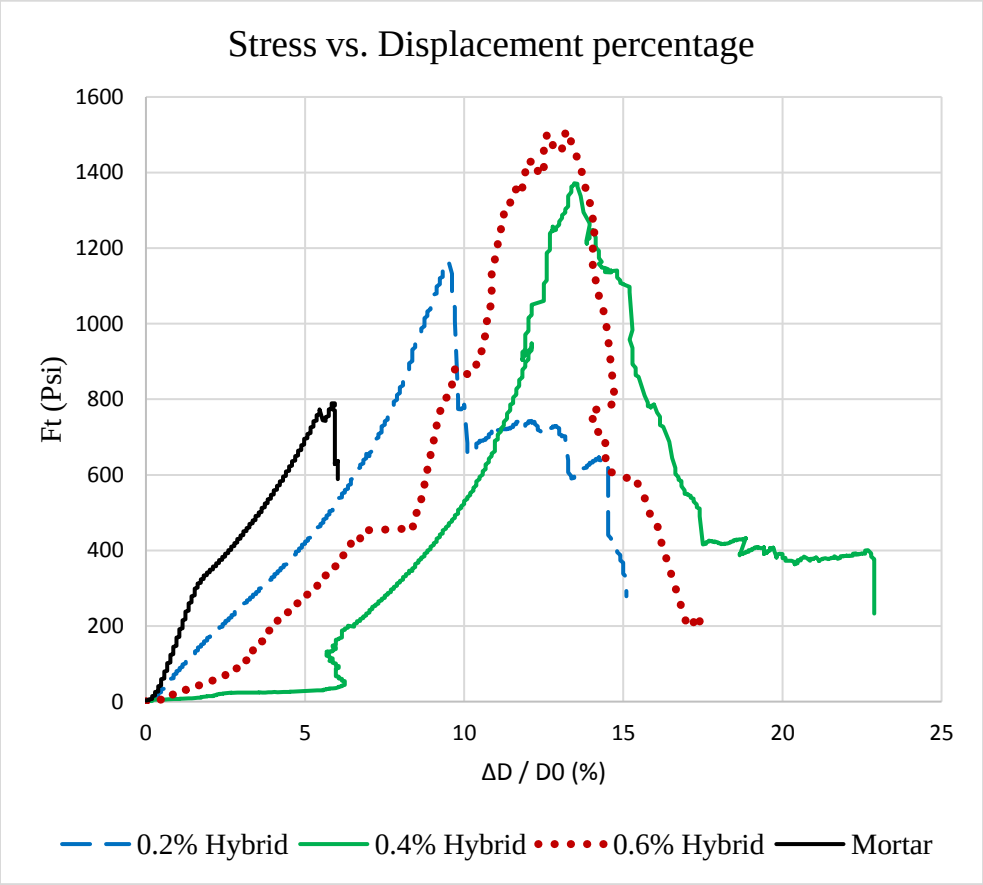


*Figure 76. Stress verses displacement percentages for nanocomposite reinforced by hybrid carbon nanotubes 0.2wt%, 0.4wt%, and 0.6wt%*

Hybrid carbon nanotubes (0.2wt %) had significantly better performance compared with the same ratio of SWCNTs and MWCNTs as shown in figure 77.

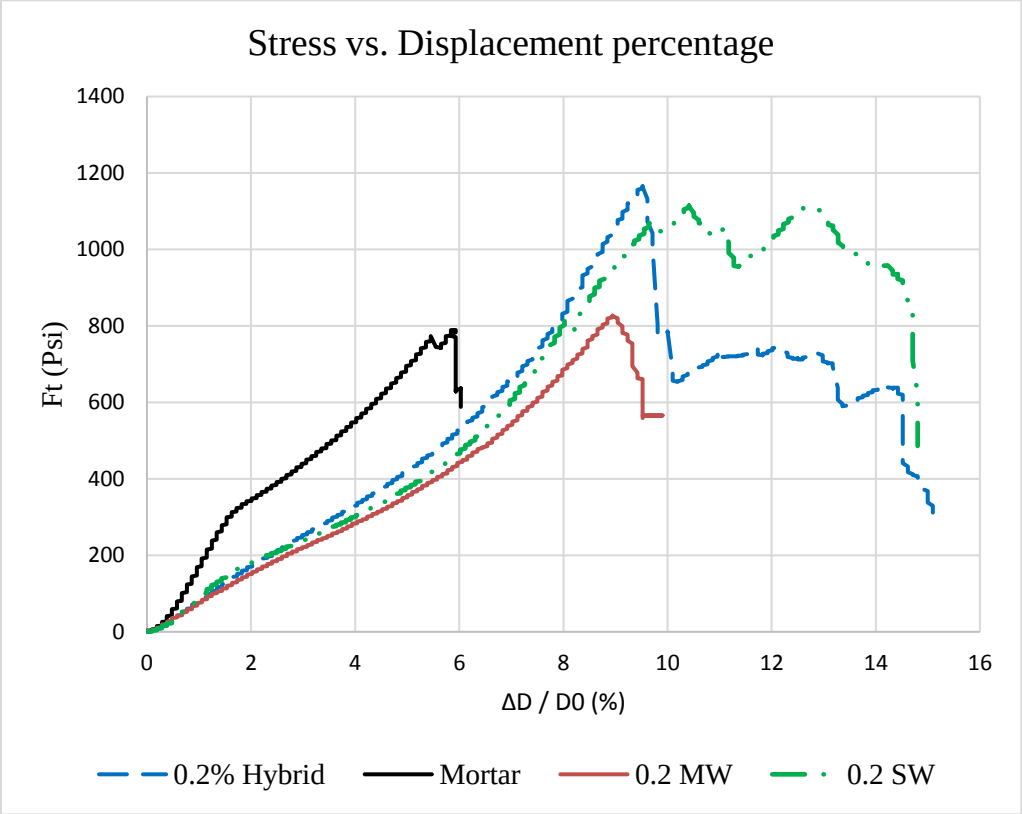


*Figure 77. Stress verses displacement percentages for nanocomposite reinforced by 0.2wt% hybrid carbon nanotubes, SWCNTs, and MWCNTs.*

Hybrid carbon nanotubes (0.6wt %) had significantly better performance compared with the same ratio of SWCNTs and MWCNTs as shown in figure 78.

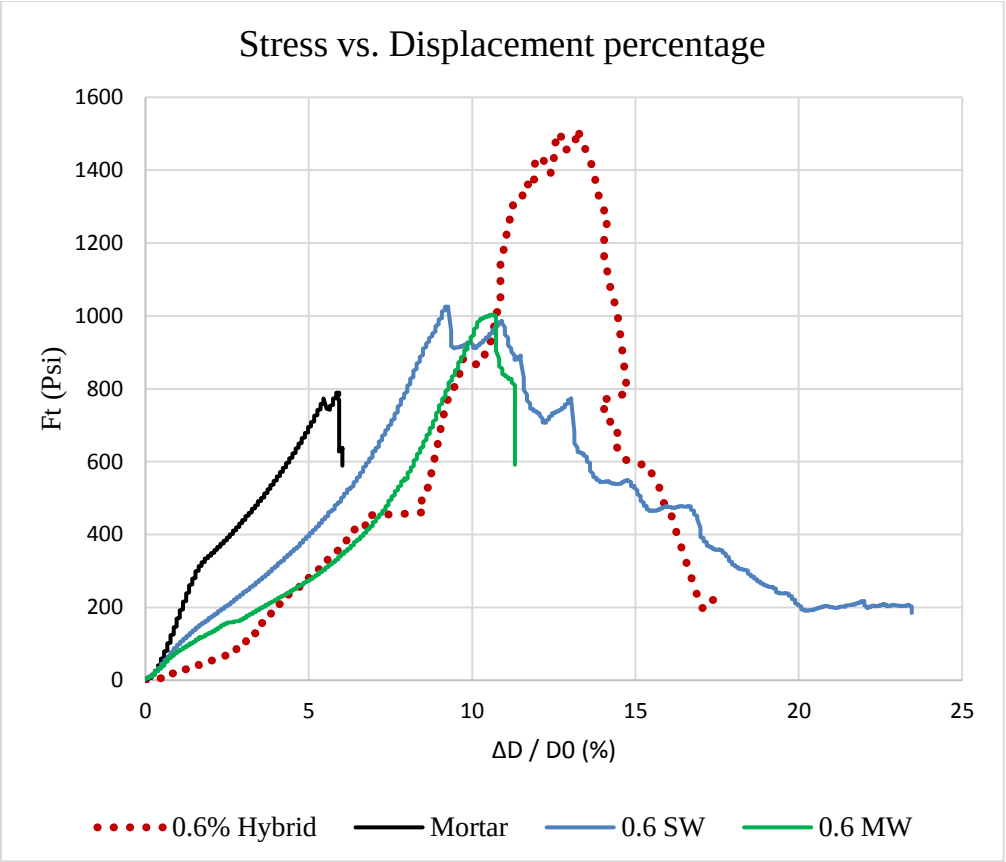


*Figure 78. Stress verses displacement percentages for nanocomposite reinforced by 0.6wt% hybrid carbon nanotubes, SWCNTs, and MWCNTs*

Hybrid carbon nanotubes (0.4wt %) had significantly better performance compared with the same ratio of SWCNTs and MWCNTs as shown in Figure 79. In summary, all volume fractions of hybrid carbon nanotubes indicated the maximum splitting tensile test.

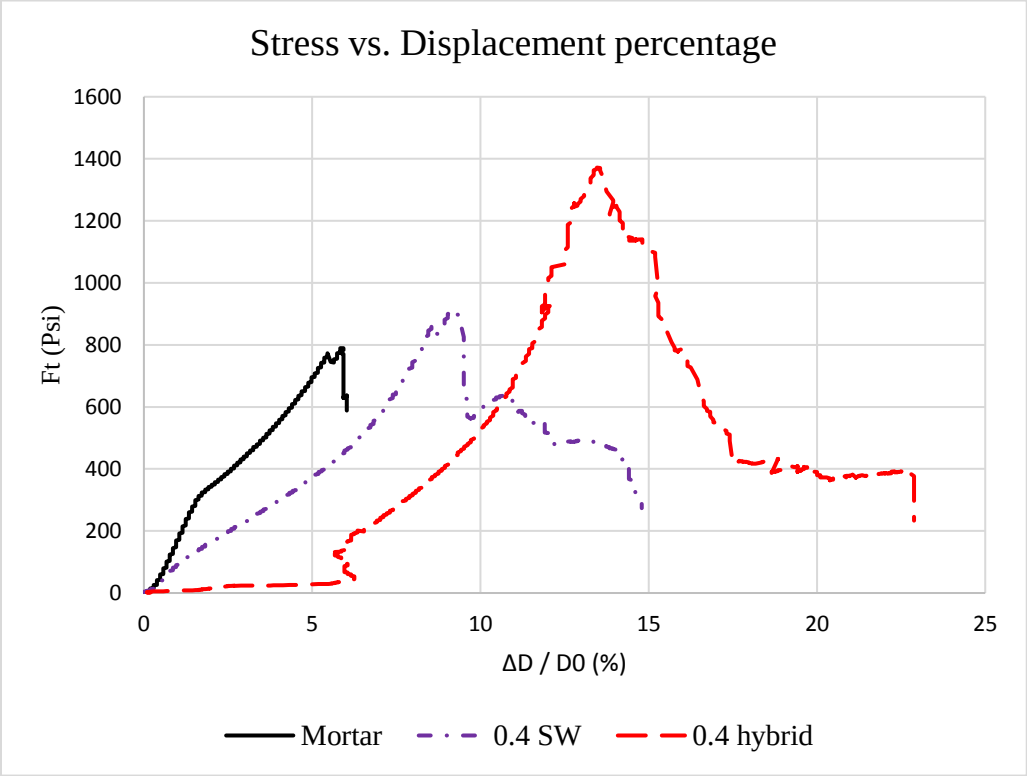


*Figure 79. Stress versus displacement percentages for nanocomposite reinforced by 0.4wt% hybrid carbon nanotubes, SWCNTs, and MWCNTs*

## 4.9 Tensile Test Results and Statistical Analysis Discussion

Table 11 summarizes the data collected from tensile strength tests. These data are illustrated in Figure 81, which shows that cementitious nanocomposites, especially those reinforced by hybrid CNTs, withstand higher tensile loads. However, Figure 81 clearly demonstrates that the ultimate tensile strength of each

composite varies widely from one specimen to another. These observations might be better understood through statistical analysis.

Average, Maximum, Minimum, and standard deviation of the ultimate tensile strength of all composites are tabulated in Table 12 in which *STD* stands for *standard deviation*. Following facts can be inferred on Table 12.

The average ultimate tensile strength of each and all composites is greater than that of plain mortar. The increment varies from 2 % (MWCNT 0.2 %) up to 36 % (Hybrid 0.4 %). The ratio of standard deviation to the average ultimate tensile strength varies from 0.1 % (MWCT 0.6 %) to 31 % (Hybrid 0.6 %). This ratio for plain mortar is 8.9 %. Increasing the dosage of CNT reinforcement does not necessarily enhance the tensile strength of the composite.

The average ultimate tensile strength is demonstrated using a column chart in Figure 81 where error bars demonstrate the standard deviation. Regarding the high standard deviations, the t-Test was conducted using Microsoft Excel software to determine whether or not the experimental results are statistically convincing.

The null hypothesis of this statistical analysis is that there is no meaningful difference between the average of ultimate tensile strength of the composite and that of the plain mortar. In the first step, the F-test was conducted to determine if the standard deviation of each composite equals the STD of the mortar. Then the outcome of each F-test is used to determine the suitable t-Test method for each composite. Lastly, two-sample t-Tests are conducted for Alpha = 0.05. The results of F-tests and t-Tests are summarized in Table 13. On each table, variable 1 with 9 observations denotes plain mortar, while variable 2 with only 3 observations refers to composite.

*Table 11. Summary of tensile strength (psi) for nanocomposite reinforced by different ratio and type of carbon nanotubes*

| Specimen | CNT | CNT % | D(in) | L(in) | P(lb.f) | Ft (psi) |
|---|---|---|---|---|---|---|
| B-1 | None | 0.0% | 1.045 | 2.260 | 3132.8 | 844.9 |
| C-1 | None | 0.0% | 1.038 | 2.211 | 2756.3 | 765.0 |
| D-1 | None | 0.0% | 1.042 | 2.200 | 3274.2 | 909.7 |
| E-1 | None | 0.0% | 1.044 | 2.255 | 3280.0 | 887.4 |
| F-1 | None | 0.0% | 1.037 | 2.300 | 3695.1 | 986.8 |
| I-1 | None | 0.0% | 1.043 | 2.216 | 3442.2 | 948.6 |
| C-1 | None | 0.0% | 1.063 | 2.165 | 2650.0 | 733.4 |
| D-1 | None | 0.0% | 1.063 | 2.087 | 2978.8 | 855.2 |
| B-1 | None | 0.0% | 1.046 | 2.130 | 2928.2 | 837.1 |
| A-2 | MWNT | 0.2% | 1.043 | 2.135 | 3147.6 | 901.2 |
| B-2 | MWNT | 0.2% | 1.043 | 2.155 | 3191.5 | 904.4 |
| C-2 | MWNT | 0.2% | 1.040 | 2.130 | 2877.6 | 827.4 |
| A-3 | MWNT | 0.4% | 1.043 | 2.130 | 3734.8 | 1070.8 |
| B-3 | MWNT | 0.4% | 1.038 | 2.090 | 4155.9 | 1220.2 |
| C-3 | MWNT | 0.4% | 1.042 | 2.194 | 3520.9 | 981.0 |
| B-4 | MWNT | 0.6% | 1.035 | 2.137 | 3485.6 | 1004.3 |
| C-4 | MWNT | 0.6% | 1.043 | 2.158 | 3541.1 | 1002.1 |
| A-2 | SWNT | 0.2% | 1.045 | 2.125 | 3103.9 | 890.3 |
| B-2 | SWNT | 0.2% | 1.047 | 2.144 | 3948.6 | 1120.4 |
| C-2 | SWNT | 0.2% | 1.038 | 2.160 | 3958.3 | 1124.5 |
| A-3 | SWNT | 0.4% | 1.043 | 2.157 | 3550.4 | 1005.2 |
| B-3 | SWNT | 0.4% | 1.041 | 2.239 | 3341.7 | 913.2 |
| C-3 | SWNT | 0.4% | 1.049 | 2.224 | 3004.0 | 820.1 |
| A-4 | SWNT | 0.6% | 1.045 | 2.255 | 3232.8 | 873.8 |
| B-4 | SWNT | 0.6% | 1.030 | 2.238 | 4047.0 | 1118.2 |
| C-4 | SWNT | 0.6% | 1.036 | 2.214 | 3695.9 | 1026.3 |

| | | | | | | |
|---|---|---|---|---|---|---|
| A-2 | Hybrid | 0.2% | 1.027 | 2.24 | 4505.4 | 1217.1 |
| B-2 | Hybrid | 0.2% | 1.047 | 2.252 | 3759.4 | 1039.7 |
| C-2 | Hybrid | 0.2% | 1.025 | 2.247 | 3683.4 | 1018.3 |
| A-3 | Hybrid | 0.4% | 1.035 | 2.226 | 2768.0 | 765.3 |
| B-3 | Hybrid | 0.4% | 1.036 | 2.226 | 5587.1 | 1543.1 |
| C-3 | Hybrid | 0.4% | 1.040 | 1.972 | 4418.8 | 1222.0 |
| A-4 | Hybrid | 0.6% | 1.040 | 2.137 | 4867.3 | 1394.9 |
| B-4 | Hybrid | 0.6% | 1.043 | 2.122 | 3209.5 | 923.7 |
| C-4 | Hybrid | 0.6% | 1.042 | 2.158 | 2296.5 | 650.5 |

*Table 12 Average, Maximum, Minimum, and Standard deviation of ultimate tensile strength of composites.*

| Composition | Percentage | Average | Maximum | Minimum | STD |
|---|---|---|---|---|---|
| Mortar | 0.0% | 863 | 987 | 733 | 77 |
| MWCNT | 0.2% | 878 | 904 | 827 | 36 |
| | 0.4% | 1,091 | 1,220 | 981 | 99 |
| | 0.6% | 1,003 | 1,004 | 1,002 | 1 |
| SWCNT | 0.2% | 1,045 | 1,124 | 890 | 109 |
| | 0.4% | 913 | 1,005 | 820 | 76 |
| | 0.6% | 1,006 | 1,118 | 874 | 101 |
| Hybrid | 0.2% | 1,092 | 1,217 | 1,018 | 89 |
| | 0.4% | 1,177 | 1,543 | 765 | 319 |
| | 0.6% | 990 | 1,395 | 651 | 307 |

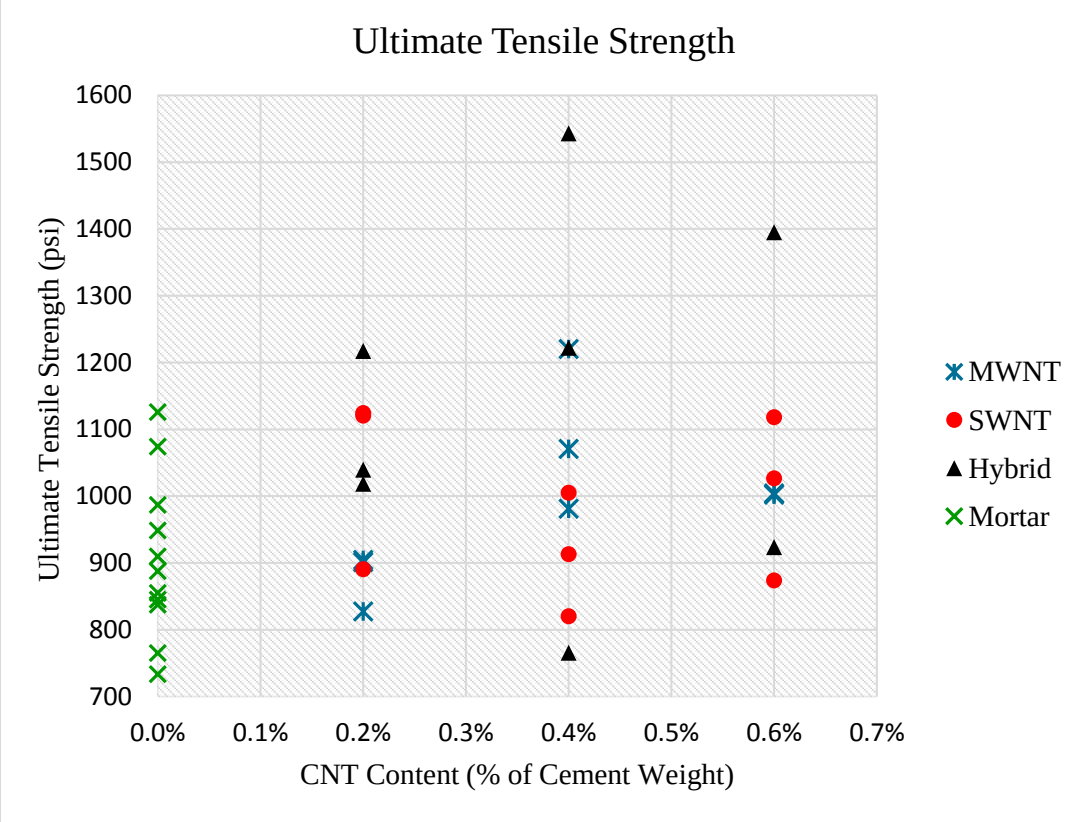


*Figure 80. Summary of stress verses displacement percentages for nanocomposite reinforced by different ratio and type of carbon nanotubes*

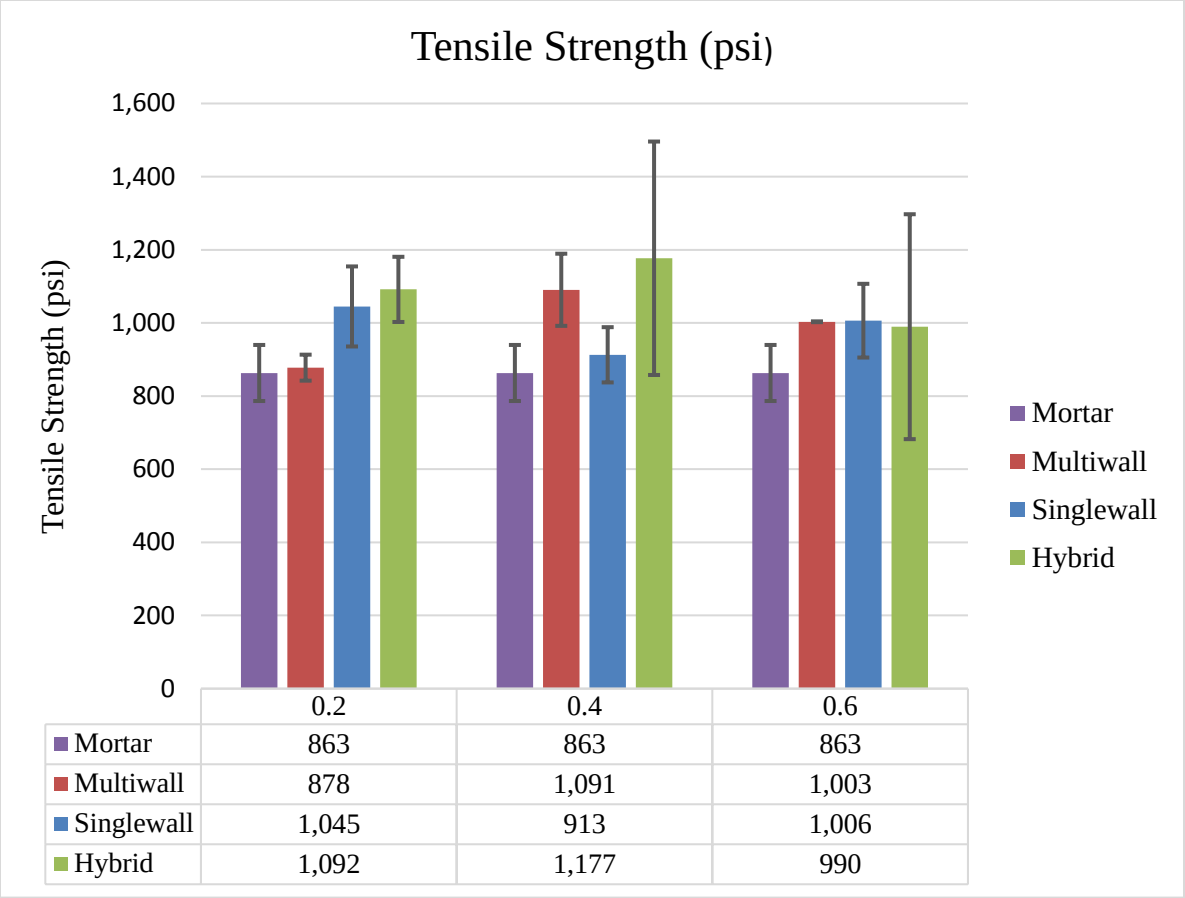


| | 0.2 | 0.4 | 0.6 |
|---|---|---|---|
| Mortar | 863 | 863 | 863 |
| Multiwall | 878 | 1,091 | 1,003 |
| Singlewall | 1,045 | 913 | 1,006 |
| Hybrid | 1,092 | 1,177 | 990 |

*Figure 81. Summary of tensile strength (psi) for nanocomposite reinforced by different ratio and type of carbon nanotubes*

A two-tail test was conducted for each composite. lf $|t_{ststst}| > t_{critical}$ two-tail, we reject the null hypothesis. This is the case for MWCNT 0.6 %, Hybrid 0.2 %, and Hybrid 0.4 %. Therefore, in these three cases the observed difference between the samples' means is statistically convincing enough to conclude that the average ultimate strength of composite and plain mortar differs significantly. In contrast, in MWCNT 0.2 %, MWCNT 0.4 %, all SWCNT-reinforced composites, and Hybrid 0.6 %, the observed data are not statistically convincing. More precise testing methods should be utilized to reach more repeatable results and lower the standard deviation of collected data. Moreover, the number of tests for each composite should be increased.

*Table 13. F-Test and t-Test of ultimate tensile strength of CNTs-reinforced composites compared to plain mortar.*

| MWCNT 0.2 % | | |
|---|---|---|
| | *Variable 1* | *Variable 2* |
| Mean | 863 | 878 |
| Variance | 6611 | 1897 |
| Observations | 9 | 3 |
| df | 8 | 2 |
| F | 3.484 | |
| P(F<=f) one-tail | 0.242 | |
| F Critical one-tail | 19.371 | |
| | Equal Variances | |

| MWCNT 0.4 % | | |
|---|---|---|
| | *Variable 1* | *Variable 2* |
| Mean | 863 | 1091 |
| Variance | 6611 | 14602 |
| Observations | 9 | 3 |
| df | 8 | 2 |
| F | 0.453 | |
| P(F<=f) one-tail | 0.172 | |
| F Critical one-tail | 0.224 | |
| | Unequal Variances | |

| MWCNT 0.6 % | | |
|---|---|---|
| | *Variable 1* | *Variable 2* |
| Mean | 863 | 1003 |
| Variance | 6611 | 2 |
| Observations | 9 | 2 |
| df | 8 | 1 |
| F | 2803.978 | |
| P(F<=f) one-tail | 0.015 | |
| F Critical one-tail | 238.883 | |
| | Unequal Variances | |

| SWCNT 0.2 % | | |
|---|---|---|
| | *Variable 1* | *Variable 2* |
| Mean | 863 | 1045 |
| Variance | 6611 | 17969 |
| Observations | 9 | 3 |
| df | 8 | 2 |
| F | 0.368 | |
| P(F<=f) one-tail | 0.126 | |
| F Critical one-tail | 0.224 | |
| | Unequal Variances | |

| SWCNT 0.4 % | | |
|---|---|---|
| | *Variable 1* | *Variable 2* |
| Mean | 863 | 913 |
| Variance | 6611 | 8560 |
| Observations | 9 | 3 |
| df | 8 | 2 |
| F | 0.772 | |
| P(F<=f) one-tail | 0.326 | |
| F Critical one-tail | 0.224 | |
| | Unequal Variances | |

| SWCNT 0.6 % | | |
|---|---|---|
| | *Variable 1* | *Variable 2* |
| Mean | 863 | 1006 |
| Variance | 6611 | 15243 |
| Observations | 9 | 3 |
| df | 8 | 2 |
| F | 0.434 | |
| P(F<=f) one-tail | 0.162 | |
| F Critical one-tail | 0.224 | |
| | Unequal Variances | |

| Hybrid 0.2 % | | |
|---|---|---|
| | *Variable 1* | *Variable 2* |
| Mean | 863 | 1092 |
| Variance | 6611 | 11906 |
| Observations | 9 | 3 |
| df | 8 | 2 |
| F | 0.555 | |
| P(F<=f) one-tail | 0.226 | |
| F Critical one-tail | 0.224 | |
| | Unequal Variances | |

| Hybrid 0.4 % | | |
|---|---|---|
| | *Variable 1* | *Variable 2* |
| Mean | 863 | 1177 |
| Variance | 6611 | 152807 |
| Observations | 9 | 3 |
| df | 8 | 2 |
| F | 0.0433 | |
| P(F<=f) one-tail | 0.0005 | |
| F Critical one-tail | 0.2243 | |
| | Equal Variances | |

| Hybrid 0.6 % | | |
|---|---|---|
| | *Variable 1* | *Variable 2* |
| Mean | 863 | 990 |
| Variance | 6611 | 141814 |
| Observations | 9 | 3 |
| df | 8 | 2 |
| F | 0.0466 | |
| P(F<=f) one-tail | 0.0006 | |
| F Critical one-tail | 0.2243 | |
| | Equal Variances | |
| | | |
| | | |
| | | |
| | | |

| MWCNT 0.2 % | | |
|---|---|---|
| | *Variable 1* | *Variable 2* |
| Mean | 863 | 878 |
| Variance | 6611 | 1897 |
| Observations | 9 | 3 |
| Pooled Variance | 5668 | |
| Hypothesized Mean Difference | 0 | |
| df | 10 | |
| t Stat | -0.290 | |
| P(T<=t) one-tail | 0.389 | |
| t Critical one-tail | 1.812 | |
| P(T<=t) two-tail | 0.778 | |
| t Critical two-tail | 2.228 | |
| t Stat is less than t Critical two-tail | | |

| MWCNT 0.4 % | | |
|---|---|---|
| | *Variable 1* | *Variable 2* |
| Mean | 863 | 1091 |
| Variance | 6611 | 14602 |
| Observations | 9 | 3 |
| Hypothesized Mean Difference | 0 | |
| df | 3 | |
| t Stat | -3.040 | |
| P(T<=t) one-tail | 0.028 | |
| t Critical one-tail | 2.353 | |
| P(T<=t) two-tail | 0.056 | |
| t Critical two-tail | 3.182 | |
| t Stat is less than t Critical two-tail | | |

| MWCNT 0.6 % | | |
|---|---|---|
| | *Variable 1* | *Variable 2* |
| Mean | 863 | 1003 |
| Variance | 6611 | 2 |
| Observations | 9 | 2 |
| Hypothesized Mean Difference | 0 | |
| df | 8 | |
| t Stat | -5.1628 | |
| P(T<=t) one-tail | 0.0004 | |
| t Critical one-tail | 1.8595 | |
| P(T<=t) two-tail | 0.0009 | |
| t Critical two-tail | 2.3060 | |
| t Stat is greater than t Critical two-tail | | |

| SWCNT 0.2 % | | |
|---|---|---|
| | *Variable 1* | *Variable 2* |
| Mean | 863 | 1045 |
| Variance | 6611 | 17969 |
| Observations | 9 | 3 |
| Hypothesized Mean Difference | 0 | |
| df | 3 | |
| t Stat | -2.219 | |
| P(T<=t) one-tail | 0.057 | |
| t Critical one-tail | 2.353 | |
| P(T<=t) two-tail | 0.113 | |
| t Critical two-tail | 3.182 | |
| t Stat is less than t Critical two-tail | | |

| SWCNT 0.4 % | | |
|---|---|---|
| | *Variable 1* | *Variable 2* |
| Mean | 863 | 913 |
| Variance | 6611 | 8560 |
| Observations | 9 | 3 |
| Hypothesized Mean Difference | 0 | |
| df | 3 | |
| t Stat | -0.830 | |
| P(T<=t) one-tail | 0.234 | |
| t Critical one-tail | 2.353 | |
| P(T<=t) two-tail | 0.467 | |
| t Critical two-tail | 3.182 | |
| t Stat is less than t Critical two-tail | | |

| SWCNT 0.6 % | | |
|---|---|---|
| | *Variable 1* | *Variable 2* |
| Mean | 863 | 1006 |
| Variance | 6611 | 15243 |
| Observations | 9 | 3 |
| Hypothesized Mean Difference | 0 | |
| df | 3 | |
| t Stat | -1.875 | |
| P(T<=t) one-tail | 0.079 | |
| t Critical one-tail | 2.353 | |
| P(T<=t) two-tail | 0.157 | |
| t Critical two-tail | 3.182 | |
| t Stat is less than t Critical two-tail | | |
| Hybrid 0.4 % | | |

| Hybrid 0.2 % | | |
|---|---|---|
| | *Variable 1* | *Variable 2* |
| Mean | 863 | 1092 |
| Variance | 6611 | 11906 |
| Observations | 9 | 3 |
| Hypothesized Mean Difference | 0 | |
| df | 3 | |
| t Stat | -3.333 | |
| P(T<=t) one-tail | 0.022 | |
| t Critical one-tail | 2.353 | |
| P(T<=t) two-tail | 0.045 | |
| t Critical two-tail | 3.182 | |
| t Stat is greater than t Critical two-tail | | |
| Hybrid 0.6 % | | |

| | *Variable 1* | *Variable 2* |
|---|---|---|
| Mean | 863 | 1177 |
| Variance | 6611 | 152807 |
| Observations | 9 | 3 |
| Pooled Variance | 35850 | |
| Hypothesized Mean Difference | 0 | |
| df | 10 | |
| t Stat | -2.485 | |
| P(T<=t) one-tail | 0.016 | |
| t Critical one-tail | 1.812 | |
| P(T<=t) two-tail | 0.032 | |
| t Critical two-tail | 2.228 | |
| t Stat is greater than t Critical two-tail | | |

| | *Variable 1* | *Variable 2* |
|---|---|---|
| Mean | 863 | 990 |
| Variance | 6611 | 141814 |
| Observations | 9 | 3 |
| Pooled Variance | 33651 | |
| Hypothesized Mean Difference | 0 | |
| df | 10 | |
| t Stat | -1.035 | |
| P(T<=t) one-tail | 0.163 | |
| t Critical one-tail | 1.812 | |
| P(T<=t) two-tail | 0.325 | |
| t Critical two-tail | 2.228 | |
| t Stat is less than t Critical two-tail | | |

## 4.10 Tensile Strength Mathematical Optimization

The data represented in the previous three graphs can be summarized in a 3D graph by introducing a new parameter. SW/ (SW+MW) denotes the amount of Single-Walled CNTs in the whole reinforcements added to the cement. When pure SWCNTs are used to reinforce the cement, this parameter equals unity. When pure MWCNTs are used to reinforce the cement, this parameter equals zero. In case of a 50% – 50% hybrids of CNTs that is investigated in this research, the SW/ (SW+MW) equals 0.5. To find the optimum mixture of MWCNTs and SWCNTs, which result in the optimum tensile strength, numerous cases between these three numbers are interpolated and the results are graphed. The numerical analysis is done using MATLAB software and the relevant code is presented in the appendices.

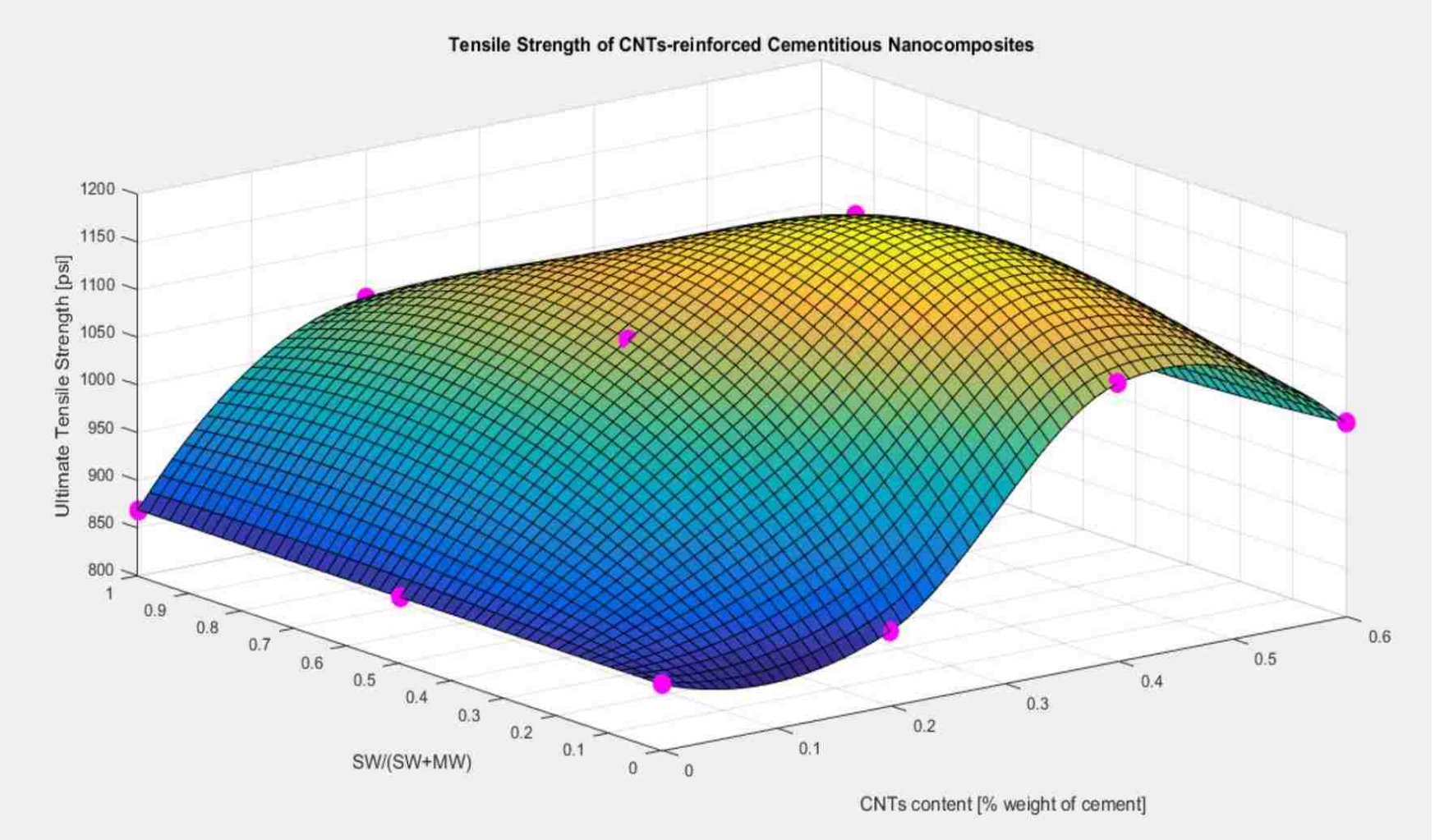


*Figure 82. Tensile strength of the full range of CNTs reinforced cementitious nanocomposites*

This graph shows that maximum tensile strength is achievable in a region around point (0.5, 0.5), which means the measured maximum tensile strength indeed provides the greatest toughness achievable with the materials used in this research. However, since Single-Walled CNTs are considerably more expensive than MWCNTs, one can mix 35% of SWCNTs with 65% of MWCNTs and reach almost the same toughness while saving about 13% in the cost of materials. The top view of this 3D graph illustrated in next picture clearly illustrates the optimum region.

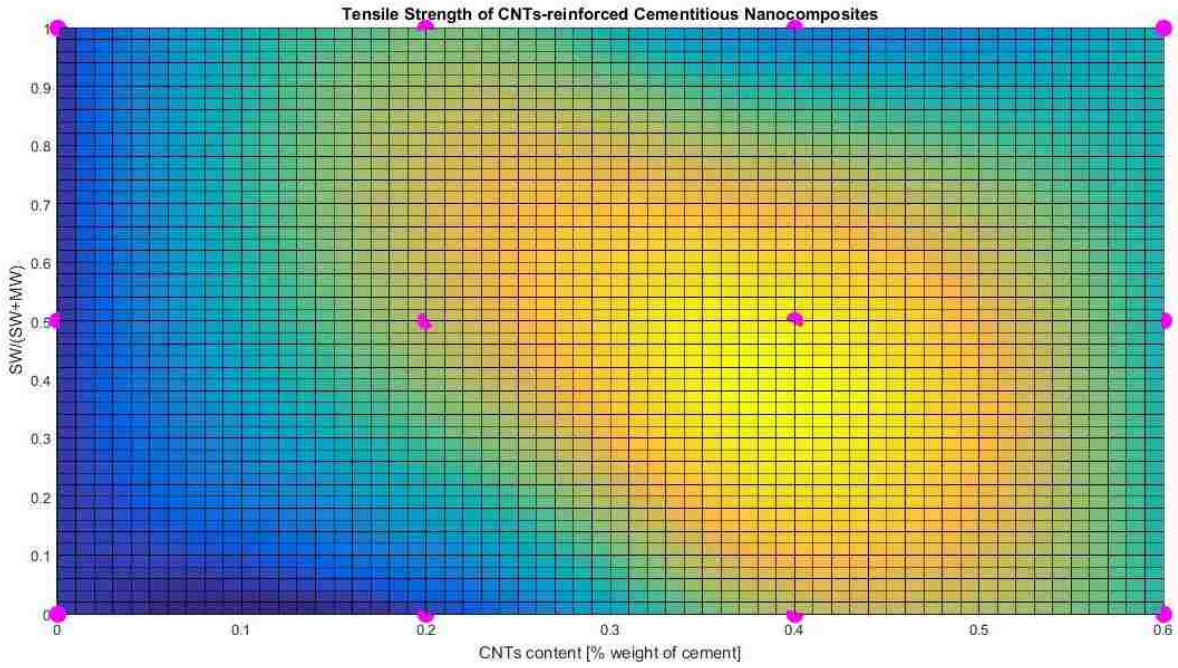


*Figure 83. Top view of tensile strength of the full range of CNTs reinforced cementitious nanocomposites*

## 4.11 Summary

In conclusion, the nanocomposite reinforced by 0.4 wt. % hybrid carbon nanotubes showed the maximum ultimate splitting tensile test. Failure mechanism also revealed more ductile behavior compared to other mixes. More importantly, after the first crack occurred, the specimens still carried load, which allowed more predictability of collapse for concrete structures--one of the superior mechanical properties of this nanocomposite. Statistical analysis, however, showed that in two-thirds of composites, the collected data are not convincing enough to conclude a significant difference between the ultimate tensile strength of the composite and that of plain mortar. To summarize, the results show considerable potential for enhancing the tensile strength of concrete by adding CNTs as reinforcement. However, more precise testing methods should be utilized to reach more repeatable results and lower the standard deviation of collected data. Moreover, the number of tests for each composite should be increase

# CHAPTER 5 RESULTS OF IMPACT TEST

## Phase III Study: Impact Experimental Analysis to Investigate the Behavior of MWCNTs, SWCNTs, and Hybrid Reinforced in Cementitious Nanocomposites

## 5.1 Introduction

Mortar, or cement paste, is a brittle material. However, it can carry a large amount of static load during structure service life, especially in compression cases. However, the behavior of cement mortar under high strain rate over a short period of time has not been fully investigated. Over the last few decades, adding fibers to cement matrix has changed the behavior of cement-based composite under dynamic loads and high strain rate tests. A review of the literature indicates that the behavior of carbon nanotube cementitious composites under impact loading has not yet been investigated. In this study, two issues were addressed, including the geometry of specimens, and the test standards of any adjusted procedure.

American Concrete Institute report (544.2R-89: Measurement of Properties of Fiber Reinforced Concrete (Reapproved 2009)) suggests a method to measure the mechanical properties of Fiber Reinforced Concrete (FRC) under impact loading [50-53]: ACI 544.2R-89 was initially developed for steel, glass, polymeric, and natural fibers cementitious composites. However, in the absence of standards specifically for CNT-reinforced cementitious composites, the ACI 544.2R-89 procedure could be followed. These standard lists are acceptable impact test methods for concrete specimens as follows:

- Weight pendulum (Charpy-type test)
- Drop weight test (singular/repeated impact)
- Constant strain test

- Projectile impact test
- Split-Hopkinson bar test
- Explosive test
- Instrumented pendulum impact test

Drop-weight test is the best method to measure small specimens. This test is based on the number of blows to appear in the specimen's initial visible crack. Additionally, the number of blows that cause the specimen's ultimate failure should be measured. The number of blows should be compared to determine different specimens' energy absorption. The cementitious composite with carbon nanotubes investigated in this study demonstrate the optimum percentage of CNTs that provided higher performance in general, but not necessarily the maximum impact strength.

## 5.2 Summary of Impact Test Literature Review

A summary of ACI-Committee 544 report [51-53] and four research papers, which followed the same procedure, is presented in the following table. This test was conducted, but one of drawback of ACI-Committee 544 is scattered results. Cement-based composite incorporating carbon nanotubes are expected to absorb an elevated level of energy due to its enhanced ductility compared to conventional cementitious composite [54].

*Table 14. Summary of Impact Test Literature Review for cementitious composite reinforced by fibers*

| No | Standard/ Procedure | Cementitious Composite Fibers | Drop Weight Test | | | | | Charpy Test |
|---|---|---|---|---|---|---|---|---|
| | | | Geometry | | Hammer | | | |
| | | | Diameter | Height | Wight | Diameter | Drop Height | |
| 1 | ACI-Committee 544 | Cementitious composite with CNTs | 2" (50mm) | 53/64" (21mm) | 3.3 lb. (1.51 kg) | 53/64" (21 mm) | 6" (152 mm) | NA |
| 2 | ACI-Committee 544 | Concrete, fiber reinforced concrete (FRC), steel, glass, polymeric, natural | 6" (152 mm) | 2 1/2" (63.5 mm) | 10 lb. (4.54 kg) | 2 1/2" (63.5 mm) | 18" (457 mm) | NA |
| 3 | Not mentioned, but it looks scaled down | Short discrete jute fiber (natural fiber) | 1 37/64" (40mm) | 6 11/16" (170mm) | 4.4 lb (2kg) | 1 37/64" (40 mm) | 6 11/16" (170mm) | NA |
| 4 | Followed ACI-Committee 544 | High-performance reinforced cement composite incorporating polypropylene fiber | 5 29/32" (150mm) | 2 1/2" (64mm) | 9.9 lb (4.5 kg) | 2" (50mm) | 18" (457 mm) | NA |
| 5 | | Glass fiber & steel ribbons | Steel ribbons 220×60×20 mm<br>Glass fibers 100×10×10 mm | | NA | NA | NA | Repeatedly blow until failure |

The Charpy and drop weight machine figures that other researchers used for cementitious composite with different fibers are shown below.

## 5.3 Suggested Impact Test Procedure

In this experiment, (ACI 544.2R-89) was used, but the geometry was scaled down from a 6-inch diameter and a 2-inch height, as shown in Table 15, below.

*Table 15. Suggest impact test procedure for cementitious nanocomposite*

| No | Standard/ Procedure | Material | Drop Weight Test | | | | |
|---|---|---|---|---|---|---|---|
| | | | Specimen | | Hammer | | |
| | | | Diameter | Height | Weight | Diameter | Drop Height |
| 1 | Modified ACI-Committee 544 | Cementitious Composite with CNTs | 2” (50 mm) | 25/32" (20 mm) | 1.36 lb (620 gr) | 53/64" (21 mm) | 4" (100 mm) |

1. Cast the cementitious composite incorporating CNTs in a 25x50 cylinder mold which is oiled prior to pure the cement mortar
2. Keep it in moist room for 24 hours to be hardened
3. Remold the specimen and keep it in moist room for 28 days
4. After 28 days the specimen reaches its ultimate strength and is ready for impact test
5. The impact load is applied with a 20-mm diameter steel hemispherical tub, 620 gr mass from 100 mm height
6. The number of blow is recorded until rupture. The first crack occurs to develop deterioration
7. The impact energy for each blow is calculated by the following equation

## 5.4 Impact Energy Equation

In compliance with the ACI 544 committee report, the static impact energy on a disk specimen for a hammer of 620 gr weight from 100 mm height is employed. The number of blows that induced failure was recorded and converted to energy using the following equation [51-53].

$$E_I = mgH\ N$$

Where

EI – Impact energy (N-m)

m – Drop hammer mass

H – Height of drop mass

N – Number of blows at ultimate failure

## 5.5 Impact Strength Test (Modified ACI 544.2R-89)

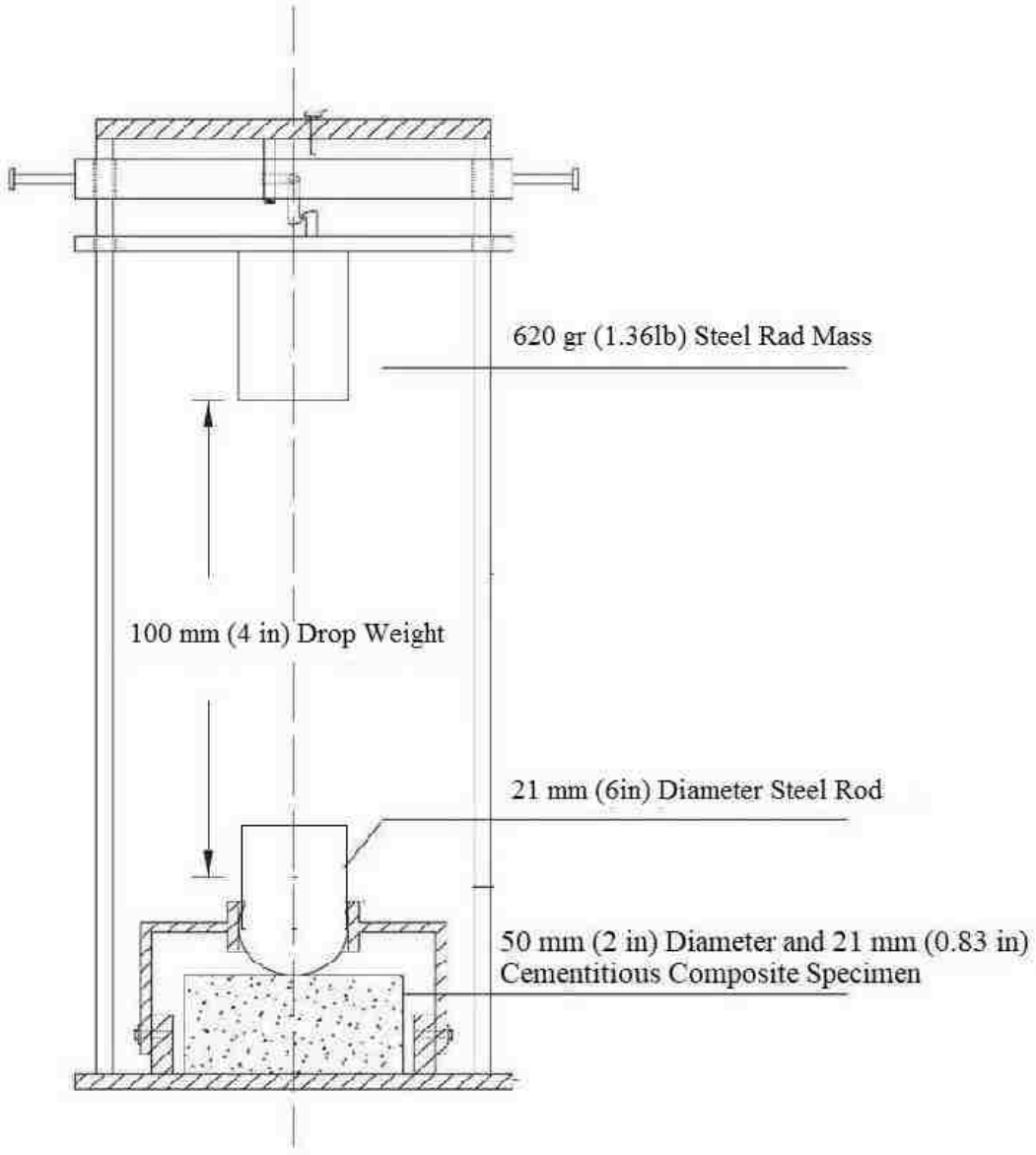


*Figure 84. Schematic diagram of general layout of the drop-weight tower for impact test*

## 5.6 Cementitious Composite with Different Mix Proportion

In this experiment, the specimens for the drop-weight impact test were scaled down to a cylinder with a 50-mm diameter and a 20-mm height.

*Table 16. Cylindrical drop-weight impact test sample geometry*

| **Impact Sample Geometry** | | |
|---|---|---|
| d | 50 | mm |
| h | 20 | mm |

Low-velocity impact test for cement matrices reinforced by multi-walled carbon nanotubes and water cement ratio of 0.4. MWCNTs sonicated for an hour. Sample A incorporated 0.2wt.% of MWCNTs; Sample B, 0.4wt%, and Sample C, 0.6wt%. Samples were mixed as shown in Table 17.

*Table 17. Mix design for cementitious nanocomposite incorporating multi-walled carbon nanotubes (all materials calculated based on weight of cement)*

| No. | MWCNTs | Materials | Sample (gr) | 3 Specimens |
|---|---|---|---|---|
| A-1 | 0.00wt% | Cement | 87.96 | 303.48 |
| B-1 | | MWCNTs | 0.00 | 0.00 |
| C-1 | | Water | 35.19 | 121.39 |
| A-2 | 0.20wt% | Cement | 87.96 | 303.48 |
| B-2 | | MWCNTs | 0.18 | 0.61 |
| C-2 | | Water | 35.19 | 121.39 |
| A-3 | 0.40wt% | Cement | 87.96 | 277.09 |
| B-3 | | MWCNTs | 0.35 | 1.11 |
| C-3 | | Water | 35.19 | 110.84 |
| A-4 | 0.60wt% | Cement | 87.96 | 271.81 |
| B-4 | | MWCNTs | 0.53 | 1.63 |
| C-4 | | Water | 35.19 | 108.72 |

*Table 18. Mix design for cementitious nanocomposite incorporating single-walled carbon nanotubes (all materials calculated based on weight of cement)*

| No. | SWCNTs | Materials | Sample (gr) | 3 Specimens |
|---|---|---|---|---|
| A-1 | 0.00wt% | Cement | 87.96 | 263.89 |
| B-1 | | SWCNTs | 0.00 | 0.00 |
| C-1 | | Water | 35.19 | 105.56 |
| A-2 | 0.20wt% | Cement | 87.96 | 263.89 |
| B-2 | | SWCNTs | 0.18 | 0.53 |
| C-2 | | Water | 35.19 | 105.56 |
| A-3 | 0.40wt% | Cement | 87.96 | 237.50 |
| B-3 | | SWCNTs | 0.35 | 0.95 |
| C-3 | | Water | 35.19 | 95.00 |
| A-4 | 0.60wt% | Cement | 87.96 | 237.50 |
| B-4 | | SWCNTs | 0.53 | 1.43 |
| C-4 | | Water | 35.19 | 95.00 |

*Table 19. Mix design for cementitious nanocomposite incorporating hybrid carbon nanotubes (all materials calculated based on weight of cement)*

| No. | SWCNTs | MWCNTs | Materials | Sample (gr) | 3 Specimens |
|---|---|---|---|---|---|
| A-1 | 0.00wt% | 0.00wt% | Cement | 87.96 | 211.12 |
| B-1 | | | CNT | 0.00 | 0.00 |
| C-1 | | | Water | 35.19 | 84.45 |
| A-2 | 0.10% | 0.10% | Cement | 87.96 | 211.12 |
| B-2 | 0.0880gr | 0.0880gr | SWCNTs | | |
| C-2 | 0.2639 | 0.2639 | Water | 35.19 | 84.45 |
| A-3 | 0.20% | 0.20% | Cement | 87.96 | 211.12 |
| B-3 | 0.1759gr | 0.1759gr | SWCNTs | | |
| C-3 | 0.5278 | 0.5278 | Water | 35.19 | 84.45 |
| A-4 | 0.30% | 0.30% | Cement | 87.96 | 211.12 |
| B-4 | 0.2639 | 0.2639 | SWCNTs | | |
| C-4 | 0.7917 | 0.7917 | Water | 35.19 | 84.45 |

*Table 20. Raw data for cementitious nanocomposite incorporating SWCNTs, MWCNTs and hybrid carbon nanotubes under drop-weight impact test with calculation of energy absorption of each specimen*

| No. | Name. | Specimen | CNT% | Number of Drop | Energy (J) | Specimen Volume ($mm^3$) | Specimen mass (gr) | Energy/Volume (kJ/m3) | Energy/mass (J/kg) |
|---|---|---|---|---|---|---|---|---|---|
| 1 | A-1 | C0 | 0% | 2 | 1.22 | 4.09E-05 | 88.3 | 30 | 13.8 |
| 2 | B-1 | C0 | 0% | 20 | 12.15 | 4.29E-05 | 92.7 | 283 | 131.0 |
| 3 | C-1 | C0 | 0% | 5 | 3.04 | 4.29E-05 | 92.7 | 71 | 32.8 |
| 4 | A-2 | MW1 | 0.20% | 1 | 0.61 | 4.09E-05 | 88.3 | 15 | 6.9 |
| 5 | B-2 | MW1 | 0.20% | 28 | 17.01 | 4.09E-05 | 88.3 | 416 | 192.6 |
| 6 | C-2 | MW1 | 0.20% | 22 | 13.37 | 4.09E-05 | 88.3 | 327 | 151.3 |
| 7 | A-3 | MW2 | 0.40% | 55 | 33.42 | 4.29E-05 | 92.7 | 779 | 360.3 |
| 8 | B-3 | MW2 | 0.40% | 85 | 51.65 | 4.29E-05 | 92.7 | 1,204 | 556.8 |
| 9 | C-3 | MW2 | 0.40% | 6 | 3.65 | 4.29E-05 | 92.7 | 85 | 39.3 |
| 10 | A-4 | MW3 | 0.60% | 300 | 226.03 | 4.32E-05 | 93.4 | 5,232 | 2420.2 |
| 11 | B-4 | MW3 | 0.60% | 4 | 4.19 | 4.32E-05 | 93.4 | 97 | 44.9 |
| 12 | C-4 | MW3 | 0.60% | 2 | 1.22 | 4.52E-05 | 90 | 27 | 13.5 |
| 13 | A-2 | SW1 | 0.20% | 310 | 188.36 | 4.42E-05 | 84.5 | 4,264 | 2229.1 |
| 14 | B-2 | SW1 | 0.20% | 15 | 9.11 | 3.93E-05 | 77 | 232 | 118.4 |
| 15 | C-2 | SW1 | 0.20% | 4 | 2.43 | 4.32E-05 | 85.5 | 56 | 28.4 |
| 16 | A-3 | SW2 | 0.40% | 59 | 35.85 | 4.32E-05 | 83.5 | 830 | 429.3 |
| 17 | B-3 | SW2 | 0.40% | 7 | 4.25 | 4.42E-05 | 84 | 96 | 50.6 |
| 18 | C-3 | SW2 | 0.40% | 5 | 3.04 | 4.09E-05 | 76.5 | 74 | 39.7 |

| | | | | | | | | | |
|---|---|---|---|---|---|---|---|---|---|
| 19 | A-4 | SW3 | 0.60% | 453 | 275.24 | 4.12E-05 | 78 | 6,675 | 3528.8 |
| 20 | B-4 | SW3 | 0.60% | 155 | 94.18 | 4.42E-05 | 84 | 2,132 | 1121.2 |
| 21 | C-4 | SW3 | 0.60% | 9 | 5.47 | 3.93E-05 | 75.5 | 139 | 72.4 |
| 22 | A-2 | HB 1 | 0.20% | 6 | 3.65 | 4.12E-05 | 78.5 | 88 | 46.4 |
| 23 | B-2 | HB 1 | 0.20% | 179 | 108.76 | 4.52E-05 | 86.5 | 2,408 | 1257.3 |
| 24 | C-2 | HB 1 | 0.20% | 253 | 153.72 | 4.42E-05 | 85.5 | 3,480 | 1797.9 |
| 25 | A-3 | HB 2 | 0.40% | 987 | 599.70 | 4.71E-05 | 91 | 12,726 | 6590.1 |
| 26 | B-3 | HB 2 | 0.40% | 8 | 4.86 | 4.22E-05 | 81.5 | 115 | 59.6 |
| 27 | C-3 | HB 2 | 0.40% | 3 | 1.82 | 4.32E-05 | 85 | 42 | 21.4 |
| 28 | A-4 | HB 3 | 0.60% | 147 | 89.32 | 4.12E-05 | 87 | 2,166 | 1026.6 |
| 29 | B-4 | HB 3 | 0.60% | 2 | 1.22 | 4.52E-05 | 80 | 27 | 15.2 |
| 30 | C-4 | HB 3 | 0.60% | 13 | 7.90 | 4.32E-05 | 81 | 183 | 97.5 |

*Table 21. Raw data for geometry of cementitious nanocomposite incorporating SWCNTs, MWCNTs and hybrid carbon nanotubes under drop-weight impact test*

| No. | Name. | Specimen | CNT% | Number of Drop | t (mm) | D (mm) | h (mm) | Drop mass(gr) |
|---|---|---|---|---|---|---|---|---|
| 1 | A-1 | C0 | 0% | 2 | 20 | 51 | 100 | 620 |
| 2 | B-1 | C0 | 0% | 20 | 21 | 51 | 100 | 620 |
| 3 | C-1 | C0 | 0% | 5 | 21 | 51 | 100 | 620 |
| 4 | A-2 | MW1 | 0.20% | 1 | 20 | 51 | 100 | 620 |
| 5 | B-2 | MW1 | 0.20% | 28 | 20 | 51 | 100 | 620 |
| 6 | C-2 | MW1 | 0.20% | 22 | 20 | 51 | 100 | 620 |
| 7 | A-3 | MW2 | 0.40% | 55 | 21 | 51 | 100 | 620 |
| 8 | B-3 | MW2 | 0.40% | 85 | 21 | 51 | 100 | 620 |
| 9 | C-3 | MW2 | 0.40% | 6 | 21 | 51 | 100 | 620 |
| 10 | A-4 | MW3 | 0.60% | 300 | 22 | 50 | 122.5 | 620 |
| 11 | B-4 | MW3 | 0.60% | 4 | 22 | 50 | 172.5 | 620 |
| 12 | C-4 | MW3 | 0.60% | 2 | 23 | 50 | 100 | 620 |
| 13 | A-2 | SW1 | 0.20% | 310 | 22.5 | 50 | 100 | 620 |
| 14 | B-2 | SW1 | 0.20% | 15 | 20 | 50 | 100 | 620 |
| 15 | C-2 | SW1 | 0.20% | 4 | 22 | 50 | 100 | 620 |
| 16 | A-3 | SW2 | 0.40% | 59 | 22 | 50 | 100 | 620 |
| 17 | B-3 | SW2 | 0.40% | 7 | 22.5 | 50 | 100 | 620 |
| 18 | C-3 | SW2 | 0.40% | 5 | 20 | 51 | 100 | 620 |
| 19 | A-4 | SW3 | 0.60% | 453 | 21 | 50 | 100 | 620 |
| 20 | B-4 | SW3 | 0.60% | 155 | 22.5 | 50 | 100 | 620 |
| 21 | C-4 | SW3 | 0.60% | 9 | 20 | 50 | 100 | 620 |
| 22 | A-2 | HB 1 | 0.20% | 6 | 21 | 50 | 100 | 620 |
| 23 | B-2 | HB 1 | 0.20% | 179 | 23 | 50 | 100 | 620 |
| 24 | C-2 | HB 1 | 0.20% | 253 | 22.5 | 50 | 100 | 620 |
| 25 | A-3 | HB 2 | 0.40% | 987 | 24 | 50 | 100 | 620 |

| | | | | | | | | |
|---|---|---|---|---|---|---|---|---|
| 26 | B-3 | HB 2 | 0.40% | 8 | 21.5 | 50 | 100 | 620 |
| 27 | C-3 | HB 2 | 0.40% | 3 | 22 | 50 | 100 | 620 |
| 28 | A-4 | HB 3 | 0.60% | 147 | 21 | 50 | 100 | 620 |
| 29 | B-4 | HB 3 | 0.60% | 2 | 23 | 50 | 100 | 620 |
| 30 | C-4 | HB 3 | 0.60% | 13 | 22 | 50 | 100 | 620 |

*Table 22 F-Test and t-Test of impact toughness of CNTs-reinforced composites compared to plain mortar4*

| MWCNT 0.2 % | | |
|---|---|---|
| | *Variable 1* | *Variable 2* |
| Mean | 128 | 253 |
| Variance | 18516 | 44454 |
| Observations | 3 | 3 |
| df | 2 | 2 |
| F | 0.417 | |
| P(F<=f) one-tail | 0.294 | |
| F Critical one-tail | 0.053 | |
| Unequal Variances | | |

| MWCNT 0.4 % | | |
|---|---|---|
| | *Variable 1* | *Variable 2* |
| Mean | 128 | 689 |
| Variance | 18516 | 319025 |
| Observations | 3 | 3 |
| df | 2 | 2 |
| F | 0.058 | |
| P(F<=f) one-tail | 0.055 | |
| F Critical one-tail | 0.053 | |
| Unequal Variances | | |

| MWCNT 0.6 % | | |
|---|---|---|
| | *Variable 1* | *Variable 2* |
| Mean | 128 | 1785 |
| Variance | 18516 | 8912605 |
| Observations | 3 | 3 |
| df | 2 | 2 |
| F | 0.002078 | |
| P(F<=f) one-tail | 0.002073 | |
| F Critical one-tail | 0.052632 | |
| Equal Variances | | |

| SWCNT 0.2 % | | |
|---|---|---|
| | *Variable 1* | *Variable 2* |
| Mean | 128 | 1517 |
| Variance | 18516 | 5664030 |
| Observations | 3 | 3 |
| df | 2 | 2 |
| F | 0.00327 | |
| P(F<=f) one-tail | 0.00326 | |
| F Critical one-tail | 0.05263 | |
| Equal Variances | | |

| SWCNT 0.4 % | | |
|---|---|---|
| | *Variable 1* | *Variable 2* |
| Mean | 128 | 334 |
| Variance | 18516 | 184914 |
| Observations | 3 | 3 |
| df | 2 | 2 |
| F | 0.100 | |
| P(F<=f) one-tail | 0.091 | |
| F Critical one-tail | 0.053 | |
| Unequal Variances | | |

| SWCNT 0.6 % | | |
|---|---|---|
| | *Variable 1* | *Variable 2* |
| Mean | 128 | 2982 |
| Variance | 18516 | 11222073 |
| Observations | 3 | 3 |
| df | 2 | 2 |
| F | 0.001650 | |
| P(F<=f) one-tail | 0.001647 | |
| F Critical one-tail | 0.052632 | |
| Equal Variances | | |

| Hybrid 0.2 % | | |
|---|---|---|
| | *Variable 1* | *Variable 2* |
| Mean | 128 | 1992 |
| Variance | 18516 | 3004915 |
| Observations | 3 | 3 |
| df | 2 | 2 |
| F | 0.00616 | |
| P(F<=f) one-tail | 0.00612 | |
| F Critical one-tail | 0.05263 | |
| Equal Variances | | |

| Hybrid 0.4 % | | |
|---|---|---|
| | *Variable 1* | *Variable 2* |
| Mean | 128 | 4294 |
| Variance | 18516 | 53320106 |
| Observations | 3 | 3 |
| df | 2 | 2 |
| F | 0.0003473 | |
| P(F<=f) one-tail | 0.0003471 | |
| F Critical one-tail | 0.0526316 | |
| Equal Variances | | |

| Hybrid 0.6 % | | |
|---|---|---|
| | *Variable 1* | *Variable 2* |
| Mean | 128 | 792 |
| Variance | 18516 | 1422337 |
| Observations | 3 | 3 |
| df | 2 | 2 |
| F | 0.0130 | |
| P(F<=f) one-tail | 0.0129 | |
| F Critical one-tail | 0.0526 | |
| Equal Variances | | |

| MWCNT 0.2 % | | |
|---|---|---|
| | *Variable 1* | *Variable 2* |
| Mean | 128 | 253 |
| Variance | 18516 | 44454 |
| Observations | 3 | 3 |
| Hypothesized Mean Difference | 0 | |
| df | 3 | |
| t Stat | -0.862 | |
| P(T<=t) one-tail | 0.226 | |
| t Critical one-tail | 2.353 | |
| P(T<=t) two-tail | 0.452 | |
| t Critical two-tail | 3.182 | |
| t Stat is less than t Critical two-tail | | |

| MWCNT 0.4 % | | | | MWCNT 0.6 % | | |
|---|---|---|---|---|---|---|
| | *Variable 1* | *Variable 2* | | | *Variable 1* | *Variable 2* |
| Mean | 128 | 689 | | Mean | 128 | 1785 |
| Variance | 18516 | 319025 | | Variance | 18516 | 8912605 |
| Observations | 3 | 3 | | Observations | 3 | 3 |
| Hypothesized Mean Difference | 0 | | | Pooled Variance | 4465561 | |
| df | 2 | | | Hypothesized Mean Difference | 0 | |
| t Stat | -1.674 | | | df | 4 | |
| P(T<=t) one-tail | 0.118 | | | t Stat | -0.961 | |
| t Critical one-tail | 2.920 | | | P(T<=t) one-tail | 0.196 | |
| P(T<=t) two-tail | 0.236 | | | t Critical one-tail | 2.132 | |
| t Critical two-tail | 4.303 | | | P(T<=t) two-tail | 0.391 | |
| t Stat is less than t Critical two-tail | | | | t Critical two-tail | 2.776 | |
| | | | | t Stat is less than t Critical two-tail | | |

| SWCNT 0.2 % | | | | SWCNT 0.4 % | | |
|---|---|---|---|---|---|---|
| | *Variable 1* | *Variable 2* | | | *Variable 1* | *Variable 2* |
| Mean | 128 | 1517 | | Mean | 128 | 334 |
| Variance | 18516 | 5664030 | | Variance | 18516 | 184914 |
| Observations | 3 | 3 | | Observations | 3 | 3 |
| Pooled Variance | 2841273 | | | Hypothesized Mean Difference | 0 | |
| Hypothesized Mean Difference | 0 | | | df | 2 | |
| df | 4 | | | t Stat | -0.789 | |
| t Stat | -1.009 | | | P(T<=t) one-tail | 0.256 | |
| P(T<=t) one-tail | 0.185 | | | t Critical one-tail | 2.920 | |
| t Critical one-tail | 2.132 | | | P(T<=t) two-tail | 0.513 | |
| P(T<=t) two-tail | 0.370 | | | t Critical two-tail | 4.303 | |
| t Critical two-tail | 2.776 | | | t Stat is less than t Critical two-tail | | |
| t Stat is less than t Critical two-tail | | | | | | |

| SWCNT 0.6 % | | | | Hybrid 0.2 % | | |
|---|---|---|---|---|---|---|
| | *Variable 1* | *Variable 2* | | | *Variable 1* | *Variable 2* |
| Mean | 128 | 2982 | | Mean | 128 | 1992 |
| Variance | 18516 | 11222073 | | Variance | 18516 | 3004915 |
| Observations | 3 | 3 | | Observations | 3 | 3 |
| Pooled Variance | 5620295 | | | Pooled Variance | 1511715 | |
| Hypothesized Mean Difference | 0 | | | Hypothesized Mean Difference | 0 | |
| df | 4 | | | df | 4 | |
| t Stat | -1.474 | | | t Stat | -1.857 | |
| P(T<=t) one-tail | 0.107 | | | P(T<=t) one-tail | 0.068 | |
| t Critical one-tail | 2.132 | | | t Critical one-tail | 2.132 | |
| P(T<=t) two-tail | 0.214 | | | P(T<=t) two-tail | 0.137 | |
| t Critical two-tail | 2.776 | | | t Critical two-tail | 2.776 | |
| t Stat is less than t Critical two-tail | | | | t Stat is less than t Critical two-tail | | |

| Hybrid 0.4 % | | |
|---|---|---|
| | *Variable 1* | *Variable 2* |
| Mean | 128 | 4294 |
| Variance | 18516 | 53320106 |
| Observations | 3 | 3 |
| Pooled Variance | 26669311 | |
| Hypothesized Mean Difference | 0 | |
| df | 4 | |
| t Stat | -0.988 | |
| P(T<=t) one-tail | 0.190 | |
| t Critical one-tail | 2.132 | |
| P(T<=t) two-tail | 0.379 | |
| t Critical two-tail | 2.776 | |
| t Stat is less than t Critical two-tail | | |

| Hybrid 0.6% | | |
|---|---|---|
| | *Variable 1* | *Variable 2* |
| Mean | 128 | 792 |
| Variance | 18516 | 1422337 |
| Observations | 3 | 3 |
| Pooled Variance | 720427 | |
| Hypothesized Mean Difference | 0 | |
| df | 4 | |
| t Stat | -0.958 | |
| P(T<=t) one-tail | 0.196 | |
| t Critical one-tail | 2.132 | |
| P(T<=t) two-tail | 0.392 | |
| t Critical two-tail | 2.776 | |
| t Stat is less than t Critical two-tail | | |

To have a better sense of the impact test results, the data recorded in the previous table were statistically analyzed and tabulated as follows.

*Table 23. Average, maximum, minimum and standard deviation for cementitious nanocomposite impact toughness of cement mortar and cementitious nanocomposite incorporation MWCNTs, SWCNTs and hybrid CNTs (0.2wt%, 0.4wt%, and 0.6wt% CNTs)*

| **Cement Mortar** | | | | |
|---|---|---|---|---|
| **CNTs** | Average | Maximum | Minimum | Standard Deviation |
| 0.0 % | 128 | 283 | 30 | 111 |

| **Multi-Walled** | | | | |
|---|---|---|---|---|
| **CNTs** | Average | Maximum | Minimum | Standard Deviation |
| 0.20 wt.% | 253 | 416 | 15 | 172 |
| 0.40 wt.% | 689 | 1,204 | 85 | 461 |
| 0.60 wt.% | 1,785 | 5,232 | 27 | 2,438 |

| **Single-Walled** | | | | |
|---|---|---|---|---|
| **CNTs** | Average | Maximum | Minimum | Standard Deviation |
| 0.20 wt.% | 1,517 | 4,264 | 56 | 1,943 |
| 0.40 wt.% | 334 | 830 | 74 | 351 |
| 0.60 wt.% | 2,982 | 6,675 | 139 | 2,735 |

| **Hybrid** | | | | |
|---|---|---|---|---|
| **CNTs** | Average | Maximum | Minimum | Standard Deviation |
| 0.20 wt.% | 1,992 | 3,480 | 88 | 1,415 |
| 0.40 wt.% | 4,294 | 12,726 | 42 | 5,962 |
| 0.60 wt.% | 792 | 2,166 | 27 | 974 |

In the next step the average, maximum, and minimum impact toughness were reorganized and graphed.

*Table 24. Average low-velocity impact toughness comparison for cementitious nanocomposite reinforced by MWCNTs, SWCNTs and hybrid CNTs*

| CNTs | Average Low-Velocity Imact Toughness (kJ/m$^3$) | | |
|---|---|---|---|
| Percentage | Multi-Walled | Single-Walled | Hybrid |
| **0.20 wt.%** | 253 | 1,517 | 1,992 |
| **0.40 wt.%** | 689 | 334 | 4,294 |
| **0.60 wt.%** | 1,764 | 2,982 | 792 |

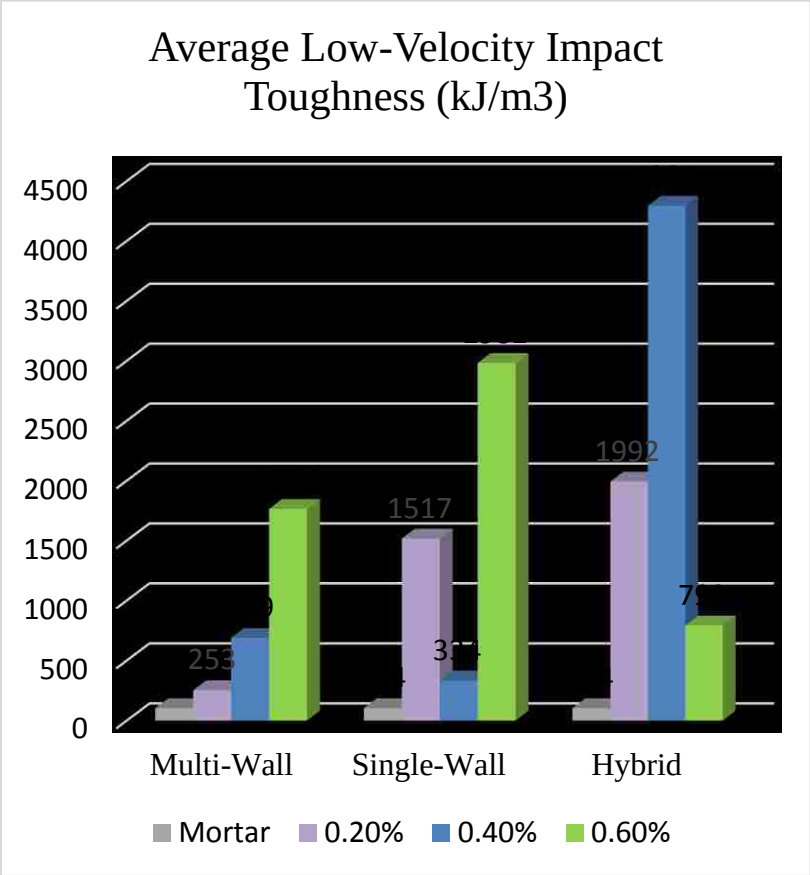


*Figure 85. Average low-velocity impact toughness comparison for cementitious nanocomposite reinforced by MWCNTs, SWCNTs and hybrid CNTs*

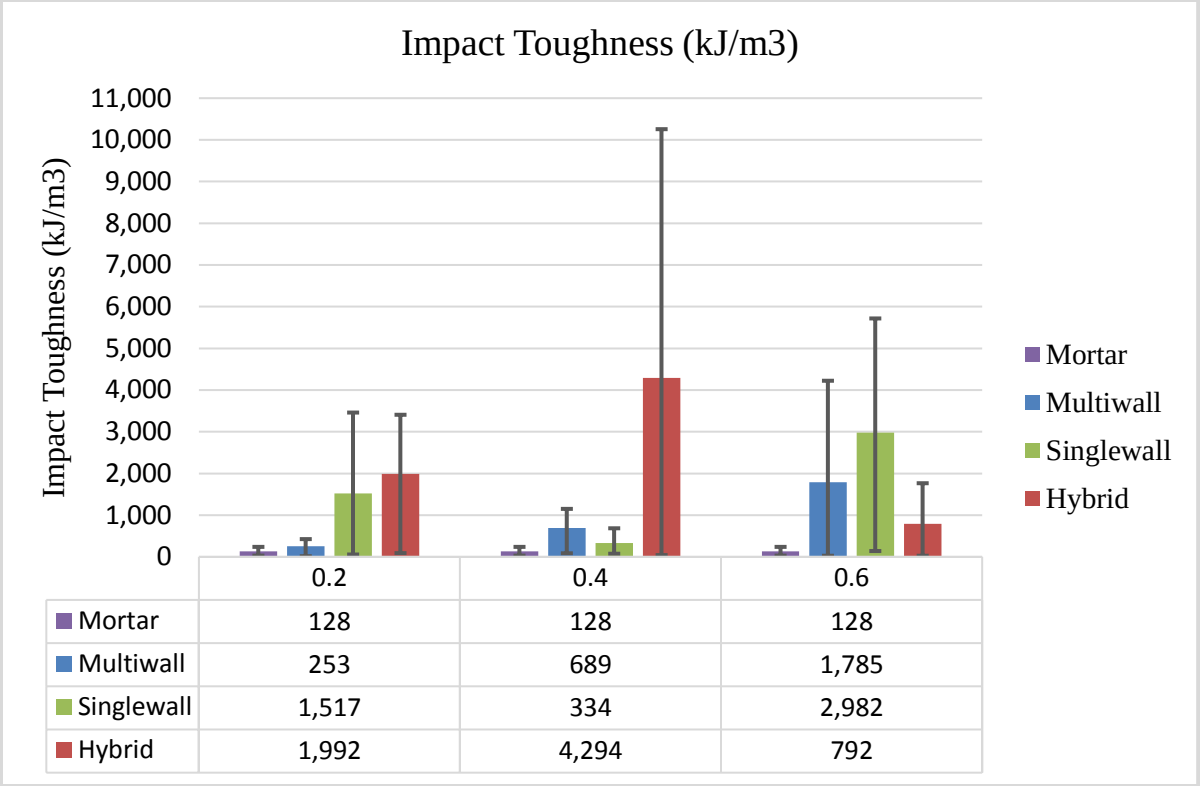


| | 0.2 | 0.4 | 0.6 |
|---|---|---|---|
| Mortar | 128 | 128 | 128 |
| Multiwall | 253 | 689 | 1,785 |
| Singlewall | 1,517 | 334 | 2,982 |
| Hybrid | 1,992 | 4,294 | 792 |

*Figure 86. Average low-velocity impact toughness with error rebar comparison for cementitious nanocomposite reinforced by MWCNTs, SWCNTs and hybrid CNTs*

The error rebars on the impact test graph demonstrate STD on upper limit, and minimum value on the lower limit.

Figure 88 illustrates the average low-velocity impact toughness of cementitious nanocomposites reinforced by multi-walled (MWCNTs), single-walled (SWCNTs), and hybrid (50-50) (HCNTs) carbon nanotubes compared to the plain cement mortar. In general, this graph shows that while both MWCNTs and SWCNTs enhance the impact toughness of cementitious composite, a hybrid of these two types of CNTs increases the impact toughness considerably more than either of them singly. A possible explanation for this quality lays in the size and shape of CNTs. Although MWCNTs are on average 2.3 times longer than SWCNTs, their average outer diameter is 6 times greater than that of SWCNTs. Considering the range of length and OD, the range of aspect ratio of the two types of CNTs are calculated as following table.

*Table 25. Type of carbon nanotubes*

| Type of Carbon Nanotubes | SWCNTs | MWCNTs |
|---|---|---|
| OD (outer diameter) | 1-4 | 30-50 |
| Length | 5-30 | 10-20 |
| Aspect Ratio | 1.25 - 30 | 1.5 - 5 |

While the average aspect ratio of MWCTs is 3.25, that of SWCNTs is 15.62. Hence, from a fibers categorization point of view, MWCNTs are indeed short fibers in contrast with SWCNTs which can be categorized under long fibers class.

Given that difference in fiber length, the mechanism of reinforcement by multi-walled CNTs is more or less close to particle reinforcements. SWCNTs on the other hand, work as long fibers and hence expectedly provide higher mechanical properties compared to MWCNTs as the same weight percentage of reinforcements. A hybrid of both types of CNTs apparently benefits from both mechanisms and hence is more successful in controlling the failure mechanism. This results in HCNTs' superior impact toughness compared to either MWCNTs or SWCNTs.

Figure 88 illustrates the maximum of low-velocity impact toughness of cementitious nanocomposites reinforced by multi-walled, single-walled, and hybrid (50-50) carbon nanotubes in comparison to the plain cement mortar. In general, this graph shows similar patterns to those found in Figure 3. The 0.40 wt.% hybrid CNTs nanocomposite set a record of 45 times stronger than plain cement mortar in this graph, which indicates that the maximum energy absorbtion achievable by this type of cementitous nanocomposite is up to 45 times greater than the maximum energy absorption of plain cement mortar.

*Table 26. Maximum low-velocity impact toughness (kJ/m3) for cementitious nanocomposite reinforced by MWCNTs, SWCNTs and hybrid CNTs*

| CNTs | Maximum Low-Velocity Imact Toughness ($kJ/m^3$) | | |
|---|---|---|---|
| Percentage | Multi-Walled | Single-Walled | Hybrid |
| **0.20 wt.%** | 416 | 4,264 | 3,480 |
| **0.40 wt.%** | 1,204 | 830 | 12,726 |
| **0.60 wt.%** | 5,232 | 6,675 | 2,166 |

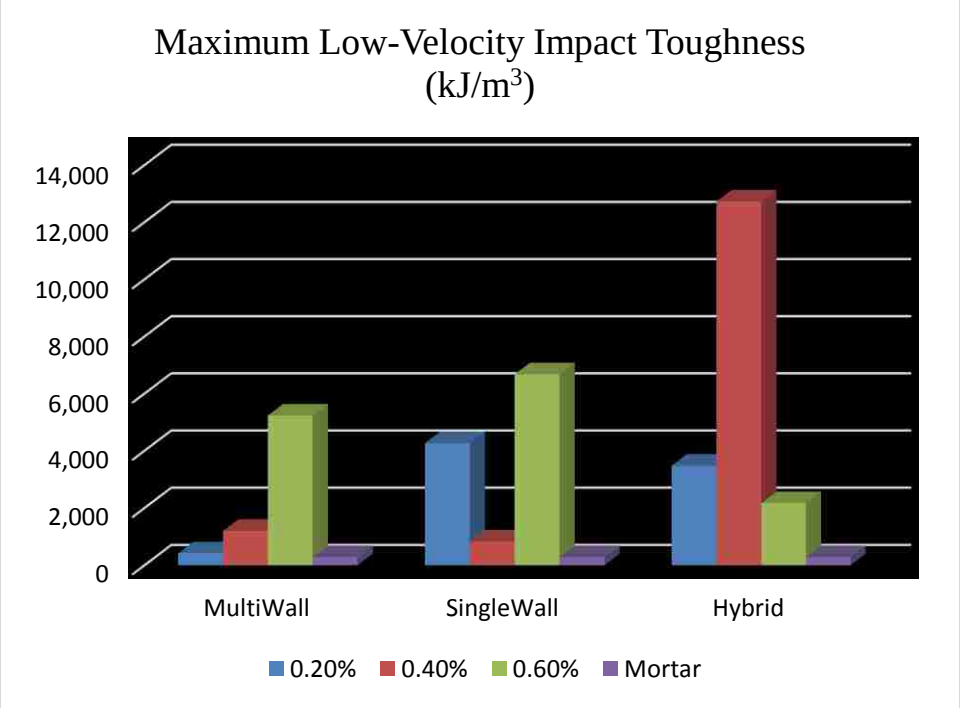


*Figure 87. Maximum low-velocity impact toughness comparison for cementitious nanocomposite reinforced by MWCNTs, SWCNTs and hybrid CNTs*

In contrast to the average and maximum toughness, the minimum toughness of MWCNTs, SWCNTs, and hybrid CNTs are very close and comparable to plain cement mortar. This observation might be explained by referring to the inhomogeneity of cementitious nanocomposites. Indeed, reinforcements are barriers that block the movement of dislocations and hence delay the growth of fracture. But regardless of the causes of the inhomogeneity, its result is to create regions and planes in the matrix composed of plain cement mortar

with no reinforcement. Micro cracks can easily nucleate in such regions and rapidly grow and propagate along the weakest planes (i.e., those containing no reinforcements). In brief, in such cases, there are pure cement mortar regions that fail under impact load long before other regions even approach failure.

*Table 27. Minimum Low-Velocity Impact Toughness (kJ/m3) for cementitious nanocomposite reinforced by MWCNTs, SWCNTs and hybrid CNTs*

| CNTs | Minimum Low-Velocity Imact Toughness (kJ/m$^3$) | | |
|---|---|---|---|
| Percentage | Multi-Walled | Single-Walled | Hybrid |
| **0.20 wt.%** | 15 | 56 | 88 |
| **0.40 wt.%** | 85 | 74 | 42 |
| **0.60 wt.%** | 27 | 139 | 27 |

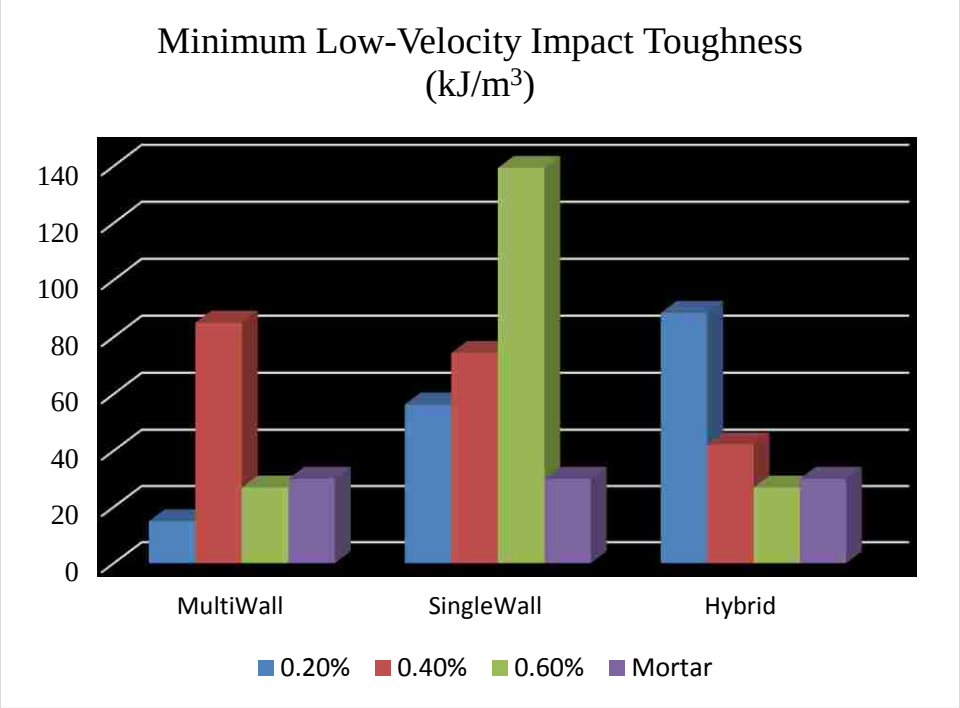


*Figure 88. Minimum low-velocity impact toughness comparison for cementitious nanocomposite reinforced by MWCNTs, SWCNTs and hybrid CNTs*

Regarding the high standard deviations, t-Test was conducted using Microsoft Excel software to discern whether the experimental results are statistically convincing or not. The null hypothesis of this statistical analysis is that there is no meaningful difference between the mean impact toughness of the composite and the plain mortar. At the first step, the F-test was conducted to determine if the standard deviation of each composite equals the STD of the mortar. Then the outcome of each F-test was used to determine the suitable t-Test method for each composite. Lastly, two-sample t-Test was conducted for Alpha = 0.05. The results of F-tests and t-Tests are summarized in Table 7. At each table variable 1 with 9 observations denotes the plain mortar while variable 2 with only 3 observations refers to the composite. A two-tail test was conducted for each composite.

lf $|t_{ststst}| > t_{critical}$ two-tail, we reject the null hypothesis, so, despite the considerable increase in the toughness of concrete, the observed data are not statistically convincing. More precise testing methods should be utilized to reach more repeatable results and lower the standard deviation of the collected data. Moreover, the number of tests for each composite should be increased.

## 5.7 Impact Test Mathematical Optimization

The data represented in the previous three graphs can be summarized in a 3D graph by introducing a new parameter. SW/(SW+MW) denotes the amount of Single-Walled CNTs in the whole reinforcements added to the cement. When pure SWCNTs are used to reinforce the cement, this parameter equals unity. When pure MWCNTs are used to reinforce the cement, this parameter equals zero. In case of a 50% – 50% hybrids of CNTs, which is investigated in this research, the SW/ (SW+MW) equals 0.5. To find the optimum mixture of MWCNTs and SWCNTs, which result in the optimum impact toughness, numerous cases in between these three numbers were interpolated and the results were graphed. The numerical analysis was done using MATLAB software and the relevant code was presented in the appendices.

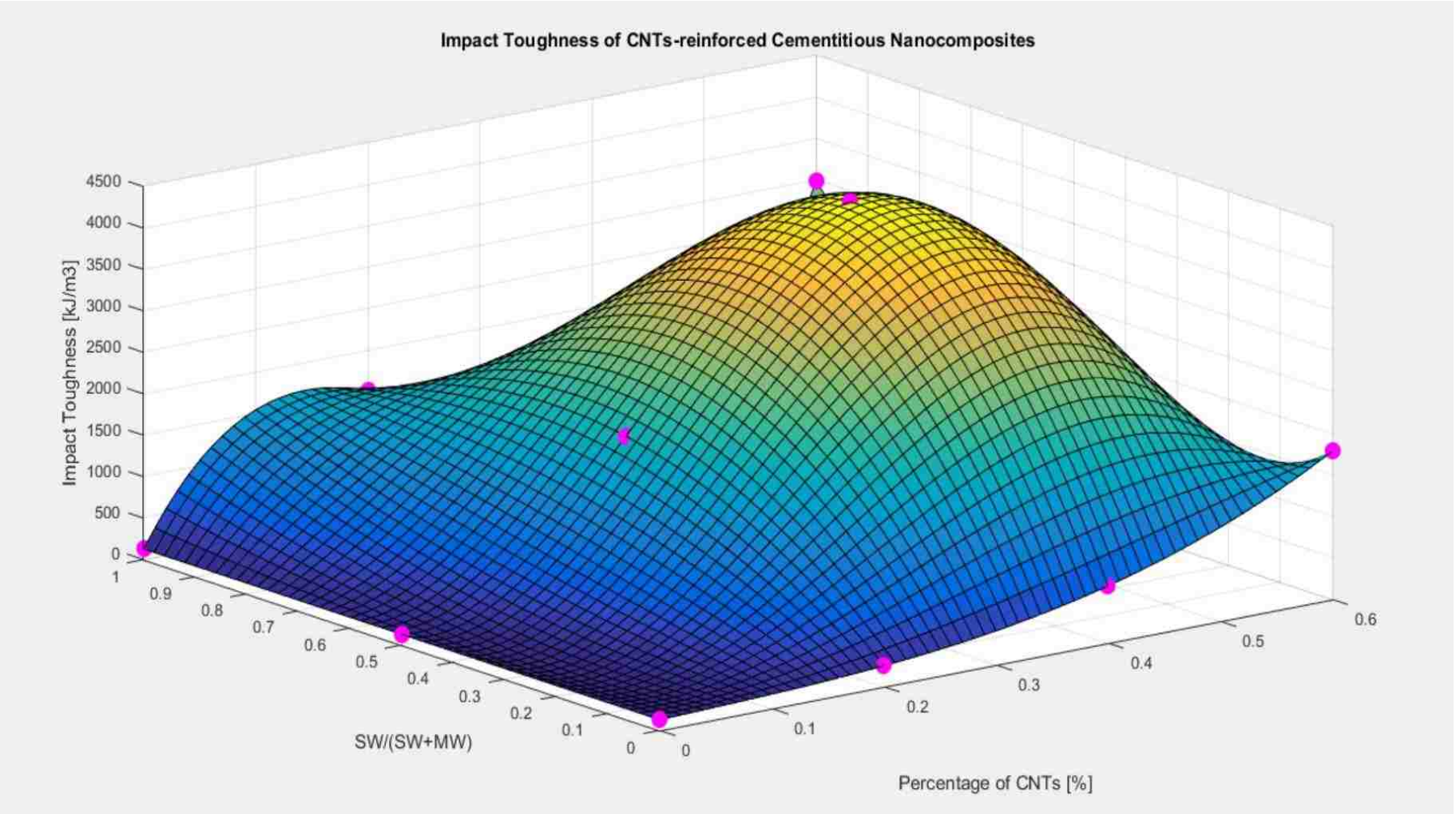


*Figure 89. Low-velocity impact toughness of the full range of CNTs reinforced cementitious nanocomposites*

This graph shows that maximum toughness is achievable in a region around point (0.5, 0.5) which means the measured maximum impact toughness is indeed the best toughness achievable with the materials used in this research. However, since the Single-Walled CNTs are considerably more expensive than MWCNTs, one can mix 35% of SWCNTs with 65% of MWCNTs and reach almost the same toughness while saving about 13% in the cost of materials. The top view of this 3D graph illustrated in next picture clearly illustrates the optimum region.

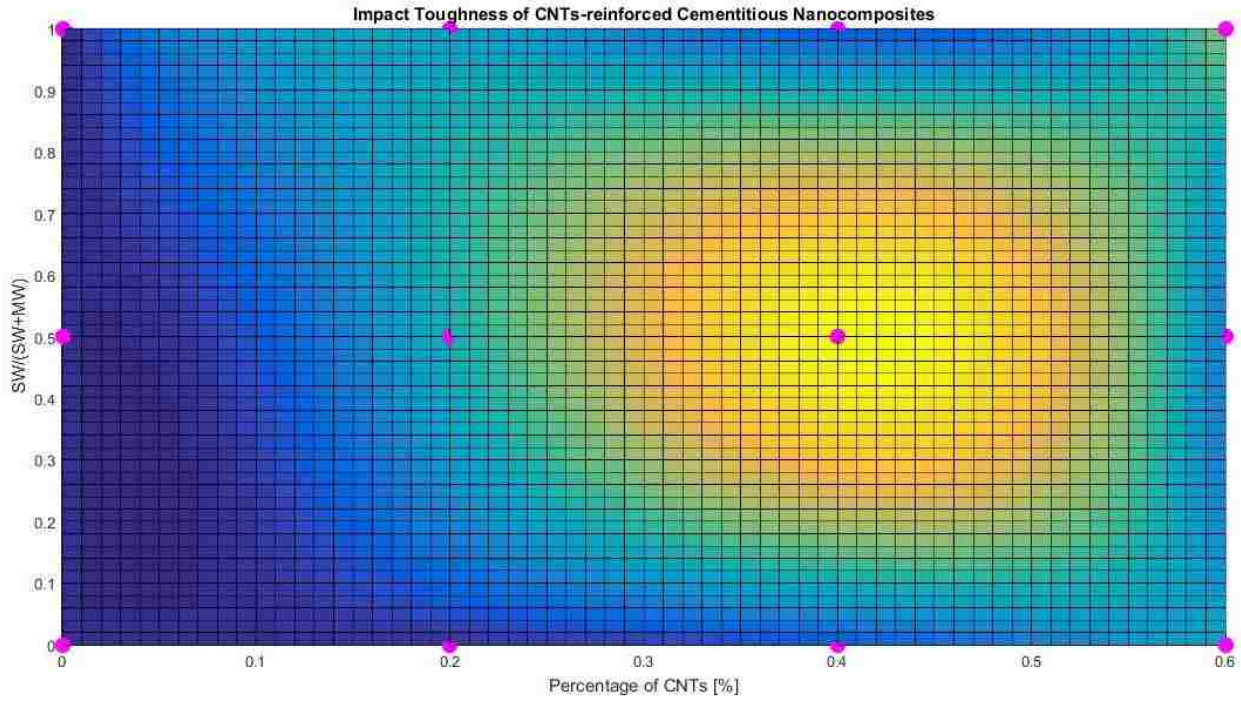


*Figure 90. Top view of low-velocity impact toughness of the full range of CNTs reinforced cementitious nanocomposites*

# CHAPTER 6 CONCLUSION AND RECOMMENDATIONS

## 6.1 Conclusion

The idea of fabricating carbon nanotubes and creating high-strength nanocomposites has attracted scholars and research professionals in various engineering disciplines as well as in medicine since the discovery of CNT 25 years ago. However, the application of carbon nanotubes in the construction industry is a newly emerging field of study that, in several aspects, has the potential to develop further.

To maximize the outstanding properties of carbon nanotubes when synthesizing them with other materials, the procedure of CNT dispersion and mixing dispersed CNTs with matrix materials plays a key role. Concrete structural stability and durability are among essential parts of any design that is rooted in physical, chemical and mechanical properties. In terms of seismic design, lightweight materials with higher energy absorption are the best candidates. Cementitious nanocomposites offer ultra-high strength and outstanding performance with considerably lower weight compared to conventional cement mortar.

Two main classes of CNT include Multi-Walled and Single-Walled Carbon Nanotubes. The main objective of this research was to investigate the effect of reinforcing cement mortar with 0.2wt%, 0.4wt%, and 0.6wt% of SWCNTs, MWCNTs, and hybrid CNTs (50% SWCNTs and 50% MWCNTs). A total of nine mixes of CNTs and one control sample were made. Each test was repeated three times for each batch. The water-to-cement ratio was 0.6 for specimens that were prepared for tensile strength, and 0.4 for specimens that were prepared for impact strength. Water was used as the CNTs' solvent.

The sonication process to disperse all mixes was performed by a tip sonicator at 30% amplitude for one hour, with a 2-second pulse on and a 1-second pulse off. After the dispersing process, CNTs dispersed in water were added to cement for the final product. The prototype samples were tested with a Field Emission

Scanning Electron Microscope (FESEM) to ensure qualitatively sufficient dispersion as cement crystals grew with CNTs. The morphology of the composite changed.

After 28 days of curing the experimental splitting tensile and drop-weight impact test (low velocity), results provided the following important conclusions:

1. Cementitious nanocomposite incorporating 0.4wt% of hybrid carbon nanotubes showed the maximum impact toughness ($kJ/m^3$) under the drop-weight (low velocity) test after 28 days of curing. The average impact toughness of hybrid cementitious nanocomposite is approximately 10 times greater than that of cement mortar.

2. Adding more than 0.4wt% of hybrid carbon nanotubes reduced the impact strength of cementitious nanocomposites, but when 0.6wt% of MWCNTs was added impact strength increased. SWCNTs behaved differently than MWCNTs. Lab observation indicated that SWCNTs require less setting time. This might be the reason for impact strength deterioration when more than 0.4wt% of SWCNTs were added: Because the cementitious nanocomposite hardened before proper mixing, it trapped more air in the composites.

3. Cementitious nanocomposites reinforced by 0.4wt% of hybrid carbon nanotubes showed the ultimate tensile strength, which increased by 50%-80% compared to cement mortar. In of all mixes (0.2wt%, 0.4wt%, and 0.6wt %), hybrid CNTs mixes had noticeably higher ultimate tensile strength compared to SWCNTs and MWCNTs.

Sudden concrete failure is due to inelastic deformations of concrete subjected to tension. However, synthesizing nanomaterials as concrete reinforcements significantly impacts cement-based composites' failure mechanisms. Nanomaterial morphology bridges micro cement crystals as homogeneous and ductile matrices. Failure mechanisms showed considerable cementitious nanocomposite ductility throughout the

splitting tensile test compared to cement mortar. Additionally, after an initial crack developed the failure pattern provided additional time before ultimate failure occurs in cementitious nanocomposites.

The evolution of crack propagation on cementitious nanocomposite surfaces through ultimate specimen failure during the splitting-tensile test was assessed. The failure mode was initiated from central axis aligned with the applied load, but cementitious nanocomposite load capacity increased after crack propagation through vertical cross section axial. The deformation of the cross section from circular to ovate augmented tensile strength by approximately 50% in cementitious nanocomposite compared to conventional cement mortar.

All CNTs' composition showed increases in ductile behavior when compared to extremly brittle conventional concrete. Concrete failure mechanisms under static and dynamic loads was identified as the first crack occurred because shortly after the first crack appears the concrete collapses. However, for cementitious nanocomposites the first material crack happened at approximately 600 psi, while the composite tensile stress increased to 1500 psi.

The outstanding performance of all types of carbon nanotube reinforcement decreased crack propagation and debris spatter of the specimen when the specimen was subjected to the impact load. Failure mechanism showed less brittleness throughout, changing from a diagonal to a radial failure pattern.

The FESEM images indicated non-uniform dispersion, but as sonication and mixing processes improved, dispersion did as well. The first prototype sample showed agglomoration of CNTs and poor bridge among CNTs and cement. However, sonication of CNTs for one hour offered the highest tensile and impact strength.

During the sonication process approximatly 1.0wt% of water was evaporated from the constant water-to-cement ratio. Therefore, the amount of evaporated water was replaced. Additionally, due to the increased

setting time required by CNTs, a higher w/c ratio was used for impact and tensile test specimens: 0.4 and 0.5 respectivly.

Another sonication improvement that influenced water evaporation throughout sonicating with ultrasonic waves involved splitting the sonication time into three intervals. Therefore, the ice bath was replaced with fresh ice every 20 minutes to cool the chemical reaction between CNTs and water. Because the specimen was small and adding CNTs expedited the hardening process, orbital vibration was applied to release trapped air and create a homogenious matrix. However, orbital vibration might not be an effective method for conventional concrete as it may cause aggregate segregation.

Results proved that specimens had higher tensile and impact strength when orbital vibration was applied compared to standard vibrating with a tapping rod. During orbital vibration, air bubbles came to the surface of the cement matrix and disappeared. This was one important issue in producing cementitious nanocomposite. Reaching the maximum potential of CNTs to enhance mechanical properties is not only dependent on the quality of CNTs' dispersion, but also on the throughness of mixing with cement. This method showed improvement, and less air remained trapped in nanoscale, as one FESEM image of cementitious nanocomposite showed.

Despite the considerable increase in the toughness of concrete, the observed data are not statistically convincing. More precise testing methods should be utilized to reach more replicable results and lower the standard deviation of collected data. Moreover, the number of tests for each composite should be increased.

The collected data for the splitting tensile test of MWCNT 0.6%, Hybrid 0.2%, and Hybrid 0.4 % suggest that the observed difference between the sample means is statistically convincing enough to conclude that the average ultimate strength between composite and plain mortar differ significantly. In contrast, in MWCNT 0.2 %, MWCNT 0.4 %, all SWCNT-reinforced composites, and Hybrid 0.6 % the observed data are not statistically convincing.

## 6.2 Research Limitation

This research was primarily conducted to shed light on and characterize two properties of a new generation of cementitious nanocomposites incorporating multi-walled, single walled, and hybrid carbon nanotubes. However, there were some limitations that might affect the results and thus need to be addressed in future research:

6 Published research on this generation of cementitious nanocomposite has been limited since CNTs were discovered 25 years ago. Additionally, the application of this class of nanocomposite is a newly emerging field in civil engineering that it is still limited to a few laboratories trying to address some specific aspect of the nanocomposite.

7 The morphology of CNT dispersion is not clear after mixing with cement, and there is not yet a standard procedure to be followed for achieving the best results.

8 Quality control of the dispersed CNTs in water cannot be checked before mixing with cement due to the limitations of electron microscopes on dried specimens.

9 As CNTs are still expensive materials, the specimen cannot be as large as conventional concrete. Therefore, scaling down the specimen might affect the accuracy of data. As can be seen from result of this research, a high standard deviation was reported after impact testing.

10 The impact test was implemented manually. Therefore, the specimen may not be have been aligned with drop hammer. Consequently, it may have affected the impact test result with scattered data. However, the tensile test results have smaller STD because it was done with an automated machine with a constant applied load.

11 There is a lack of ACI or ASTM standards for cementitious nanocomposites and modifying the procedure, which might have affected the results.

12 The number of test repetitions was limited to three, which makes it challenging to determine conclusive results.

## 6.3 Future Research

This experimental research has advanced the state-of-art for synthesizing multi-walled, single-walled, and hybrid carbon nanotubes to reinforce cementitious composite. The cementitious composite thus syhtesized offers ultra-high impact strength and remarkable tensile strength. However, investigation of all physical, chemical, and mechanical properties requires further research to fully study the single-walled, multi-walled, and, especially, hybrid carbon nanotube reinforcements to create a new generation of nanocomposites suitable for structural stability and durability under applied static and dynamic loads. The most important recommendations that would help future research development are listed below:

1 The cost of carbon nanotubes is still greater than all other reinforcements available to the construction industry. Single-walled carbon nanotubes are very expensive. However, the excellent engineering properties that SWCNTs offer may justify the cost.

2 Creating cementitious nanocomposites with hybrid carbon nanotubes showed outstanding properties. However, it should be more efficient and economical when the optimum percentage is found. Synthesizing less than 50% SWCNTs may produce a nanocomposite with higher mechanical properties without scarifying the effectiveness of SWCNTs, and simultaneously reduce the disadvantages of SWCNTs such as increased setting time and air void.

3 Other mechanical properties of hybrid and SWCNTs need evaluation and comparison with current research results.

4 The chemical process of combining SWCNTs and MWCNTs should be studied.

5 These classes of nanocomposite are costly. Therefore, the effect of scaling down should be taken into consideration.

6 Although this research illuminated the potential of CNT reinforcement, comprehensive laboratory research is needed before utilizing this class of nanocomposite in field applications. The samples should be scaled up for more accurate results.

7 Morphology of a different type of carbon nanotube should be clarified to realize optimum dispersion of carbon nanotubes. A standard method of dispersion is needed to ensure uniform dispersion to maximize the superior properties of carbon nanotubes reinforcement, and should be developed. Further micro-structural research is necessary as nanomaterials bridge with cement crystals while cement is hydrating.

8 As the specimens were scaled down, the ACI 544.2R-89 for drop-weight impact test was modified. It is worthwhile to consider implementing additional impact test methods.

9 Optimum hybrid carbon nanotubes are 0.4wt% in this experiment. However, percentages of 0.3 and 0.5wt% hybrid CNTs should be tested to determine maximum optimization.

10 Failure mechanism should be tracked to discover the potential of health monitoring systems in real time beginning when the initial crack develops until ultimate stress occurs. It is vital to be able to predict nanocomposites' failure in structural applications.

11 Numerical analysis can be conducted to find mathematical models for cementitious nanocomposite behavior.

12 A standard procedure can be developed to enhance the quality of mixing, vibrating, and curing cementitious nanocomposites.

## 6.4 Impact of the Research Effort

This research was pioneering and innovative in terms of investigation of cementitious nanocomposites incorporating hybrid carbon nanotubes. The results provided convincing evidence of the importance of this product, especially under impact load and the splitting tensile test. The behavior of this hybrid cementitious nanocomposite and failure mechanism made this class of composite uniquely applicable where structural health monitoring should be predictable and trackable. This research offers ultra-high impact resistance cement mortar without adding any aggregate, additive, or superplasticizer. The results indicated this cement-based nanocomposite has at least twicethe average impact toughness compared to available fiber-reinforced concrete products [35]. Hybrid carbon nanotubes make important contributions to producing ultra-high- strength and ultra-high-performance cement-based composites with outstanding ductility properties.

This experimental research provided the hybrid system with SWCNTs and MWCNTs. Additionally, it was found that the optimum percentage of hybrid CNTs (0.4wt %) enhances impact and tensile strength of cement-based nanocomposites while other research pointed out the range of 0.01-2.00 wt%.

The dispersion method of CNTs developed in this experiment prevented unnecessary ultra-sonic energy that damages CNTs, but provided yet enough energy to disperse CNT and incorporate the superior mechanical properties of nanocomposites. The dispersion method in this research reduced the amount of water evaporation during sonication process. More importantly, the process of mixing dispersed CNT in water with cement to produce a homogeneous matrix was modified with an innovative vibration process to release air bubbles trapped in the cement mortar before completing cement hydration process and beginning the hardening phase.

# APPENDIX

# APPENDIX 1 MATLAB CODE FOR MATHEMATICAL OPTIMIZATION OF ULTIMATE TENSILE STRENGTH

```
clc
clear
%
%
        [X,Y] = meshgrid(0:.2:0.6,0:0.5:1);
        % X axis demonstrates the percentage of nanoparticles.
        % Y axis shows the ratio SW/(SW+MW). When pure single
        % walled CNT is used Y = 1, when 50 % of SW and 50% of MW is used
        % Y=0.5 and when pure multy-walled CNT is used Y = 0
        Z = [869,878,1091,1003;869,1092,1177,990;869,1045,913,1006];

 Xq = 0:0.01:0.6; Yq = 0:0.02:1;
[Xq,Yq] = meshgrid(Xq,Yq);
Zq = interp2(X,Y,Z,Xq,Yq,'cubic');
figure
surf(Xq,Yq,Zq);
hold on;
plot3(X,Y,Z,'.','MarkerSize',40,'markeredge','m')
xlabel('CNTs content [% weight of cement]')
ylabel('SW/(SW+MW)')
zlabel('Ultimate Tensile Strength [psi]')
legend
title('Tensile Strength of CNTs-reinforced Cementitious Nanocomposites')
format short
Max_Tensile = max(max(Zq));
%
%
```

# APPENDIX 2 MATLAB CODE FOR MATHEMATICAL OPTIMIZATION OF IMPACT TOUGHNESS

```
clc
clear
%
%
        [X,Y] = meshgrid(0:.2:0.6,0:0.5:1);
        % X axis demonstrates the percentage of nanoparticles.
        % Y axis shows the ratio SW/(SW+MW). When pure single
        % walled CNT is used Y = 1, when 50 % of SW and 50% of MW is used
        % Y=0.5 and when pure multy-walled CNT is used Y = 0
        Z = [128,253,689,1785;128,1992,4294,792;128,1517,334,2982];

 Xq = 0:0.01:0.6; Yq = 0:0.02:1;
[Xq,Yq] = meshgrid(Xq,Yq);
Zq = interp2(X,Y,Z,Xq,Yq,'spline');
figure
surf(Xq,Yq,Zq);
hold on;
plot3(X,Y,Z,'.','MarkerSize',35,'markeredge','m')
xlabel('Percentage of CNTs [%]')
ylabel('SW/(SW+MW)')
zlabel('Impact Toughness [kJ/m3]')
legend
title('Impact Toughness of CNTs-reinforced Cementitious Nanocomposites')
format short
Max_Toughness = max(max(Zq));
```

# REFERENCES

[1] Siddique, R., & Mehta, A. (2014). Effect of carbon nanotubes on properties of cement mortars. Construction and Building Materials, 50, 116-129.

[2] Liu, Z., Tabakman, S., Welsher, K. et al. Nano Res. (2009) 2: 85. https://doi.org/10.1007/s12274-009-9009-8

[3] Eftekhari, M., & Mohammadi, S. (2016). Molecular dynamics simulation of the nonlinear behavior of the CNT-reinforced calcium silicate hydrate (C–S–H) composite. Composites Part A: Applied Science and Manufacturing, 82, 78-87.

[4] Eatemadi A, Daraee H, Karimkhanloo H, Kouhi M, Zarghami N, Akbarzadeh A, Abasi M, Hanifehpour Y, Joo SW. Carbon nanotubes: properties, synthesis, purification, and medical applications. Nanoscale Res Lett. 2014; 9:1–13.

[5] Sadiq, M. M. (2013). Reinforcement of cement-based matrices with graphite nanomaterials (Order No. 3554877).

[6] Muhammad Maqbool Sadiq, Anagi Manjula Balachandra, Parviz Soroushian, patent US 8951343 B2

[7] Chen, Z., Lim, J. L. G., & Yang, E. (2016). Ultra-high-performance cement-based composites incorporating low dosage of plasma synthesized carbon nanotubes. Materials & Design, 108, 479-487.

[8] Mohsen, M. O., Al-Nuaimi, N., Abu Al-Rub, R. K., Senouci, A., & Bani-Hani, K. A. (2016). Effect of mixing duration on flexural strength of multi walled carbon nanotubes cementitious composites. Construction and Building Materials, 126, 586-598.

[9] Kim, H. (2015). Chloride penetration monitoring in reinforced concrete structure using carbon nanotube/cement composite. Construction and Building Materials, 96, 29-36.

[10] Eftekhari, M., & Mohammadi, S. (2016). Multiscale dynamic fracture behavior of the carbon nanotube reinforced concrete under impact loading. International Journal of Impact Engineering,87, 55-64.

[11] Annamalai, S. K., Arunachalam, K. D., & Sathyanarayanan, K. S. (2012). Production and characterization of bio caulk by bacillus pasteurii and its remediation properties with carbon nano tubes on concrete fractures and fissures. Materials Research Bulletin, 47(11), 3362-3368.

[12] Shen, H., & Xiang, Y. (2015). Nonlinear response of nanotube-reinforced composite cylindrical panels subjected to combined loadings and resting on elastic foundations. Composite Structures, 131, 939-950.

[13] Kim, H. K., Park, I. S., & Lee, H. K. (2014). Chloride penetration monitoring and stability of CNT/cement mortar composites with low water–binder ratio. Composite Structures, 116, 713-719.

[14] Kim, G. M., Naeem, F., Kim, H. K., & Lee, H. K. (2016). Heating and heat-dependent mechanical characteristics of CNT-embedded cementitious composites. Composite Structures, 136, 162-170.

[15] Kim, H. (2015). Chloride penetration monitoring in reinforced concrete structure using carbon nanotube/cement composite. Construction and Building Materials, 96, 29-36.

[16] Kim, H. K., Nam, I. W., & Lee, H. K. (2014). Enhanced effect of carbon nanotube on mechanical and electrical properties of cement composites by incorporation of silica fume. Composite Structures, 107, 60-69.

[17] Stynoski, P., Mondal, P., & Marsh, C. (2015). Effects of silica additives on fracture properties of carbon nanotube and carbon fiber reinforced portland cement mortar. Cement and Concrete Composites, 55, 232-240.

[18] Nam, I. W., Kim, H. K., & Lee, H. K. (2012). Influence of silica fume additions on electromagnetic interference shielding effectiveness of multi-walled carbon nanotube/cement composites. Construction and Building Materials, 30, 480-487.

[19] Chew, K., Low, K., Sharif Zein, S. H., McPhail, D. S., Gerhardt, L., Roether, J. A., & Boccaccini, A. R. (2011). Reinforcement of calcium phosphate cement with multi-walled carbon nanotubes and bovine serum albumin for injectable bone substitute applications. Journal of the Mechanical Behavior of Biomedical Materials, 4(3), 331-339.

[20] Eftekhari, M., & Mohammadi, S. (2016). Molecular dynamics simulation of the nonlinear behavior of the CNT-reinforced calcium silicate hydrate (C–S–H) composite. Composites Part A: Applied Science and Manufacturing, 82, 78-87.

[21] Eftekhari, M., Hatefi Ardakani, S., & Mohammadi, S. (2014). An XFEM multiscale approach for fracture analysis of carbon nanotube reinforced concrete. Theoretical and Applied Fracture Mechanics, 72, 64-75.

[22] Malla, S. (2008). Effect of multi-walled carbon nanotubes on characteristics of cement paste (Order No. 1460077). Available from ProQuest Dissertations & Theses Global. (304474925). Retrieved from

[23] Manzur, T. (2011). Nano-modified cement composites and its applicability as concrete repair material (Order No. 3473989). Available from ProQuest Dissertations & Theses Global. (896959071). Retrieved from

[24] Mohanam, V. (2012). Comparative application of two nanoparticles in cement mortar (Order No. 1541320). Available from ProQuest Dissertations & Theses Global. (1418271246). Retrieved from http://ezproxy.library.unlv.edu/login?url=https://search.proquest.com/docview/1418271246?accountid=3611

[25] Jeevanagoudar, Y. V., Krishna, R. H., Gowda, R., Preetham, R., & Prabhakara, R. (2017). Improved mechanical properties and piezoresistive sensitivity evaluation of MWCNTs reinforced cement mortarsdoi:http://dx.doi.org/10.1016/j.conbuildmat.2017.03.139

[26] Wang, S., Zhang, S., Wang, Y., Sun, X., & Sun, K. (2017). Reduced graphene oxide/carbon nanotubes reinforced calcium phosphate cement doi:http://dx.doi.org/10.1016/j.ceramint.2017.06.196

[27] Sun, G., Liang, R., Lu, Z., Zhang, J., & Li, Z. (2016). Mechanism of cement/carbon nanotube composites with enhanced mechanical properties achieved by interfacial strengtheningdoi:http://dx.doi.org/10.1016/j.conbuildmat.2016.04.034

[28] Nadiv, R., Shtein, M., Refaeli, M., Peled, A., & Regev, O. (2016). The critical role of nanotube shape in cement composites doi:https://doi-org.ezproxy.library.unlv.edu/10.1016/j.cemconcomp.2016.05.012

[29] Jiang, S., Zhou, D., Zhang, L., Ouyang, J., Yu, X., Cui, X., & Han, B. (2018). Comparison of compressive strength and electrical resistivity of cementitious composites with different nano- and micro-fillers doi:https://doi-org.ezproxy.library.unlv.edu/10.1016/j.acme.2017.05.010

[30] https://www.concrete.org/store/productdetail.aspx?ItemID=544289&Format=DOWNLOAD

[30] Park, H. M., Kim, G. M., Lee, S. Y., Jeon, H., Kim, S. Y., Kim, M., . . . Yang, B. J. (2018). Electrical resistivity reduction with pitch-based carbon fiber into multi-walled carbon nanotube (MWCNT)-embedded cement composites. Construction and Building Materials, 165, 484-493. doi:https://doi-org.ezproxy.library.unlv.edu/10.1016/j.conbuildmat.2017.12.205

[31] Lim, M., Lee, H. K., Nam, I., & Kim, H. (2017). Carbon nanotube/cement composites for crack monitoring of concrete structures doi:https://doi-org.ezproxy.library.unlv.edu/10.1016/j.compstruct.2017.08.042

[32] Yin, X., Li, S., He, G., Feng, Y., & Wen, J. (2018). Preparation and characterization of CNTs/UHMWPE nanocomposites via a novel mixer under synergy of ultrasonic wave and extensional deformationhttps://doi-org.ezproxy.library.unlv.edu/10.1016/j.ultsonch.2017.12.039

[33] Baig, Z., Mamat, O., Mustapha, M., Mumtaz, A., Munir, K. S., & Sarfraz, M. (2018). Investigation of tip sonication effects on structural quality of graphene nanoplatelets (GNPs) for superior solvent dispersionhttps://doi-org.ezproxy.library.unlv.edu/10.1016/j.ultsonch.2018.03.007

[34] ASTM Standard C192/C192MMaking and Curing Concrete Test Specimens in the Laboratory

ASTM International, West Conshohocken, PA, U.S.A (2002)

[35] Gerges, N. N., Issa, C. A., & Fawaz, S. (2015). Effect of construction joints on the splitting tensile strength of concretehttps://doi-org.ezproxy.library.unlv.edu/10.1016/j.cscm.2015.07.001

[36] Wang, Y., Colas, G., & Filleter, T. (2016). Improvements in the mechanical properties of carbon nanotube fibers through graphene oxide interlockinghttps://doi-org.ezproxy.library.unlv.edu/10.1016/j.carbon.2015.11.008

[37] Routray, K. L., Saha, S., & Behera, D. (2017). Effect of CNTs blending on the structural, dielectric and magnetic properties of nanosized cobalt ferritehttps://doi-org.ezproxy.library.unlv.edu/10.1016/j.mseb.2017.09.021

[38] Bor, A., Ichinkhorloo, B., Uyanga, B., Lee, J., & Choi, H. (2018). Cu/CNT nanocomposite fabrication with different raw material properties using a planetary ball milling processhttps://doi-org.ezproxy.library.unlv.edu/10.1016/j.powtec.2016.06.042

[39] Chen, P., Jing, S., Chu, Y., & Rao, P. (2018). Improved fracture toughness of CNTs/SiC composites by HF treatmenthttps://doi-org.ezproxy.library.unlv.edu/10.1016/j.jallcom.2017.09.265

[40] Ramli, N. I. T., Rashid, S. A., Mamat, M. S., Sulaiman, Y., & Krishnan, S. (2018). Incorporation of iron oxide into CNT/GNF as a high-performance supercapacitor electrodehttps://doi-org.ezproxy.library.unlv.edu/10.1016/j.matchemphys.2018.03.044

[41] Dolati, S., Azarniya, A., Azarniya, A., Eslami-shahed, H., Hosseini, H. R. M., & Simchi, A. (2018). Toughening mechanisms of SiC-bonded CNT bulk nanocomposites prepared by spark plasma sinteringhttps://doi-org.ezproxy.library.unlv.edu/10.1016/j.ijrmhm.2017.10.024

[42] Maho, B., Jamnam, S., Sukontasukkul, P., Fujikake, K., & Banthia, N. (2017). Preliminary study on multilayer bulletproof concrete panel: Impact energy absorption and failure pattern of fibre reinforced concrete, para-rubber and styrofoam sheetshttps://doi-org.ezproxy.library.unlv.edu/10.1016/j.proeng.2017.11.090

[43] Reuter, U., Sultan, A., & Reischl, D. S. (2018). A comparative study of machine learning approaches for modeling concrete failure surfaceshttps://doi-org.ezproxy.library.unlv.edu/10.1016/j.advengsoft.2017.11.006

[44] Wu, J., Ning, J., & Ma, T. (2017). The dynamic response and failure behavior of concrete subjected to new spiral projectile impactshttps://doi-org.ezproxy.library.unlv.edu/10.1016/j.engfailanal.2017.05.037

[45] Sarfarazi, V., Haeri, H., Ebneabbasi, P., Bagher Shemirani, A., & Hedayat, A. (2018). Determination of tensile strength of concrete using a novel apparatushttps://doi-org.ezproxy.library.unlv.edu/10.1016/j.conbuildmat.2018.01.157

[46] Du, X., Jin, L., & Ma, G. (2014). Numerical simulation of dynamic tensile-failure of concrete at meso-scalehttps://doi-org.ezproxy.library.unlv.edu/10.1016/j.ijimpeng.2013.12.005

[47] Mohammadhosseini, H., Tahir, M. M., & Sam, A. R. M. (2018). The feasibility of improving impact resistance and strength properties of sustainable concrete composites by adding waste metalized plastic fibreshttps://doi-org.ezproxy.library.unlv.edu/10.1016/j.conbuildmat.2018.02.210

[48] Geng, J., Sun, Q., Zhang, Y., Cao, L., & Zhang, W. (2017). Studying the dynamic damage failure of concrete based on acoustic emissionhttps://doi-org.ezproxy.library.unlv.edu/10.1016/j.conbuildmat.2017.05.054

[49] Wolf, J., Pirskawetz, S., & Zang, A. (2015). Detection of crack propagation in concrete with embedded ultrasonic sensorshttps://doi-org.ezproxy.library.unlv.edu/10.1016/j.engfracmech.2015.07.058

[50] Bhogayata, A. C., & Arora, N. K. (2018). Impact strength, permeability and chemical resistance of concrete reinforced with metalized plastic waste fibershttps://doi-org.ezproxy.library.unlv.edu/10.1016/j.conbuildmat.2017.11.135

[51] Siddique, S., Shrivastava, S., Chaudhary, S., & Gupta, T. (2018). Strength and impact resistance properties of concrete containing fine bone china ceramic aggregatehttps://doi-org.ezproxy.library.unlv.edu/10.1016/j.conbuildmat.2018.02.213

[52] ACI544.2R-89, Measurement of properties of fiber reinforced concrete, ACI, West Conshohocken, PA, 1999.

[53] AbdelAleem, B. H., Ismail, M. K., & Hassan, A. A. A. (2018). The combined effect of crumb rubber and synthetic fibers on impact resistance of self-consolidating concretehttps://doi-org.ezproxy.library.unlv.edu/10.1016/j.conbuildmat.2017.12.077

[54] Khalil, E., Abd-Elmohsen, M., & Anwar, A. M. (2015). Impact resistance of rubberized self-compacting concrete doi:http://dx.doi.org/10.1016/j.wsj.2014.12.002

[55] Annamalai, S. K., Arunachalam, K. D., & Sathyanarayanan, K. S. (2012). Production and characterization of bio caulk by bacillus pasteurii and its remediation properties with carbon nano tubes on concrete fractures and fissures. Materials Research Bulletin, 47(11), 3362-3368.

[56] Sindu, B. S., Sasmal, S., & Gopinath, S. (2014). A multi-scale approach for evaluating the mechanical characteristics of carbon nanotube incorporated cementitious composites. Construction and Building Materials, 50, 317-327.

[57] American Concrete Institute (ACI) Committee 440, 440.6-08 "Specification for Carbon and Glass Fiber-Reinforced Polymer Bar Materials for Concrete Reinforcement," 2008 -

[58] Jang, S., Hochstein, D. P., Kawashima, S., & Yin, H. (2017). Experiments and micromechanical modeling of electrical conductivity of carbon nanotube/cement composites with moisture doi: http://dx.doi.org/10.1016/j.cemconcomp.2016.12.003

[59] Magalhães, A. G., Marques, A. T., Oliveira, F. M. F., Soukatchoff, P., & de Castro, P. T. (1996). Mechanical behaviour of cementitious matrix composites doi:http://dx.doi.org/10.1016/0958-9465(95)00035-6

[60] Fakharifar, M., Dalvand, A., Arezoumandi, M., Sharbatdar, M. K., Chen, G., & Kheyroddin, A. (2014). Mechanical properties of high performance fiber reinforced cementitious composites doi:http://dx.doi.org.ezproxy.library.unlv.edu/10.1016/j.conbuildmat.2014.08.068

[61] Zhou, X., Ghaffar, S. H., Dong, W., Oladiran, O., & Fan, M. (2013). Fracture and impact properties of short discrete jute fibre-reinforced cementitious composites doi:http://dx.doi.org.ezproxy.library.unlv.edu/10.1016/j.matdes.2013.01.029

[62] Yoo, D., You, I., & Lee, S. (2018). Electrical and piezoresistive sensing capacities of cement paste with multi-walled carbon nanotubes https://doi-org.ezproxy.library.unlv.edu/10.1016/j.acme.2017.09.007

[63] ASTM C496. Standard test method for splitting tensile strength of cylindrical concrete specimens, Annual Book of ASTM Standards: American Society of Testing Materials; 2004.

[66] Kim, G. M., Park, S. M., Ryu, G. U., & Lee, H. K. (2017). Electrical characteristics of hierarchical conductive pathways in cementitious composites incorporating CNT and carbon fiber doi:https://doi-org.ezproxy.library.unlv.edu/10.1016/j.cemconcomp.2017.06.004

[64] Baig, Z., Mamat, O., Mustapha, M., Mumtaz, A., Munir, K. S., & Sarfraz, M. (2018). Investigation of tip sonication effects on structural quality of graphene nanoplatelets (GNPs) for superior solvent dispersionhttps://doi-org.ezproxy.library.unlv.edu/10.1016/j.ultsonch.2018.03.007

[65] Nadiv, R., Vasilyev, G., Shtein, M., Peled, A., Zussman, E., & Regev, O. (2016). The multiple roles of a dispersant in nanocomposite systemshttps://doi-org.ezproxy.library.unlv.edu/10.1016/j.compscitech.2016.07.008

[66] Choi, Y., & Yuan, R. L. (2005). Experimental relationship between splitting tensile strength and compressive strength of GFRC and PFRChttps://doi-org.ezproxy.library.unlv.edu/10.1016/j.cemconres.2004.09.010

# CURRICULUM VITAE

## ROBABEH JAZAEI, PH.D.

E-Mail address: Robabeh.jazaei@gmail.com

Dr. Robabeh Jazaei has more than ten years of professional and academic experience in civil engineering, and project management. She has received his Bachelor of Science degree in Civil Engineering from the Shahrood University of Technology (2002); Master's degree in Structural Engineering from Tehran Azad University (2009); and Ph.D. degree in Civil and Environmental Engineering from the University of Nevada, Las Vegas (2018). Currently, Dr. Jazaei is the Statics instructor at the UNLV.

In the past few years, Dr. Jazaei's dissertation title is "preliminary investigation of tensile strength and impact characterization of cementitious composite incorporating carbon nanotubes". Her research has focused on structural applications of cementitious nanocomposites, with particular emphasis on impact characterization to increase energy absorption under static impact loads and tensile strength to increase deformation. Dr. Jazaei investigated the failure mechanisms and ductile behavior of nanocomposites incorporating carbon nanotubes, carbon nanofibers and graphene under tensile stress and drop-weight impact loads. Her interdisciplinary dissertation was collaborative research with faculty members from Department of Civil and Environmental Engineering (Dr. Moses Karakouzian, Dr. Ying Tian, and Dr. Pramen Shrestha) and Department of Mechanical Engineering (Dr. Brendan O'Toole and Jeayun Moon).

Dr. Jazaei has also conducted research on multifunctional nanoparticles for structural health monitoring in concrete structures. This research was awarded by National Science Foundation Innovation Corp in 2016 and 2018. The aim of producing this generation of cement-based nanocomposites is to be commercialized for construction industry applications.

Other areas of Dr. Jazaei's research have been focused on finite element analysis and seismic performance of ferrocement-composite shells as well as experimental research on fiber reinforced concrete. She has patented an invention that won a bronze medal at the Tecnopol Moscow Science and Technology Association, Russia, 2010 and a gold medal at the European Exhibition of Creativity and Innovation, Romania, 2012. Her hard work and dedication have earned him several academic and professional certifications for design, construction management, academic, and professional development.

She is a voting member of American Concrete Institute (ACI) Committee 241-A01 (The Application and Implementation of Nano-Engineered Concrete, member of American Society of Civil Engineers (ASCE), American Society of Mechanical Engineering (ASME), American Society of Heating, Refrigerating and Air-Conditioning Engineers (ASHRAE), National Society of Professional Engineers (NSPE).